Geodätisch-geophysikalische Arbeiten in der Schweiz

(Fortsetzung der Publikationsreihe
«Astronomisch-geodätische Arbeiten in der Schweiz»)

herausgegeben von der

Schweizerischen Geodätischen Kommission
(Organ der Schweizerischen Akademie der Naturwissenschaften)

Achtundvierzigster Band
Volume 48

IONOSPHERE AND GEODETIC SATELLITE SYSTEMS: PERMANENT GPS TRACKING DATA FOR MODELLING AND MONITORING

Urs Wild

1994

Geodätisch-geophysikalische Arbeiten in der Schweiz

(Fortsetzung der Publikationsreihe
«Astronomisch-geodätische Arbeiten in der Schweiz»)

herausgegeben von der

Schweizerischen Geodätischen Kommission
(Organ der Schweizerischen Akademie der Naturwissenschaften)

Achtundvierzigster Band
Volume 48

IONOSPHERE AND GEODETIC SATELLITE SYSTEMS: PERMANENT GPS TRACKING DATA FOR MODELLING AND MONITORING

Urs Wild

1994

Adresse der Schweizerischen Geodätischen Kommission:

Institut für Geodäsie und Photogrammetrie
Eidg. Technische Hochschule Zürich
ETH-Hönggerberg
CH-8093 Zürich
Switzerland

Redaktion des 48. Bandes:
Dr. U. Wild
Dr. B. Bürki

Druck: OWADRUCK, CH - 3173 Oberwangen

VORWORT

Mit der Entwicklung von Satellitensystemen zur Positionierung und Navigation ab Mitte der 60-er Jahre wurde eine satellitengestützte Erforschung der Ionosphäre möglich. Es erwies sich nämlich als unbedingt erforderlich, die Navigationssignale von diesen Satelliten auf zwei kohärenten Trägerwellen auszusenden, um die ionosphärisch bedingten Laufzeitkorrekturen zu bestimmen. Diese Korrekturen enthalten naturgemäss Information über die Ionosphäre; insbesondere erlauben sie die Bestimmung des "totalen Elektroneninhalts", der Gesamtzahl der Elektronen in einem Zylinder gegebener Grundfläche zwischen Satellit und Beobachter. Legt man der Ionosphäre ein mathematisches Modell (z.B. das Einschichtmodell) zugrunde, wird die Bestimmung der Elektronendichte in diesem Modell möglich.

Dies ist der allgemeine Rahmen, in den Herr Urs Wild seine Dissertation stellt. Als sehr nützlich für Astronomen und Geodäten wird sich der Überblick über den Stand der Ionosphärenforschung in Kapitel 3 erweisen. Eigentlicher Kern der Arbeit sind die Kapitel 4 und 5: In Kapitel 4 werden die mathematischen Modelle der Ionosphäre vorgestellt, die Computer-Programme zu deren Bestimmung werden eingehend diskutiert. Herr Wild unterscheidet zwischen einem deterministischen Ionosphärenmodell, welches es gestattet, zu einer beliebigen Zeit die mittlere Elektronendichte in der erwähnten Schicht an einem beliebigen Punkt über der Erdoberfläche zu berechnen und einem "stochastischen" Anteil, welcher Auskunft über ionosphärische Turbulenzen gibt. Wichtig ist, dass die Modelle regionaler oder gar lokaler Natur sind: Mit den Beobachtungen weniger (im Grenzfall sogar nur eines) GPS Empfänger(s) lässt sich ein zuverlässiges regionales Modell der Ionosphäre mit einer hohen zeitlichen Auflösung (wenige Stunden) angeben. Ebenso zuverlässig lässt sich die (Un)ruhe der Ionosphäre in der Region beschreiben. Da die Programme sehr wenig Interaktion verlangen, und da zudem nur die rohen, unbehandelten Messdaten eines einzelnen Empfängers benötigt werden, lassen die entwickelten Verfahren eine Analyse in "fast" Echtzeit ("real-time") zu. Die so erarbeiteten Ionosphärenmodelle gestatten eine Prognose für die Laufzeitkorrekturen von Radiosignalen beliebiger Wellenlänge und die Abschätzung des stochastischen Anteils der Ionosphäre am Gesamtrauschen.

In Kapitel 5 werden die entwickelten Verfahren angewandt. Der Autor unterscheidet zwischen geodätischen und geophysikalischen Anwendungen. Zunächst wird anhand des Turtmann-Netzes im Wallis gezeigt, dass in kleinen Netzen das Ionosphärenmodell zusammen mit den Messungen in den beiden echten Trägerwellen wesentlich bessere Resultate ermöglicht als die Auswertung der sogenannten ionosphärenfreien Linearkombination. Das zweite Beispiel, die Eichung des Altimeters des ESA Satelliten "European Remote Sensing Satellite 1 (ERS-1)" zeigt, dass die GPS Resultate von Herrn Wild den Vergleich mit unabhängigen Techniken durchaus nicht zu scheuen brauchen. Das letzte geodätische Beispiel zeigt, dass Ionosphärenmodelle auch in mittelgrossen Netzen ihre Bedeutung haben. Zukunftsweisend ist das geophysikalische Beispiel. Herr Wild zeigt mit einem sich über mehrere Wochen erstreckenden Test mit mehr als 20 in allen geographischen Breiten verteilten Empfängern, dass seine Verfahren im Rahmen des "International GPS Service for Geodynamics (IGS)" bei einer minimalen Mehrbelastung (Rechenzeit und Speicherkapazität) zu einem eigentlichen satellitengestützten Ionosphärendienst verwendet werden könnten. Es wäre zu wünschen, dass der IGS tatsächlich um diese Dienstleistung erweitert würde.

Prof. Dr. G. Beutler
Direktor des Astronomischen Instituts der Universität Bern

Direktor F. Jeanrichard
Bundesamt für Landestopographie
Vizepräsident der SGK

Prof. Dr. H.-G. Kahle
ETH-Zürich
Präsident der SGK

PREFACE

L'investigation de l'ionosphère assistée par satellites est désormais possible grâce au développement, dès le milieu des années soixante, des systèmes de satellites pour le positionnement et la navigation. En effet, il s'avéra absolument nécessaire d'émettre les signaux de ces satellites sur deux ondes porteuses cohérentes afin de déterminer les corrections ionosphérique du temps de propagation. De par leur nature, ces corrections contiennent des informations concernant l'ionosphère et, en particulier, permettent la détermination du "contenu total des électrons", c'est-à-dire, le nombre total des électrons dans un cylindre de section donnée entre le satellite et l'observateur. Si l'on décrit l'ionosphère avec un modèle mathématique (par exemple le modèle d'une couche unique), la détermination de la densité des électrons est alors possible pour le modèle choisi.

Voilà pour le cadre général de la dissertation de Monsieur Urs Wild. La vue d'ensemble concernant l'état de l'investigation de l'ionosphère donnée dans le chapitre 3 est très utile aux astronomes et aux géodésiens. Mais le point fort du travail se trouve dans les chapitres 4 et 5. Dans le chapitre 4, les modèles mathématiques de l'ionosphère sont présentés et les logiciels de calcul pour les déterminer sont discutés. Monsieur Wild fait la distinction entre un modèle déterministe de l'ionosphère qui permet, à un instant donné, de calculer la densité moyenne des électrons d'une couche donnée en un point quelconque de la surface terrestre et une partie stochastique qui donne des informations sur les turbulences ionosphériques. Les modèles, et ceci est important, peuvent être de nature régionale, voire locale: ainsi, il suffit de faire des observations avec un nombre restreint de récepteurs GPS (à la limite, un seul suffit) pour obtenir un modèle régional fiable de l'ionosphère en quelques heures seulement. La turbulence de l'ionosphère peut être également décrite très exactement dans la région considérée. Comme les logiciels n'exigent que peu d'interventions interactives et, qu'en plus, seules les données brutes et non traitées sont nécessaires, les procédés développés ici permettent de faire une analyse presque en temps réel. Les modèles de l'ionosphère déterminés par ces procédés permettent de faire des prévisions concernant le temps de propagation de signaux radio de longueur d'onde quelconque ainsi que l'estimation de la part stochastique de l'ionosphère par rapport à la somme des perturbations.

Le chapitre 5 montre quelques applications des procédés développés dans les chapitres précédents. L'auteur distingue les applications géodésiques et les applications géophysiques. Tout d'abord, en prenant l'exemple du réseau-test de Turtmann, il démontre que dans les petits réseaux, le modèle ionosphérique avec les mesures effectuées à l'aide de deux ondes porteuses donne des résultats bien meilleurs que l'élimination de l'influence de l'ionosphère par la méthode de l'analyse de combinaisons linéaires. Le second exemple, le calibrage de l'altimètre du satellite ERS-1 (European Remote Sensing Satellite 1) de l'ESA, montre que les résultats obtenus par la méthode GPS de Monsieur Wild ne craignent pas la comparaison avec d'autres techniques indépendantes. Le dernier exemple géodésique montre que le modèle ionosphérique a son importance également dans des réseaux d'étendue moyenne. Le dernier exemple géophysique est orienté vers le futur. Monsieur Wild montre, avec un test s'étendant sur plusieurs semaines et effectué avec plus de 20 récepteurs répartis sous toutes les latitudes géographiques, que ses procédés pourraient être utilisés par un service de l'ionosphère assisté par satellites dans le cadre du "International GPS Service for Geodynamics (IGS)" et ceci avec une charge supplémentaire minime touchant le temps de calcul et la capacité en mémoires. Il serait souhaitable que l'IGS élargisse son champs d'activité et offre cette prestation.

Prof. Dr. G. Beutler
Directeur de l' Institut
d' astronomie
de l'Université de Berne

F. Jeanrichard, Directeur
de l' Office fédéral de topographie
Vice-président de la CGS

Prof. Dr. H.-G. Kahle
ETH Zurich
Président de la CGS

PREFACE

With the development of satellite systems for positioning and navigation during the 1960s, the satellite-based exploration of the ionosphere became available. It was also obvious that it would be absolutely necessary to transmit the navigation signals on two different frequencies in order to determine the ionospheric run-time corrections of the satellite signals. These run-time corrections allow to compute the 'total electron content' of the ionosphere, i.e. the number of free electrons in a cylinder with a given cross-section between satellite and observer. Assuming a mathematical model for the ionosphere (like e.g. the 'single layer' model), the determination of the electron density in the ionosphere will be possible.

This is the general context of the thesis of U. Wild. Chapter 3 gives an interesting overview (especially for astronomers and geodesists) over the exploration methods of the ionosphere. Chapters 4 and 5 form the kernel of the dissertation: the mathematical models of the ionosphere are discussed in chapter 4, where also the software developments are presented. U. Wild distinguishs between a deterministic model of the ionosphere, which allows for a given point on the Earth and a given time to compute the total electron content in the ionosphere, and a stochastical part, which gives information about the irregular part of the ionosphere. It is important, that the models are of regional or even local nature: using the observations of one or more dual frequency GPS receivers a reliable regional ionosphere model may be computed with a high temporal resolution (several hours). In the same way also the irregular part of the ionosphere may be described. Because the programs do not need a lot of interaction and because they just use the raw measurements of a single GPS receiver, the presented algorithms allow to perform an almost "real-time" analysis of the ionosphere. The computed ionosphere models allow the prediction for the run-time corrections for radio signals of different wavelengths and they also give an estimate of the influence of the irregular part of the ionosphere on the total signal noise.

Chapter 5 shows the application of the developed methods. The author makes the distinction between geodetic and geophysical applications. In a first example the Turtmann network in the Swiss Alps is used to demonstrate, that in small networks the introduction of ionosphere models together with the observations of the original GPS carriers gives significantly better results than the use of the so-called ionosphere free linear combination. A second example, the altimeter calibration of the ESA satellite "European Remote Sensing Satellite 1 (ERS-1)" shows, that the results of U. Wild are absolutely comparable to other independent observation techniques. The last geodetic example shows the application of ionosphere models in medium-scale networks. The geophysical example may be regarded as very promising for the future. U. Wild uses 20 globally distributed stations (in different geographical latitudes) over a time span of several weeks in order to show, that all the programs and algorithms could be used also for the "International GPS Service for Geodynamics (IGS)" in order to establish a 'satellite-aided ionosphere service'. It is desirable, that the IGS will be enhanced by this new service.

Prof. Dr. G. Beutler
Director of the Astronomical
Institute, University of Berne

Director F. Jeanrichard
Federal Office of Topography
Vice president SGC

Prof. Dr. H.-G. Kahle
ETH Zurich
President SGC

DANK

Ich möchte an dieser Stelle Herrn Prof. G. Beutler herzlich für seine Unterstützung während der ganzen Arbeit danken.

Mein Dank gilt ebenso meinen Vorgesetzten am Bundesamt für Landestopographie, allen voran Herrn Direktor F. Jeanrichard, Herrn Vizedirektor E. Gubler und Herrn Dr. D. Schneider für ihr Verständnis und insbesondere die Erteilung der Urlaubstage während den Jahren 1992 und 1993, ohne die die vorliegende Arbeit nicht hätte vollendet werden können.

Nicht zuletzt gilt mein Dank auch Frau Ch. Gurtner für die sorgfältige Reinschrift der Arbeit.

Bern, im Juni 1994 Urs Wild

IONOSPHERE AND GEODETIC SATELLITE SYSTEMS: PERMANENT GPS TRACKING DATA FOR MODELLING AND MONITORING

C o n t e n t

1. INTRODUCTION

1.1 History

In 1901 the first **transmission of radio signals over the atlantic ocean** was performed by G. Marconi (1874-1937). The success of this transmission gave a first hint for the existence of a reflecting layer guiding the electromagnetic waves around the earth. An other hint was the observation of large variations of the signal strength for radio transmissions during the night over distances longer than 150 km. These variations were explained by the superposition of two different waves: a ground wave and a wave reflected somewhere in the atmosphere. When the two waves are superposed either addition or subtraction (fading) of the signal may occur. The (still hypothetic) **reflecting layer** was called **Heaviside-Kenelly-Layer.**

It was now obvious that waves propagating non-perpendicularly to the atmospheric layers could be reflected back to earth. Would the same be true for waves hitting the layers perpendicularly? In 1924 several groups in England and in the USA started to use radio waves in order to study the structure of the atmosphere. In 1925 the existence of the Heaviside-Kenelly-Layer was proved experimentally by different groups in England and in the USA. The name **ionosphere** was introduced by R.A. Watson Watt around 1930.

It was found that the ionosphere consists of different layers and that ionospheric disturbances are highly correlated with the activity of the sun. The impact of the ionosphere on civil and military radio networks was one of the main reasons for the establishment of a **global network of ionosphere observation stations** from 1930 onwards in order to obtain ionosphere maps and predictions of ionospheric behaviour.

1.2 Satellite Systems

Until 1962 only ground-based ionosphere measurement techniques were used and therefore no information of the higher ionospheric layers and the topside of the ionosphere was available. In 1962 the first

satellite with a so-called topside-sounder was launched, giving now also information about the upper part of the ionosphere.

Other satellite systems transmitting radio signals became available in the sixties and seventies: geostationary satellites for telecommunication and e.g. the **U.S. American Navy Navigation Satellite System (NNSS or TRANSIT)** for military and civil navigation purposes. Different measurement techniques were developped to use the signals of such satellite systems in order to determine the amount and the variations in time and space of the total electron content of the ionosphere. (Leitinger et al., 1984) are using signals of the polar orbiting satellites of the NNSS to compute latitude profiles of the total electron content for specific times. The main problem of this method is the restriction to profiles in latitude due to the polar orbits of the satellites.

The **Global Positioning System (GPS)**, sometimes also called **NAVSTAR (NAVigation System using Time and Ranging)** is a satellite navigation system developed by the U.S. Departement of Defense (DoD) for real time navigation. The original goal was to achieve an accuracy of the geocentric position of 10 - 15 m in real time. A first test configuration of 7 satellites became available in 1983. At present (summer 1993) 23 satellites are available. The final configuration will be reached around 1994. It will consist of 24 satellites (including 3 active spares), distributed in 6 different orbit planes with an inclination of 55° with respect to the earth's equatorial plane a semi-major axis of about 26'500 km and a revolution period of about 12 hours. The GPS satellites are transmitting signals on two carrier frequencies: L_1 = 1575.42 MHz and L_2 = 1227.60 MHz.

In the former USSR, today in Russia, a similar satellite navigation system is under development: the **GLObal NAvigation Satellite System (GLONASS)** (Anodina and Prilepin, 1989). Today a test configuration of 10-12 satellites is available. The final configuration should be available in 1995 and will consist of 24 satellites (including 3 spares). The satellites are distributed in 3 orbital planes with 64.8° inclination with respect to the earth's equatorial plane. The semi-major axes of the satellites are about 25'500 km, the revolution period 11 hours 15 minutes.

Both satellite systems are primarily designed for real-time navigation. Apart from that GPS and GLONASS may also be used for high precision applications in geodesy and geophysics: reconstructing directly the carrier phase of the signals relative accuracies (errors in baseline components and lengths) of 10^{-8} to 10^{-9} are achievable today (Beutler et al., 1987a), (Blewitt et al., 1988).

Apart from the two systems mentioned, **civil satellite navigation systems** will become available (e.g. NAVSAT (Carnebianca et al., 1985)) within the next years, too, in order to become independent from military and political authorities in the USA or in Russia.

In the present study we will confine ourselves to the discussion of the **capabilities of the GPS for ionosphere modelling and mapping.** But it should be kept in mind that every satellite system transmitting signals on two or more frequencies might be used in the same way.

Because of the frequency dependence of ionospheric refraction (see section 3.2) the difference of the refraction between the L_1 and L_2 carriers may be measured and related to the electron content of the ionosphere. The determination of the electron content using GPS has obvious advantages compared to that using the NNSS:

- Satellite geometry:
  The GPS satellites are distributed in 6 different orbit planes (see section 2.1). This satellite distribution allows to compute electron density profiles in latitude **and** longitude.

- Satellite availability:
  The NNSS satellites are available (from one specific ground site) usually for 15 - 20 minutes every 2 hours ("satellite pass"), whereas for a given position and a given time of the day at least 4 GPS satellites are available.

1.3 Motivation

Satellite navigation systems will become more and more important in the near future. They will be used for different purposes in navigation, geophysics, and in geodesy. The orbit parameters broadcast by the satellite systems allow relative point accuracies of about 10^{-6} for geodetic networks. For high precision applications in geodesy (10^{-8}-10^{-9}) the **International GPS Geodynamics Service (IGS)** (Mueller and Beutler, 1992), (Beutler, 1992a), (Beutler, 1992b) was established.

The **Swiss astro-geodetic fundamental station in Zimmerwald** may be considered as an example for a station in a permanent civil GPS tracking network. The Astronomical Institute of the University of Berne (AIUB) and the Swiss Federal Office of Topography (L+T) are closely cooperating in order to establish and to improve this permanent tracking station. The station contributes to the determination of GPS orbit parameters within the IGS. It also serves as the reference for Swiss first order surveys.

Since June 1992 the station is equipped with a permanently operated GPS receiver (Trimble 4000SSE). The data are collected in a completely automated way, reformated and distributed to the **CODE processing center** (see below) and to the **IGS data center for Europe** at the Institute for Applied Geodesy (IfAG) in Frankfurt, Germany. At the AIUB programs for highly automated orbit determination using GPS code and phase observations have been developed since spring 1992. The AIUB, the L+T, the IfAG, and the french Institut Géographique National (IGN) operate the so-called **Center for Orbit Determination in Europe (CODE)** processing center for IGS.

The data of permanent GPS tracking stations may also be used to extract useful information about the regional/global behaviour of the ionosphere: ionosphere models may be used for geodetic purposes or to draw maps of the total electron content. These ionosphere programs use exactly the same data as the orbit determination programs and they are designed as batch programs (i.e. they do not need much user interaction), the information about the ionospheric behaviour is thus easily obtainable.

We see two principal applications for ionosphere models or maps:

- *Ionosphere Models for Geodesy*

For surveys made with single frequency receivers the main impact of the ionosphere consists of a scale factor in the network of up to 10 ppm (depending on the total electron content of the ionosphere). This scale factor may be eliminated or greatly reduced with a regional ionosphere model derived from observations of one or more dual frequency receiver(s) operated in the region of the geodetic network (Georgiadiou et al., 1988), (Wild et al., 1989). The practical importance of this method will depend on the future development of receiver costs: if dual frequency receivers become achievable even for small survey companies, the main influence of the ionosphere will be eliminated using the so-called "ionosphere-free" linear combination of the observation equations of the two carriers L_1 and L_2 (see section 2.3) and the use of ionosphere models for local or regional surveys will be more of theoretic interest.

Preprocessing of GPS observations (= checks for discontinuities or outliers in the phase observable) made under extreme ionospheric conditions may be very difficult, because the changes of the ionospheric refraction between two subsequent observation epochs may be of the order of a few centimeters up to a few decimeters (Beutler et al., 1988), i.e. they may be of the order of one wavelength of the GPS carrier and may be misinterpreted as discontinuities in the phase observations. This problem may be solved if not only the original carriers L_1 and L_2, but also linear combinations of L_1 and L_2 (especially the "ionosphere-free" linear combination L_3) are used in the preprocessing. A detailled discussion of such algorithms may be found in (Beutler et al., 1988). Ionosphere models give useful information about ionospheric conditions and therefore help to define appropriate values for preprocessing parameters (e.g. the maximum allowed change of ionospheric refraction per minute). For two cases ionosphere models are of vital interest:

- Preprocessing of single frequency data,

- Preprocessing observations made in the presence of large systematic changes of the ionospheric electron content between subse-

quent observation epochs (especially if the data rate of the receiver was low).

The accuracy obtained by GPS phase observations is much improved if the real-valued estimates of the phase ambiguities (see section 2.2) may be replaced by the corresponding correct integer number of cycles. This process is called ambiguity resolution. For longer baselines (> 20 km) and dual-frequency receivers without P-code (see section 2.1.1) this ambiguity resolution becomes more and more difficult or even impossible. The use of special linear combinations of the carriers L_1 and L_2 (especially the "wide-lane" linear combination, see chapter 2.3) may help to solve this problem (Beutler et al., 1988). The most important limiting factor is the systematic influence of the ionosphere on the "wide-lane" linear combination. Introducing an ionosphere model considerably helps the ambiguity resolution for longer baselines.

- *Ionosphere Models for Geophysics*

Whereas geodesists try to eliminate all systematic and stochastic influences of the ionosphere, geophysicists are interested exactly in these phenomena. During the work on the elimination of ionosphere biases in geodetic networks the idea came up to use GPS observations to monitor the total electron content (and its changes) in the ionosphere.

The data of permanent GPS tracking stations seemed to be suited to study the capabilities of GPS for ionospheric studies and ionosphere mapping:

- Permanent GPS tracking stations may be equipped with the necessary programs for the computation of the total electron content in the ionosphere.

- The data are available for 24 hours per day, i.e. the daily variations of the electron density in the ionosphere may be studied.

- The stations of the GPS tracking networks are well distributed over the earth (e.g. the IGS stations) and allow to study the variations of the ionosphere for different latitudes.

In this study we will present programs for the computation of the total electron content in the ionosphere and for stochastical modelling (measures for short period perturbations and correlation functions in time and space giving an idea of the distances where similar ionospheric conditions may be expected).

All these GPS-derived results (electron content, correlation functions etc.) are compared to the results of other geophysical measurement techniques (see section 3.3) and to other relevant geopysical parameters (like number of sunspots, solar flares, disturbances in the geomagnetic field etc.).

It is one goal of the present study to show that GPS observations from permanent tracking stations may be used as an independent source of information for the investigation of the ionosphere.

2. GPS AS A TOOL FOR IONOSPHERE MODELLING

2.1 The Segments of the GPS

The GPS consists of three different segments, the space segment, the control segment, and the user segment, each of which will briefly be discussed below.

2.1.1 The Space Segment

The **full constellation of the GPS** (which will be available in 1994) will consist of **21 operational and 3 active spare satellites.** They will be distributed in **6 orbital planes** with **inclinations of 55°** with respect to the earth's equator each. The difference in right ascension of the ascending nodes between two neighbouring planes is 60°. The satellite orbits are almost circular with a **height** of about **20'000 km above the earth's surface** and with a **period of 12 sidereal hours.** A specific satellite constellation is therefore repeated every sidereal day (from day to day a shift of 4 minutes in Universal Time occurs due to the difference between the solar and the sidereal day).

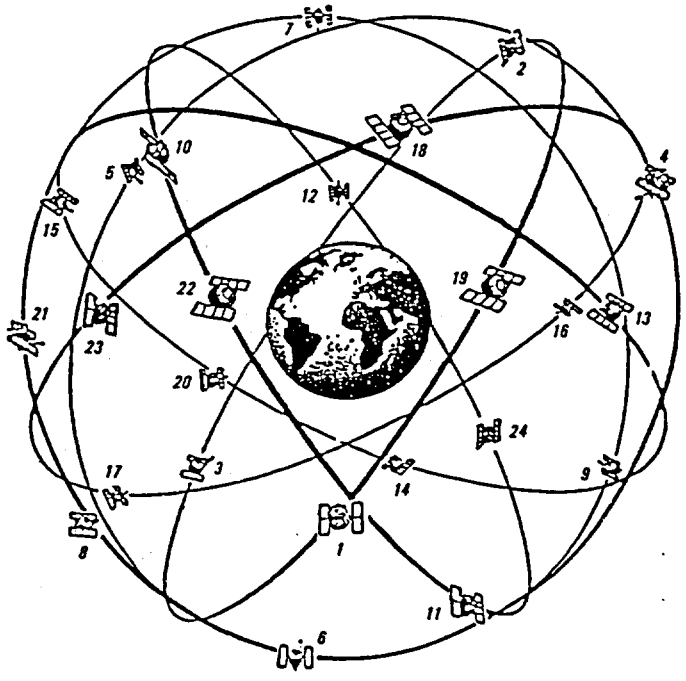

Figure 2-1
GPS Satellite Constellation

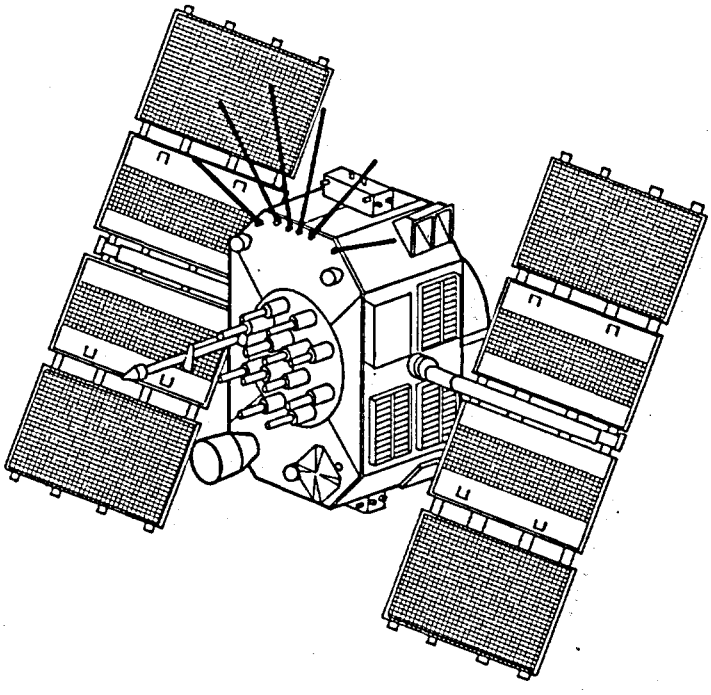

Figure 2-2
GPS Satellite

Figure 2-2 shows a GPS satellite (schematic). The weight is about 500 kg for Block I satellites, about 880 kg for Block II satellites, and 975 kg for Block IIA satellites. The satellites are equipped with an engine for orbit manoeuvres and gyroscopes for the satellite stabilization. The power supply is guaranteed by two solar panels. The oscillators in the GPS satellites have a stability of about 10^{-12} to 10^{-13}. This stability is needed for time transfer and precise range measurements.

The GPS satellites transmit signals on **two different frequencies:**

L_1 = 1575.42 MHz
L_2 = 1227.60 MHz

The two carriers (L_1 and L_2) are **frequency-modulated:** the transmitted information consists of the **navigation signals (codes)** as well as the **navigation- and system data.** The ensemble of navigation data is also called **broadcast message.** Each message contains the Keplerian elements (plus some of the time derivatives) for each satellite orbit and satellite clock information. The codes are rea-

lized through so-called Pseudo Random Noise (PRN) - sequences (Spilker, 1978). The P-code (precise code) is available on both carriers (L_1 and L_2) whereas the C/A-code (clear acquisition code) is only available on the L_1 carrier.

2.1.2. The Control Segment

The GPS control segment consists of one **master control station (Colorado Springs, USA)** and several **monitor stations** and **ground antennas** distributed over the world (Figure 2-3).

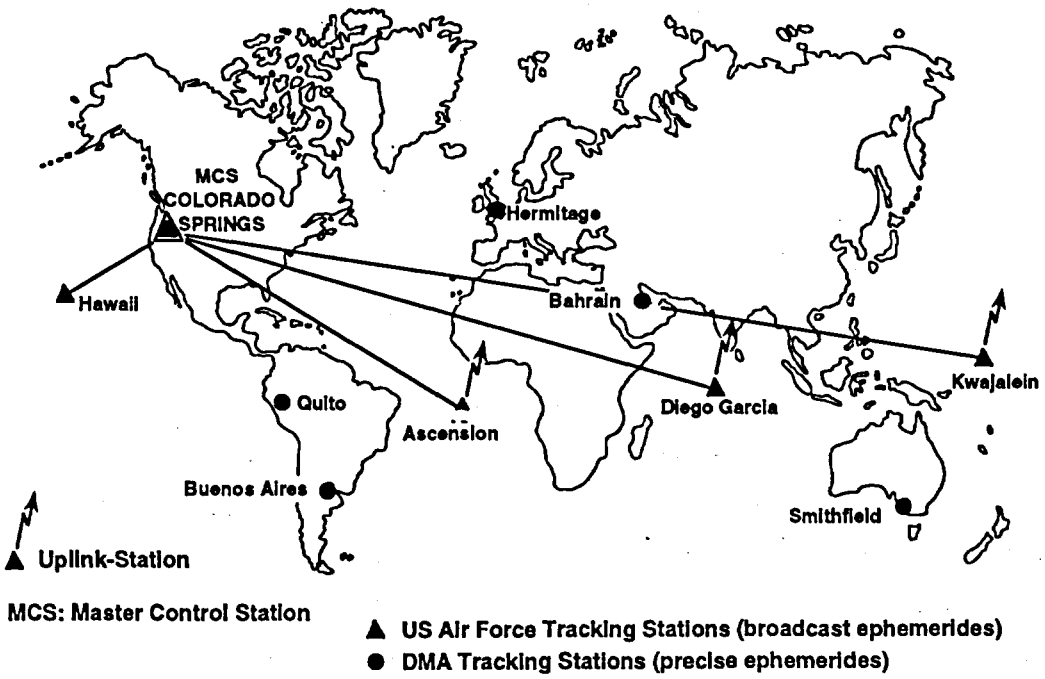

Figure 2-3
GPS Control Segment

The main tasks of the control segment are:

- Control of the satellite system,
- determination of GPS system time,
- determination and control of the satellite clocks,
- computation of operational satellite orbits (using the observations of the monitor and ground stations), and
- transfer of the computed orbital elements and satellite clock information to the GPS satellites.

The GPS system time is directly related to the time standard of the U.S. Naval Observatory. For all stations of the control segment clock corrections are computed.

2.1.3. The User Segment

The user segment consists of GPS receivers. A broad variety of receiver types are available today.

The GPS offers two different classes of positioning accuracies:

- Precise Positioning Service (PPS)
- Standard Positioning Service (SPS)

The PPS allows a real-time positioning **accuracy of 10 - 15 m** in geocentric coordinates using the P-code. The PPS may be restricted in future to U.S. military GPS users (see below). The SPS may be accessed by all users. The mean error of a point determined in the **SPS** mode (C/A - code) is of the order of **10 m if Selective Availability (S/A) is not active,** of the order of **200 m if S/A is on** (see below).

The US Department of Defence (DoD) has two options to degrade the accuracy of the GPS:

(1) The P-code may be inaccessible to the general user because of the **"Anti-Spoofing" - technique (A-S)**, which essentially consists in an encryption of the P-code. The encrypted code is called Y-code.

(2) The technique of the **"Selective Availability" (S/A)** degrades the accuracy of the C/A - code by superposing a random-walk to the satellite clock oscillator (= clock dithering). In addition the broadcast messages may be deteriorated.

The degradation of the accuracy of the GPS primarily affects the real-time GPS users (e.g. navigation applications). The influence of A-S and S/A on geodetic applications has been investigated in detail: it seems that most of the problems (like e.g. bad orbit

quality due to S/A) may be overcome by using appropriate observation and computation strategies (like orbit improvement techniques, simultaneous observations to eliminate short-term variations of the satellite clocks etc.)

2.2 Observation Equations

The GPS signals may be used in two different observation modes:

- By comparing the observed satellite codes **(C/A or P-code)** to the receiver generated reference code the travel time of the signal between receiver and satellite (and therefore the range) may be directly measured. This range is biased by receiver and satellite clock errors and is therefore called **pseudorange.** The observation noise for P-code is 0.5-5 m, for C/A-code 3-10 m depending on the antenna used.

- The difference of the incoming **carrier phase** and the receiver generated reference phase may be measured with a resolution of a few millimeters. The low measurement noise of the phase observation makes it the main observable for geodetic applications.

For our purpose it is sufficient to use the following simplified observation equations for the basic "Satellite S^i-Receiver R_k" combination (Beutler et al., 1989) at time t_m:

$$\text{Code:} \quad C^i_{k;m} = d^i_{k;m} + c\cdot\tau^i_m - c\cdot\tau_{k;m} \tag{2-1}$$

$$\text{Phase:} \quad \Phi^i_{k;m} = d^i_{k;m} + c\cdot\tau^i_m - c\cdot\tau_{k;m} + N^i_k\cdot\lambda \tag{2-2}$$

where: Φ: Phase observation (in meters)
C: Code observation (in meters)
d: Distance between satellite S^i (at time $t_m - d_{k;m}/c$) and receiver R_k (at time t_m) including the terms for tropospheric and ionospheric refraction
c: Speed of light in vacuum
t_m: Observation time in GPS system time

τ^i_m: Satellite clock error (with respect to GPS system time)

$\tau_{k;m}$: Receiver clock error (with respect to GPS system time)

λ: Wavelength

N^i_k: Initial phase ambiguity of a satellite - receiver combination

The difference between eqn. (2-1) and eqn. (2-2) is obvious: phase observations are biased by an integer number of cycles, the so-called **initial phase ambiguity**. The resolution of the phase ambiguities to integer numbers may be crucial for the use of GPS in small networks.

For ionosphere modelling in principle both observation types may be used. Phase observations have the advantage of the lower observation noise, but for each satellite (and for each discontinuity detected in the data) at least one parameter has to be introduced. This may weaken the estimated ionosphere parameters. The use of code observations for ionospheric modelling has become possible with the modern dual-frequency P-code receivers. However the noise level of these receivers still seems to be too high for the determination of the total electron content in the ionosphere. In the following we will only use GPS phase observations.

In order to reduce or eliminate systematic effects (such as receiver- or satellite-clock errors, ionospheric or tropospheric biases etc.) **several types of differences** may be formed:

Forming for each observation epoch t_m the differences between the two observation equations for receivers R_k and R_ℓ refering to the same satellite S^i we obtain the **single-difference** observation equation:

$$\Delta\Phi^i_{k\ell;m} = \Delta d^i_{k\ell;m} - c\cdot\Delta\tau_{k\ell;m} + N^i_{k\ell}\cdot\lambda \qquad (2\text{-}3)$$

with $\Delta\Phi^i_{k\,\ell\,;\,m} = \Phi^i_{k\,;\,m} - \Phi^i_{\ell\,;\,m}$

$\Delta d^i_{k\,\ell\,;\,m} = d^i_{k\,;\,m} - d^i_{\ell\,;\,m}$

$\Delta\tau_{k\,\ell\,;\,m} = \tau_{k\,;\,m} - \tau_{\ell\,;\,m}$

$N^i_{k\,\ell} = N^i_k - N^i_\ell$

We assume that the satellite clock term cancels out, which in turn means that (under S/A with typical frequency changes of about 1 Hz) the receivers k and ℓ have to be synchronized against each other within about 1 msec. The systematic effects of orbit errors, ionospheric and tropospheric refraction are considerably reduced by forming single differences.

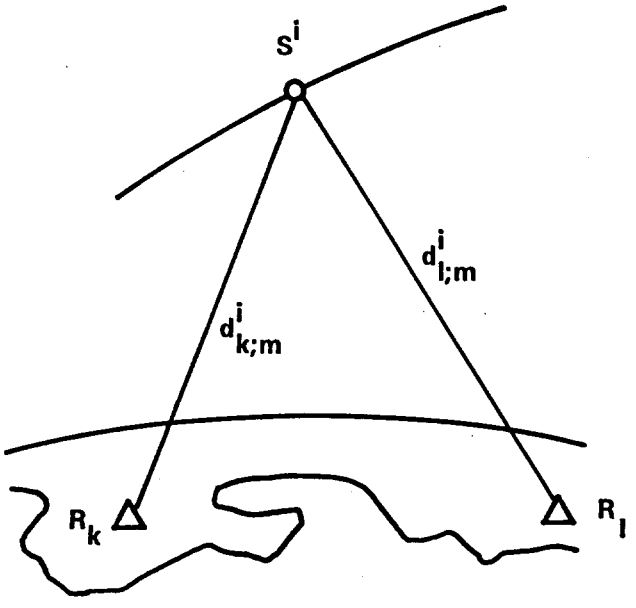

Figure 2-4
Single-difference Observable

In a next step the difference of two single-difference equations may be formed, i.e. the differences between the observations of two receivers and two satellites are formed (see Figure 2-5). The **double-difference** observation equation may be written as:

$$\nabla\Delta\Phi^{i\,j}_{k\,\ell\,;\,m} = \nabla\Delta d^{i\,j}_{k\,\ell\,;\,m} + N^{i\,j}_{k\,\ell}\,\lambda \qquad (2\text{-}4)$$

with $\nabla\Delta\Phi^{i\,j}_{k\,\ell\,;\,m} = \Delta\Phi^{i}_{k\,\ell\,;\,m} - \Delta\Phi^{j}_{k\,\ell\,;\,m}$

$\nabla\Delta d^{i\,j}_{k\,\ell\,;\,m} = \Delta d^{i}_{k\,\ell\,;\,m} - \Delta d^{j}_{k\,\ell\,;\,m}$

$N^{i\,j}_{k\,\ell} = N^{i}_{k\,\ell} - N^{j}_{k\,\ell}$

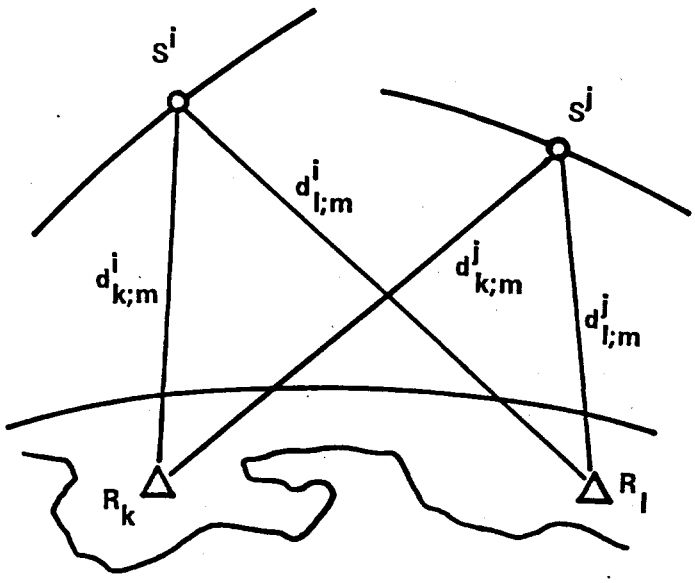

Figure 2-5
Double-difference Observable

By forming double differences the relative influence $\Delta\tau_{k\,\ell\,;\,m}$ of the receiver clocks cancels out. However the receiver clocks have to be synchronized at the 1 μs level to GPS time in order to be able to compute accurately enough the satellite positions contained in $\nabla\Delta d^{i\,j}_{k\,\ell\,;\,m}$.

By forming the difference between the double-difference observations of two subsequent observation epochs the so called **triple-difference** observable results. In the triple-differences the integer phase ambiguity cancels out.

When forming differences mathematical correlations between the differenced observations have to be taken into account in the adjust-

ferenced observations have to be taken into account in the adjustment process. There are other approaches for the evaluation of GPS data, see e.g. (Landau, 1989): for each difference a new clock parameter is introduced into the adjustment process, i.e. systematic effects are not eliminated by forming differences but they are modelled. This is mathematically equivalent to forming differences.

2.3 Linear Combinations

Table 2-1 (from (Beutler et al., 1989)) gives an overview over linear combinations of the original carrier (or code) observations which are frequently used in practice. We assume that all observations (L_1, L_2 and linear combinations) are expressed in meters.

Ionosphere-free linear combination L_3:
By multiplying the L_1 observation with the factor $\nu_1^2/(\nu_1^2-\nu_2^2)$ and the L_2 observation with the factor $-\nu_2^2/(\nu_1^2-\nu_2^2)$ and then adding the two results, a linear combination is obtained which does no longer contain systematic biases due to the ionosphere. This L_3 linear combination also has its disadvantage: The noise is about three times higher than the noise of the original observations L_1 and L_2. This may cause problems especially for smaller networks (Bock et al., 1986): "if by forming single differences the effect of the ionosphere is eliminated to a large extent, then the L_3 linear combination will just increase the observation noise and will not help to eliminate systematic effects."

Geometry-free linear combination L_4:
In the linear combination L_4 (difference L_1 - L_2 (both expressed in meters)) all terms relating to the geometry (distances) and clocks cancel out. What remains may be interpreted as the difference between the ionospheric refraction in L_1 and L_2. In the case of phase observations the difference of the ambiguities in L_1 and L_2 is an additional unknown constant. The L_4 linear combination is used to estimate ionosphere parameters and will be discussed in detail in section 4.1

LC	λ	LC-Factors		Tropospheric/Orbit Biases		Ionospheric Biases		Observation Noise	
	[m]	$x_{\ell,1}$	$x_{\ell,2}$	[length]	[cycles]	[length]	[cycles]	[length]	[cycles]
L_1	c/ν_1 0.19	1	0	1	1	1	1	1	1
L_2	c/ν_2 0.24	0	1	1	$\frac{\nu_2}{\nu_1}$ 0.78	$\frac{\nu_1^2}{\nu_2^2}$ 1.6	$\frac{\nu_1}{\nu_2}$ 1.3	$\frac{\nu_1}{\nu_2}$ 1.3	1
L_3	0	$\frac{\nu_1^2}{\nu_1^2-\nu_2^2}$ 2.5	$\frac{-\nu_2^2}{\nu_1^2-\nu_2^2}$ -1.5	1	-	0	-	$\frac{\nu_1\sqrt{\nu_1^2+\nu_2^2}}{\nu_1^2-\nu_2^2}$ 3.1	-
L_4	∞	1	-1	0	-	$-\frac{\nu_1^2-\nu_2^2}{\nu_2^2}$ -0.6	-	$\sqrt{1+\frac{\nu_1^2}{\nu_2^2}}$ 1.6	-
L_5	$\frac{c}{\nu_1-\nu_2}$ 0.86	$\frac{\nu_1}{\nu_1-\nu_2}$ 4.5	$\frac{-\nu_2}{\nu_1-\nu_2}$ -3.5	1	$\frac{\nu_1-\nu_2}{\nu_1}$ 0.22	$-\frac{\nu_1}{\nu_2}$ -1.3	$\frac{\nu_2-\nu_1}{\nu_2}$ -0.28	$\frac{\nu_1}{\nu_1-\nu_2}\sqrt{2}$ 6.4	$\sqrt{2}$ 1.4
L_5'	$\frac{c}{\nu_1-2\nu_2}$ -0.34	$\frac{\nu_1}{\nu_1-2\nu_2}$ -1.8	$\frac{-2\nu_2}{\nu_1-2\nu_2}$ 2.8	1	$\frac{\nu_1-2\nu_2}{\nu_1}$ -0.56	$\frac{(\nu_2-2\nu_1)\nu_1}{(\nu_1-2\nu_2)\nu_2}$ 2.8	$\frac{\nu_2-2\nu_1}{\nu_2}$ -1.6	$\frac{\nu_1}{\nu_1-2\nu_2}\sqrt{5}$ -4.0	$\sqrt{5}$ 2.2

Table 2-1
Summary of Linear Combinations (LC) (Factors to be Applied to Observations ℓ_1 and ℓ_2) (given in meters)

"Wide-lane" linear combination L_5:

By multiplying the L_1 and L_2 observations by $\nu_1/(\nu_1-\nu_2)$ and $-\nu_2/(\nu_1-\nu_2)$ and then adding the two terms the wide-lane" linear combination (expressed in meters) with a formal wavelength of 86 cm results. This linear combination is mainly used for ambiguity resolution on longer baselines (> 50 km): the L_5 linear combination has an integer L_5 ambiguity (the difference between the ambiguities in L_1 and L_2). Because of the long wavelength the determination of the L_5 ambiguities is much easier and more reliable than the ambiguity resolution on the original carriers L_1 or L_2. The resolved L_5 ambiguities may then be used in subsequent steps for the ambiguity resolution in the original carriers L_1 and L_2.

3. THE IONOSPHERE

3.1 The Solar-Terrestrial System

In this chapter the basic facts concerning the ionosphere which give the background for the following discussions and developments are presented. For more information the reader is referred to (Rishbeth and Garriot, 1969), (Kertz, 1971), (Kelley, 1989), and (Gorney, 1990).

3.1.1 Introduction

The **ionosphere of the Earth** is strongly related to the **solar activity.** In order to understand the parameters influencing the ionosphere we briefly discuss the solar - terrestrial system. A polar view of the ecliptic plane is given in Figure 3-1 showing the propagation of solar X-rays, solar energetic particles, and the solar wind from the Sun to the vicinity of the Earth. The field lines of the **interplanetary magnetic field** form the so-called Archimedean spiral. This pattern is due to the rotation of the sun and the outward velocity of the solar wind.

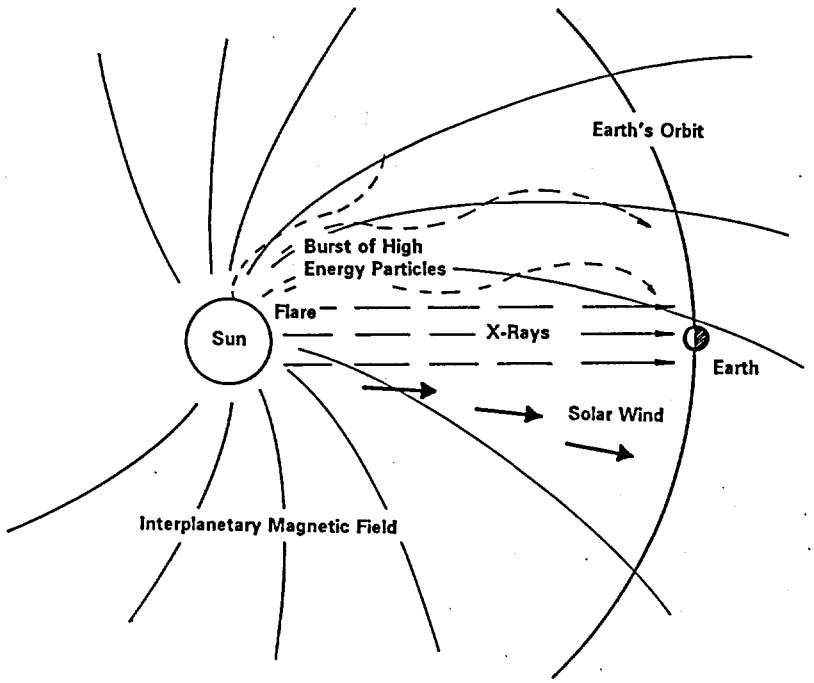

Figure 3-1
Polar View of the Ecliptic Plane

Figure 3-2 shows the environment of the Earth in more detail. The configuration of the geomagnetic field within the interplanetary magnetosphere is shown. The **Earth's magnetosphere** extends over several earth radii.

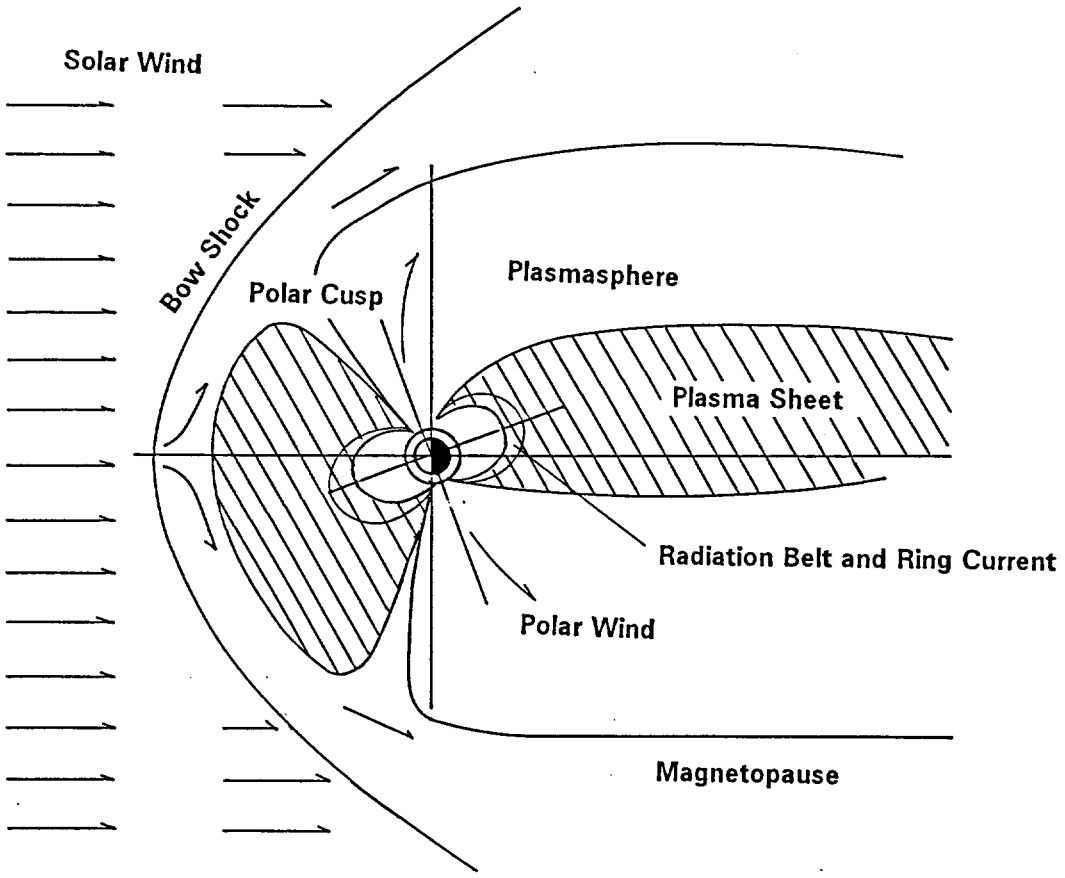

Figure 3-2
Earth's Magnetosphere

The most reliable measure for the activity of the sun is the **relative sunspot number R:**

$$R = 10 \cdot g + f \qquad (3\text{-}1)$$

where: R: Relative sunspot number
g: Number of sunspot groups
f: Number of sunspots

The sunspot number as a function of time shows a period of 11 years (see Figure 3-3).

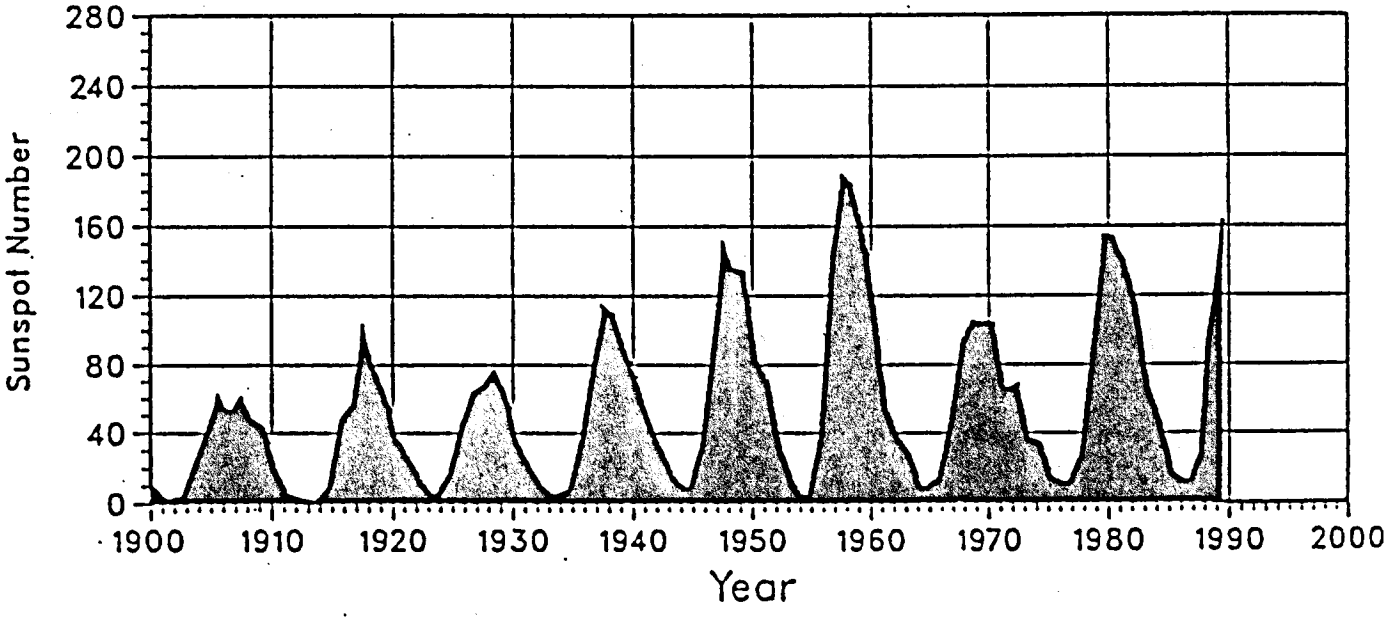

Figure 3-3
Sunspot Numbers from 1900 - 1989

Two different types of solar radiation influence the space around the Earth:

(1) ***Wave radiation:***
Two types of wave radiation are important for the ionosphere: the **UV radiation,** which causes the ionization of the gases in the upper atmosphere (see section 3.1.3) and **radiation with radio wavelengths (from cm to m).** The intensity of this radio radiation is a good measure for the activity of the sun: for higher solar activity the radio radiation is greatly enhanced. The radio radiation at a wavelength of 10.7 cm is observed by different observatories distributed around the globe. One of these observatories is the Algonquin Radio Observatory (ARO) of the National Research Council of Canada. The local-noon values of the solar flux at 10.7 cm at this observatory are published in the Solar-Geophysical Data Prompt Reports of the National Ocean and Atmosphere Administration (NOAA).

(2) Corpuscular radiation (particles, solar wind):
The occurrence of high-energetic (10 MeV to 1 GeV) **solar particle events** is one of the most direct influences of solar activity on the Earth's space environment. The reason for such particle events are **solar flares** in the solar corona. The time development of a typical solar particle event is shown in Figure 3-4.

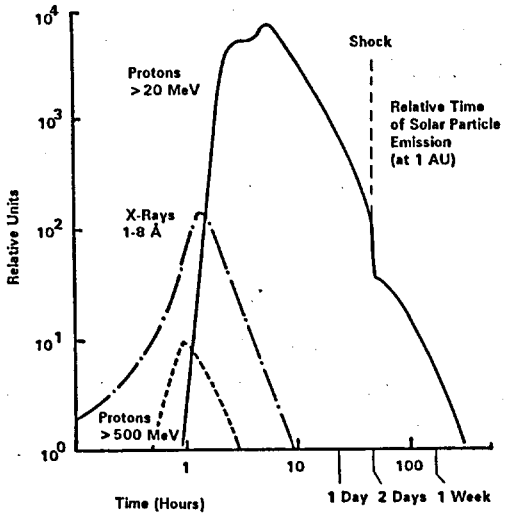

Figure 3-4
Time Evolution of a Solar Particle Event

Protons of relativistic energies arrive at the Earth within seconds or minutes after the electromagnetic radiation of the solar particle event. The high-energy particles propagate along the field lines of the interplanetary magnetic field and arrive with the corresponding time-of-flight delays. The number of particles decreases after the event over a time span of several days to the original background value. The total amount of particles and the time development of the event depends on the location of the solar flare relative to the footprint of the magnetic field line actually connected to Earth.

Solar particle events do not occur very frequently (only a few events per year). The frequency of occurrence tends to be maximal around the sunspot maximum. During the years surrounding the sunspot minimum the frequency of occurrence of particle events tends to be minimal.

3.1.2. Geomagnetic Activity

The **geomagnetic field** extends to a region of several earth radii around the earth. This region is also called **magnetosphere** (see Figure 3-2).

The **geomagnetic field** may be approximated by a simple (best fitting) earth-centered **dipole**. The **dipole axis** is given by the **geomagnetic poles** (Gm.P.), which have the (geographical) coordinates 78.3°N/69°W (north pole) and 78.3°S/111°E (south pole). Dip coordinates are used in geophysics to describe the actual geomagnetic field, i.e. at the dip poles (D.P.) the field lines are vertical and at the dip equator they are horizontal with respect to the Earth's surface (see Figure 3-5).

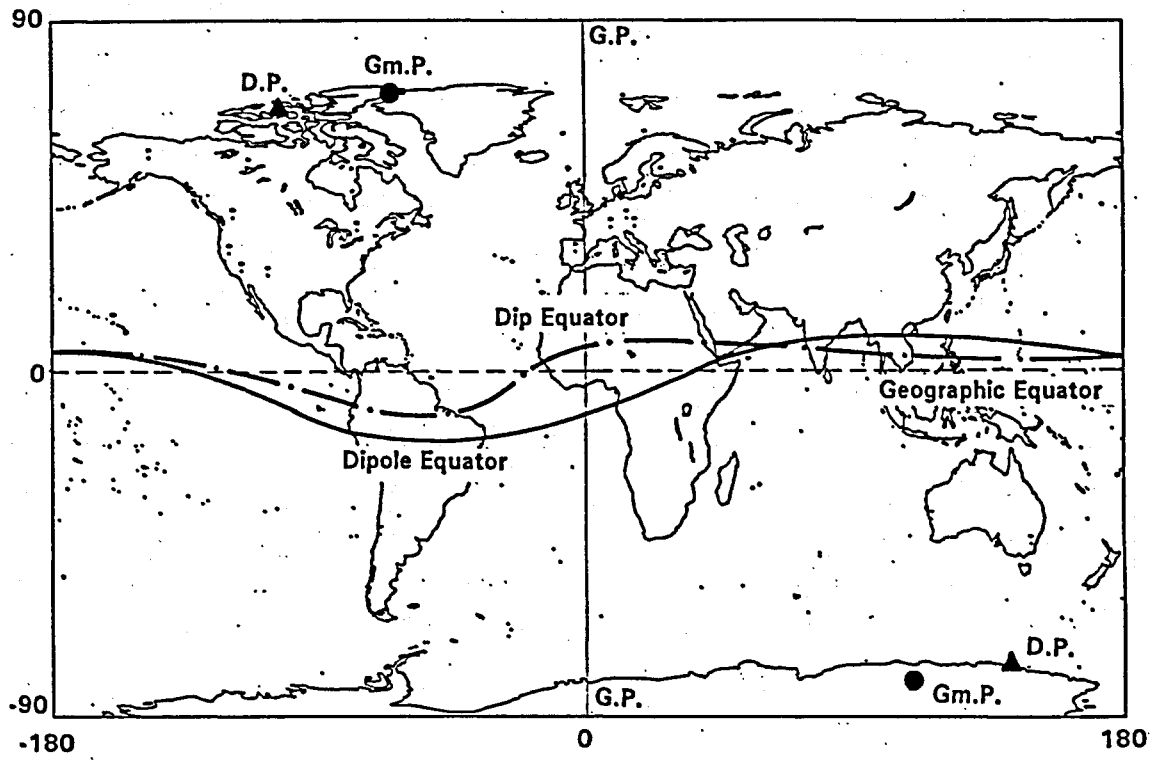

Figure 3-5
The Geomagnetic Field:
Dip Poles (D.P.) and Geomagnetic Poles (Gm.P.)
and Corresponding Equators

The strength of the geomagnetic field is measured at different observation stations around the world. The recorded components or elements are (Risbeth and Garriot, 1969) either

- north component X, east component Y, and down component Z

or

- eastern declination D = arctan(Y/X), horizontal intensity

$H = \sqrt{x^2+y^2}$ and vertical intensity $V = |Z|$

Different units are used for the measurement of the geomagnetic field:

$$1 \text{ gamma} = 10^{-5} \text{ Gauss} = 1 \text{ Nanotesla} \qquad (3\text{-}2)$$

The **geomagnetic elements (X,Y,Z)** undergo a **daily variation** about their mean values. In addition the geomagnetic field is frequently disturbed. If the field is severely disturbed, the disturbance is called a **geomagnetic storm.** There are different patterns for geomagnetic storms: the SSC (Sudden Storm Commencement) followed by a magnetic storm and the SI (Sudden Impulse) without a subsequent storm.

In a typical geomagnetic storm the SSC is followed by an increase of all geomagnetic field components for a few hours. This increase is probably due to the compression of the geomagnetic field by the solar plasma. After a few hours the main phase of the storm starts and the geomagnetic field decreases for approximately one day. Within one or two days the storm enters into its recovery phase and the magnetic field returns to normal.

Various empirical indices have been defined in order to describe the behaviour of the geomagnetic field. The most important index is the so-called **K_p-index** (p stands for planetary). This index is computed in the following way: at all observation stations for each three-hour period of a day (UT) the range of the variation of each of the Cartesian field components X,Y,Z is observed. The greatest of these ranges is called the amplitude (in gammas). The amplitudes of 12 representative (well distributed) stations are combined to obtain a "planetary" value for every three-hours period.

The index K_p runs from 0 to 9 and is related to the amplitude by a quasi-logarithmic scale which is chosen individually for each station according to its activity. The qualification for $K_p = 9$ is typically a disturbance of 300 gammas for a low-latitude station, 500 gammas for a mid-latitude, and 2000 gammas for an auroral zone station. The K_p-indices from the 12 stations are combined to obtain the K_p-index, which is determined to an accuracy of one-third of a unit, running as: 0_0, 0_+, 1_-, 1_0, 1_+, 2_-, 2_0 etc.

The geomagnetic activity shows a clear correlation with the 11-year sunspot cycle: there is a major peak of geomagnetic activity during the declining phase of the solar cycle and a secondary peak occuring close to the sunspot maximum.

3.1.3. Morphology of the Ionosphere

Table 3-1 gives an overview over the structure of the atmosphere:

Name	Height above Surface (km)	Electron Density (cm^{-3}) Night	Day
Troposphere	0 - 10	---	---
Stratosphere	10 - 50	---	---
Mesosphere	50 - 80	10^3	10^3
Thermosphere	80 - 500	10^5	10^6
Exosphere	> 500	10^4	10^5

Table 3-1
Nomenclature of the Atmosphere

The part of the atmosphere **above 50 km** is called **the upper atmosphere.** The main gases in this region are nitrogen (N_2), atomic (O) and molecular (O_2) oxygen. This part (up to about 1000 km) is also called **the ionosphere** because of the presence of **ionized gas** and **free electrons.**

The most frequent **ionization processes** are:

$$N_2 + h\nu \rightarrow N_2^+ + e^- \qquad \lambda < 796\ Å \qquad (3\text{-}3)$$

$$O + h\nu \rightarrow O^+ + e^- \qquad \lambda < 911\ Å \qquad (3\text{-}4)$$

$$O_2 + h\nu \rightarrow O_2^+ + e^- \qquad \lambda < 1027\ Å \qquad (3\text{-}5)$$

with h : Planck's constant
e^- : Electron
λ : Maximum wave length for the ionisation
ν : Frequency of the incoming radiation

Due to the absorption of different wavelengths of the solar radiation in different heights the distribution of the ions and the free electrons is not homogeneous. Figure 3-6 gives an overview over the distribution of the different ions in the upper atmosphere (daily mean values).

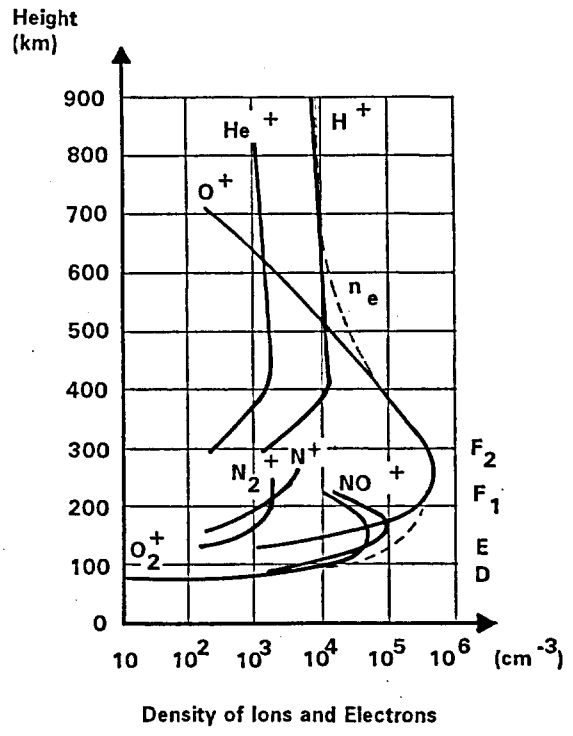

Figure 3-6
Ion and Electron Concentration in the Upper Atmosphere as a Function of the Height

Ionization is produced by a wide spectrum of solar X-ray and extreme ultraviolet (EUV) radiation. Apart from the ionization by so-

lar photon radiation free electrons may also be produced by corpuscular radiation (but to a much lesser extent). The production rate depends on the energy and the direction of motion of the incoming particles. The production, which varies with latitude, is present by day and by night. The solar cycle variation is opposite to the corresponding variation of solar photon radiation because the flux of galactic cosmic rays reaching the Earth is smaller at sunspot maximum than at minimum (due to the shielding effect of the enhanced interplanetary magnetic field).

The absorption of solar radiation of different wavelengths in different heights and the different types of ionization lead to a **layer structure** of the ionosphere. Figure 3-7 shows the distribution of the ionospheric layers on the day and the night side of the Earth.

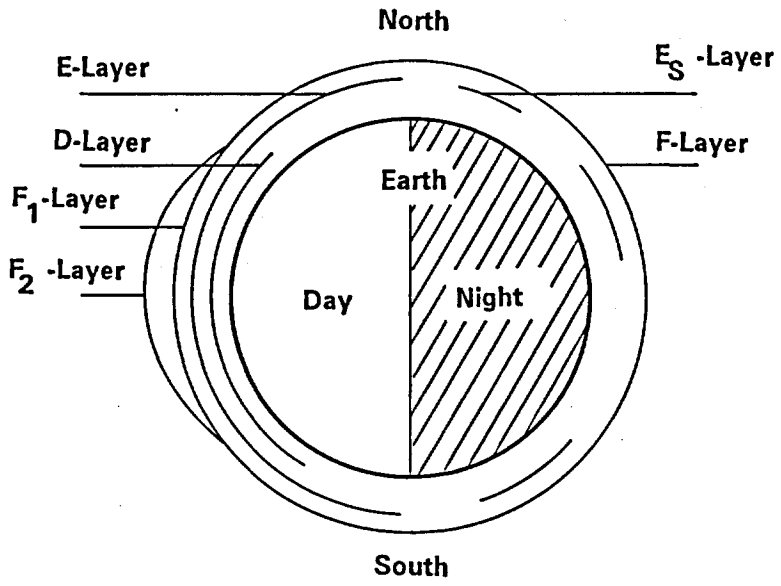

Figure 3-7
Ionospheric Layers (Schematic)

Table 3-2 gives an overview over the main characteristics of the different layers.

	D	E	F_1	F_2
Height (in km)	60 -85	85 - 140	140 - 200	200 - 1000
Electron Density (cm^{-3})				
Day	10^2-10^4	10^5	3×10^5	5×10^5
Night	——	2×10^3	10^3	3×10^5
Density of Neutral Gas (cm^{-3})	10^{15}	2×10^{12}	10^{10}	10^6-10^{10}

Table 3-2
Main Characteristics of the Ionospheric Layers

The ionization in the **D-layer** is mainly solar controlled: the profiles of the electron concentration show a building up of the D-layer ionization from sunrise to noon. The D-layer shows one important anomaly: on certain days in winter the absorption of solar radiation is greatly enhanced and leads to an extra ionization in the D-layer. This phenomenon is known as "winter anomaly" and is absent in low latitudes, but it is found in southern mid-latitude regions.

The normal **E-layer** is produced by ionizing solar radiation, too. The height of the peak production for overhead sun is found to be about 108 km. There are some latitudinal variations in the E-layer ionization which might be caused by transport effects due to the currents of the geomagnetic field flowing in the E-region. After sunset the ionization decreases to its nighttime value of about 5×10^3 cm^{-3}, which can probably be maintained by the extreme ultraviolet radiations of the night sky. During geomagnetic disturbances a pronounced night E-layer may be observed especially in auroral latitudes. In addition to the regular E-layer sometimes one or more irregular layers are observed in heights of 100 to 120 km. These layers are called "sporadic E" (E_S).

On the day side of the earth the **F-layer** is splitted up into an F_1- and an F_2-layer:
whereas the F_1-layer shows a more or less solar-controlled and regular behaviour, the behaviour of the F_2-layer is usually very irregular. More than other layers the F_2-layer is subject to day-to-day variations of about 20 %, and may even change appreciably from one hour to the next.

On a global scale there exists an annual variation of the electron concentration in the F_2-layer (about 20 % larger in December than in June). This may partially be explained by the 6 % variation of the solar flux, which has its maximum in January due to the variation of the distance between sun and earth. In addition there is a winter anomaly: the noon values for the electron concentration tend to be greater in winter than in summer. Furthermore the winter anomaly does not exist at solar cycle minimum.

At nighttime the electron concentration in the F_2-layer decreases irregularly. There is some sort of base level for the ionization in the layer of about 10^5 electrons/cm^3. How this "base level" is maintained is not clear yet. One possible source of ionization is corpuscular radiation of the night sky. Increases and decreases of the ionization may be observed in the hours before the F-layer sunrise. Some of these phenomena may be attributed to an influx of photoelectrons along geomagnetic field lines, when the conjugated point is illuminated by the sun.

The F_2-layer shows a special behaviour in the polar regions: although the changes of the solar zenith angle are neglectible at the geographic south pole, there are diurnal changes in the electron concentration which must be due to movement processes. These changes are correlated to Universal Time (UT). One possible explanation for this phenomenon is that the neutral air winds blow across polar regions from the day hemisphere towards the night hemisphere, producing vertical drifts in the F-region. During the polar winter the ionization in the polar F_2-layer is maintained although no direct solar radiation is present. The possible sources for the ionization are corpuscular radiation or transport effects between lower latitudes and polar regions produced by electric fields. Of great interest in this context was the discovery of a "trough" between the polar and the mid-latitude F-region.

The F_2-layer in the equatorial region shows a very irregular behaviour: sometimes the electron concentration at midnight is higher than at noon. These irregularities might be due to the fact that the free electrons are prohibited to move across the geomagnetic field lines, but may easely move along these lines and therefore

produce a high variability in latitude.

Figure 3-8 illustrates a second phenomenon of this region: the existence of an eastward electric field during the day in the equatorial region produces an upward plasma drift. The lifted plasma diffuses down the magnetic field lines and away from the equator. This phenomenon is also called the "equatorial fountain effect". The result is a "trough" of the noon values of electron concentration around the geomagnetic dip equator (± 15°-20° geographical latitude).

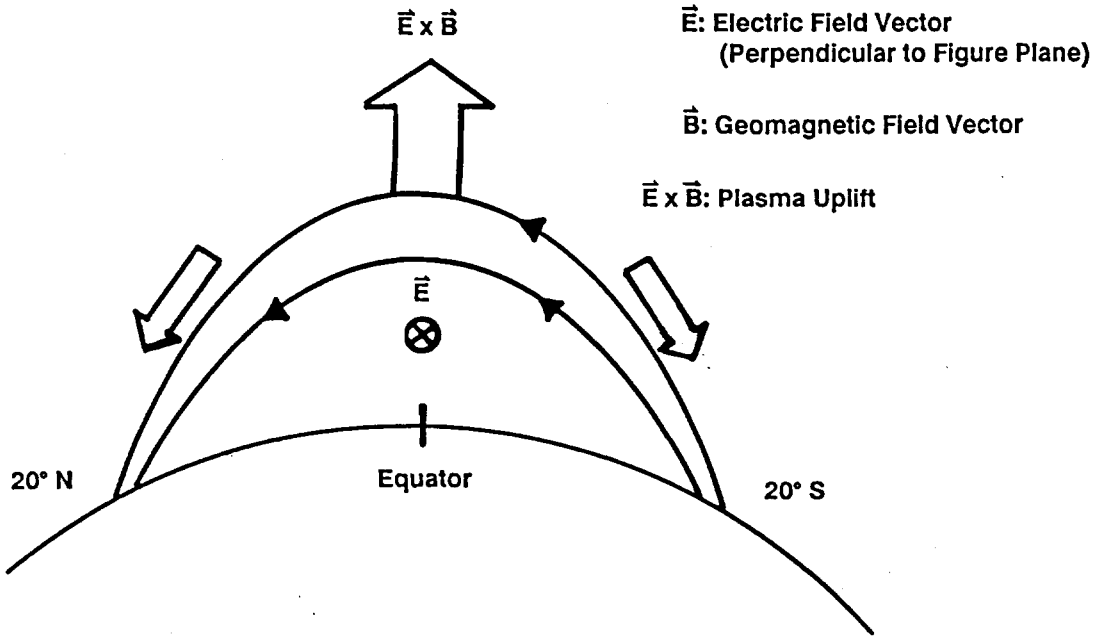

Figure 3-8
Equatorial Fountain Effect

The goal of this chapter was to point out that for all discussions concerning the behaviour of the ionosphere at least three different regions in geographical latitude have to be distinguished:

- the auroral region,
- the mid-latitude region, and
- the equatorial region.

Figure 3-9 shows these major geographic regions of the ionosphere.

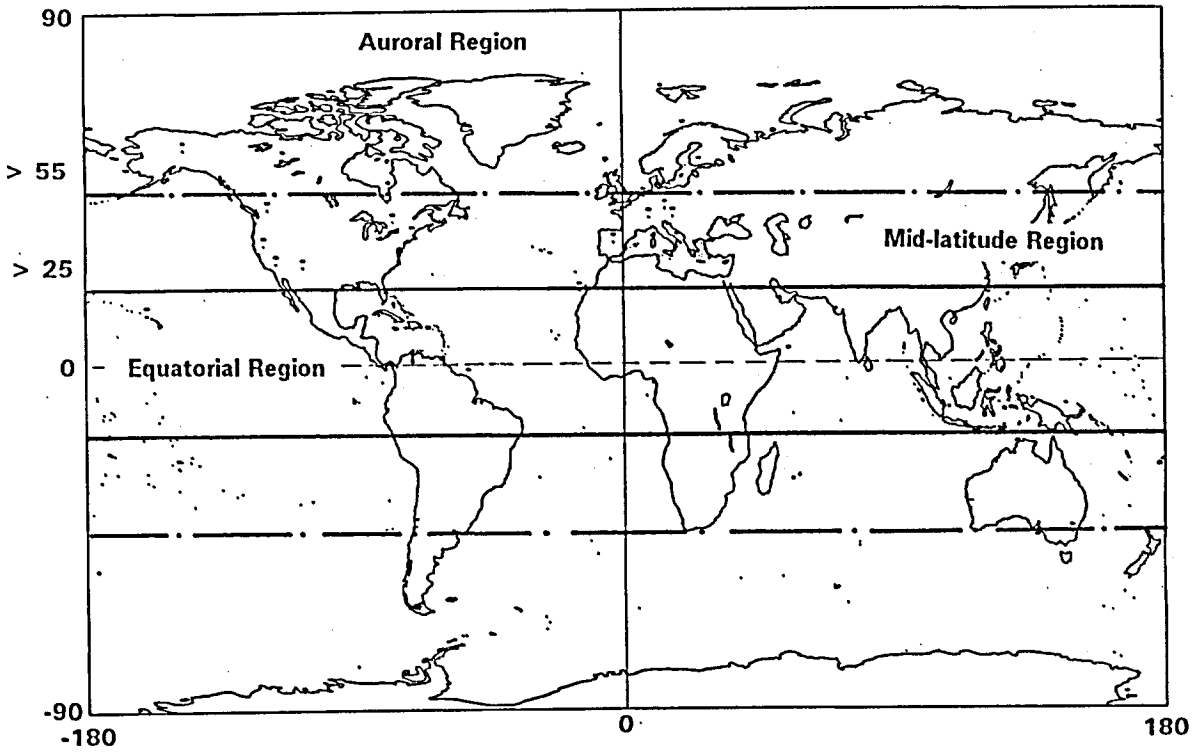

Figure 3-9
Major Geographic Regions of the Ionosphere

3.2 Propagation of Electromagnetic Waves Through the Ionosphere

The influence of the ionosphere on radio signals with frequencies > 100 MHz has been studied in detail by several authors, e.g. (Hartmann and Leitinger, 1984). We summarize the most relevant results.

The **refractive index n** describes the propagation of an electromagnetic wave in a specific medium. It is defined as:

$$n = c / v \qquad (3\text{-}6)$$

with c : speed of light (in the vacuum)
v : speed of the electromagnetic wave in the medium

For GPS observations one additional fact has to be taken into account: the signal carriers are propagating with the phase velocity v_p whereas the codes are propagating with the group velocity v_G. We therefore also have to distinguish between a phase refractive index

n_p and a group refractive index n_G.

Two different atmospheric regions have to be distinguished: the **lower atmosphere** (troposphere) with a refractive index $n_p > 1$ and the **upper atmosphere** (ionosphere, magnetosphere) with a refractive index $n_p < 1$. In the ionosphere the refractive index n is **frequency dependent.** Such a propagation medium is also called a **dispersive medium.**

The ionospheric refractive index n_p may be written as (Brunner and Gu, 1991):

$$n_p^2 = 1 - \frac{2X(1-X)}{2(1-X)-Y^2\sin^2\nu \pm \sqrt{Y^4\sin^4\nu+4Y^2\cos^2\nu(1-X)^2}} \qquad (3\text{-}7)$$

with $X = f_p/f$; $Y = f_H/f$

f_p : Plasma frequency; $f_p = \sqrt{\frac{e\,N_e}{4\pi^2\varepsilon_0 m_e}}$

f_H : Gyrofrequency; $f_H = \frac{\mu_0 e H_0}{2\pi m_e}$

f : Frequency of the electromagnetic wave
e : Electron charge
N_e : Electron density
ε_0 : Permittivity in vacuum
m_e : Electron mass
H_0 : Amplitude of the geomagnetic field
μ_0 : Permeability in vacuum
ν : Angle between geomagnetic field vector H and the propagation direction of the electromagnetic wave

The ionospheric refractive index n_p depends mainly on the density of free electrons, the direction of wave propagation with respect to the geomagnetic field, and the strength of the geomagnetic field.

Assuming transmission frequencies > 100 MHz (for GPS: 1575.42 and 1227.60 MHz) the following approximations may be made (see e.g. Hartman and Leitinger, 1984):

$$n_p^2 = 1 - \frac{f_p^2}{f^2 \pm f \cdot f_H \cdot |\cos\nu|} \qquad (3\text{-}8)$$

with
- f_p : Plasma frequency
- f_H : Gyrofrequency
- f : Frequency of the electromagnetic wave
- ν : Angle between geomagnetic field vector H and the propagation direction of the electromagnetic wave

The different signs (±) in eqn. (3-8) are due to the fact that the ionosphere is a birefringent medium, i.e. the electromagnetic wave is splitted up into two different propagation modes: a left-hand circular polarized mode (+ sign) and a right-hand mode (- sign). For f > 100 MHz it is allowed to neglect the term $f_H \cdot |\cos\nu|$, because f_H is always < 1.4 MHz (Hartmann and Leitinger, 1984) and because for most practical applications at the receiver location no information on the polarization of the electromagnetic waves is available anyway.

Therefore eqn. (3-8) may be rewritten neglecting terms of order f_p^4/f^4 as

$$n_p = 1 - \frac{1}{2}\frac{f_p^2}{f^2} \qquad (3\text{-}9)$$

and evaluating the expression for the plasma frequency f_p we obtain:

$$n_p = 1 - \frac{40.3}{f^2} N_e \qquad (3\text{-}10)$$

Taking into account the different refractive indices for phase and code GPS observations (see above) we may summarize:

$$n_p = 1 - \frac{40.3}{f^2} N_e \qquad (3\text{-}11)$$

$$n_G = 1 + \frac{40.3}{f^2} N_e \qquad (3\text{-}12)$$

with n_p : Refractive index for phase observations
n_G : Refractive index for code observations
N_e : Electron density
f : Signal frequency

The actual range s between receiver R and satellite S is given by the integral over the path from R to S:

$$s = \int_R^S n_p \, ds \qquad (3\text{-}13)$$

(with ds: infinitesimal line element). We therefore obtain the **ionospheric distance correction for GPS observations** (Spilker, 1978):

$$\Delta d_i^{ion} = \frac{\pm \, a \cdot TEC}{f_i^2} \quad ; \quad i=1,2 \qquad (3\text{-}14)$$

with Δd_i^{ion} : Ionospheric distance correction for frequency i
f_i : Frequency of the GPS carriers i = 1,2
TEC : Total Electron Content (Electrons/m^2)
\+ : Sign for code observations
\- : Sign for phase observations
a : Constant (a = 40.3 $s^{-2}m^3$)

3.3 Ionosphere Measurement Techniques

In this section a short overview over the ionospheric measurement techniques used today will be given. We will focus on measurement techniques using radio signals.

The total electron content of the ionosphere along a straight line between observer and satellite is measured in so-called Total Electron Content Units (TECU's), 1 TECU corresponding to 10^{16} electrons per m^2.

3.3.1 Ionosondes

Principle: a radio wave signal with a frequency f of 1-20 MHz is emitted into the ionosphere. Such a signal is reflected by the different layers of the ionosphere when its frequency f is equal to the **local plasma frequency** f_p (Kelley, 1989):

$$f_p = \frac{1}{2\pi} \sqrt{\frac{eN_e}{m_e \varepsilon_0}} \qquad (3\text{-}15)$$

with f_p : plasma frequency
N_e : electron density
e : electron charge
m_e : electron mass
ε_0 : permittivity in the vacuum

Eqn. (3-15) may be approximated by

$$f_p = 9000 \sqrt{N_e} \quad [Hz] \qquad (3\text{-}16)$$

The frequency which is no longer reflected by an ionospheric layer but penetrates it, is called the **critical frequency** f_0 for the specific layer (see Figure 3-10).

The ionosonde is varied from 1 - 20 MHz. For each emitted frequency the ionosonde measures the time of flight of the radio pulse and computes a so-alled "virtual" height h' of the reflecting layer. The plot of these virtual heights h' as a function of the emitted frequency is called ionogram. Figure 3-10 shows a schematic ionogram.

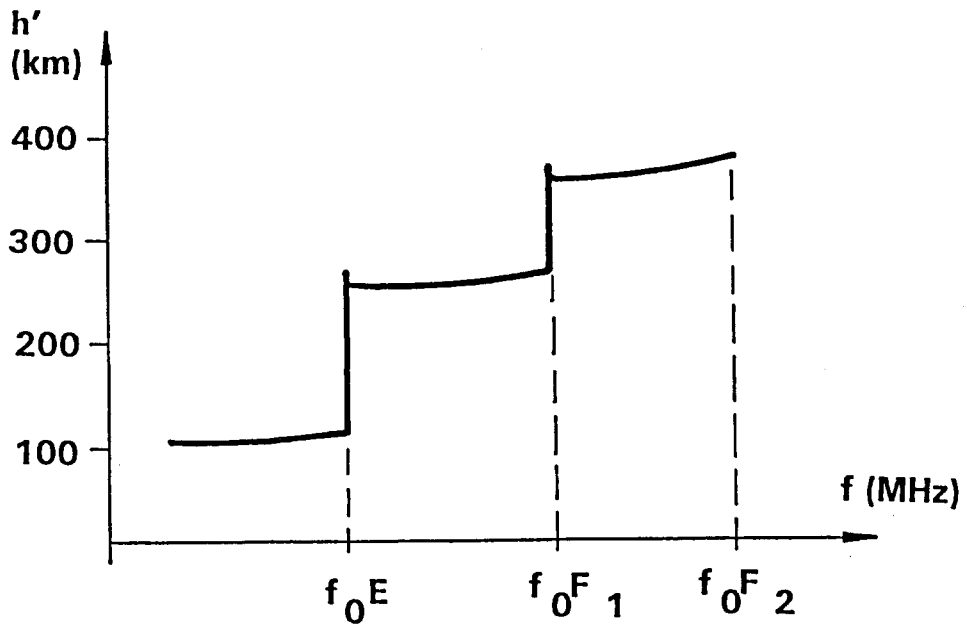

Figure 3-10
Ionogram (schematic)

The virtual height h' differs from the real geometrical height h of the reflection point due to the fact, that with increasing ionization the speed of the radio pulse is changed, too.

Ionosphere sondes operated at the earth surface do not give any information about the electron distribution above the peak of electron concentration of the F-layer. Therefore ionosondes are also used nowadays on board of satellites. This so-called top-side sounding gives useful information about the electron concentration above the F-layer.

3.3.2 Incoherent Scatter Radars

Since 1958 there exists a new method for the determination of the total electron content, called Thomson-Scatter-Sounding: Radio waves with a frequency much higher than the critical frequency of the F-layer are transmitted vertically trough the ionosphere. The electric field in the transmitted wave causes the free electrons in the ionosphere to oscillate. This oscillation creates a signal at almost the same frequency as the original wave (secondary radia-

tion). The power of this radiation is measured on the ground by a large antenna. The measured power is proportional to the number of free electrons in the ionosphere because each electron incoherently radiates back a small amount of the incident energy.

Table 3-3 gives an overview over the operational incoherent scatter radars around the world (Kelley, 1989).

Observatory	Frequency (MHz)	Lat.	Long.
Jicamarca (Peru)	49.9	12°S	76°W
Millstone Hill (USA)	440	43°N	72°W
Chatanika (Alaska)	1290	65°N	148°W
Arecibo (Puerto Rico)	430	18°N	67°W
St. Santin (France)	935	45°N	2°E
EISCAT (Tromso, Norway)	224/933	70°N	19°E
Sondre Stromfjord (Greenland)	1290	67°N	51°W
Altair (Kwajalein)	155.5	9°N	168°E
MU (Japan)	46.5	35°N	136°E

Table 3-3
Incoherent Scatter Radar

3.3.3 Geostationary Satellites

Another method to determine the total electron content is the **Faraday rotation** measurement technique using signals of geostationary satellites. In order to understand this method we briefly resume a few results of the magneto-ionic theory. A detailed discussion may be found e.g. in (Ratcliffe, 1970).

In the presence of a magnetic field the ionosphere is a doubly refracting medium. There exist **two modes of wave propagation**, an "ordinary" and an "extraordinary" one. The two modes are **circularly polarized in opposite senses** and a linearly polarized wave traversing the ionosphere may be regarded as the sum of the ordinary and the extraordinary component. The two components have **different phase velocities** and therefore the **plane of polarization** continually **rotates along the path of the wave (Faraday rotation)**. The total rotation of the polarization plane (in radians) is related to the electron concentration (Rishbeth and Garriot, 1969):

$$\Omega = \frac{2.36 \cdot 10^4}{f^2} \int_0^\infty \left(B \frac{\cos\nu}{\cos X} \right) N_e \, dh \qquad (3\text{-}17)$$

where Ω : total rotation of the polarization plane (in rad),
f : radio wave frequency,
B : local magnetic flux density,
ν : angle between radio wave normal and magnetic field direction,
X : angle between wave normal and the vertical, and
N_e : electron concentration.

If the total rotation of the polarization plane is measured the electron concentration may be computed using eqn. (3-17).

3.3.4 The Global Positioning System (GPS)

The use of the GPS satellite signals to measure the total electron content has been proposed by different authors, see e.g. (Royden et al., 1984).

There are two ways to use the GPS to measure the total electron content of the ionosphere:

(1) Use of dual-frequency data forming the L_4 linear combination (see section 2.3). In the case of code observations the total electron content is proportional to the difference of the ionospheric refraction on the two frequencies (see section 4.1). This method has been used e.g. by (Lanyi et al., 1987) for the calibration of the total electron content for the Deep Space Network (DSN). We use the same method for the computation of our single-layer models (see section 4.1).

If phase observations are used the method is biased by an unknown (real valued) differential ambiguity term. This ambiguity may either be estimated together with the ionosphere model parameters (Wild et al., 1989) or be calibrated using the P-code (Lanyi et al., 1987). In the latter case multipatheffects have to be considered (Bishop et al., 1985).

The formal accuracy of this method is quoted to be about 1 TECU (Lanyi et al., 1987) by comparing GPS derived total electron contents with Faraday rotation data. Our experiments indicate accuracies in the same order of magnitude (see section 5.2).

(2) (Smith, 1987) proposed a method for TEC determination using a single-band receiver. The basic concept of the method is:

a) Observe for two different observation epochs t_m and t_{m+1} the pseudoranges $C^i_{k;m}$ and $C^i_{k;m+1}$ (see eqn. 2-1):

$$C^i_{k;m} = d^{i\,\prime}_{k;m} + \Delta d_{ion;m} + c\cdot\tau^i_m - c\cdot\tau_{k;m} \qquad (3\text{-}18)$$

$$C^i_{k;m+1} = d^{i\,\prime}_{k;m+1} + \Delta d_{ion;m+1} + c\cdot\tau^i_{m+1} - c\cdot\tau_{k;m+1} \qquad (3\text{-}19)$$

with $d^{i\,\prime}_{k;m}$: geometrical distance (without ionospheric refraction term) receiver k-satellite i

$\Delta d_{ion;m}$: ionospheric refraction

τ^i_m : satellite clock bias

$\tau_{k;m}$: receiver clock error

and for the time interval $\Delta t = t_{m+1} - t_m$ the accumulated changes in phase (see eqn. 2-2):

$$\Delta\Phi^i_{k;\Delta t} = \Delta d^{i\,\prime}_{k;\Delta t} - (\Delta d_{ion;m+1} - \Delta d_{ion;m}) + c\cdot\Delta\tau^i_{\Delta t} - c\cdot\Delta\tau_{k;\Delta t} \qquad (3\text{-}20)$$

with
$$\Delta d^{i\,\prime}_{k;\Delta t} = d^{i\,\prime}_{k;m+1} - d^{i\,\prime}_{k;m}$$
$$\Delta\tau^i_{\Delta t} = \tau^i_{m+1} - \tau^i_m$$
$$\Delta\tau_{k;\Delta t} = \tau_{k;m+1} - \tau_{k;m}$$

b) Compute the difference of the ionospheric refraction $dion_{\Delta t}$ between the two observation epochs t_m and t_{m+1} using the observations $C^i_{k;m}$, $C^i_{k;m+1}$ and $\Delta\Phi^i_{k;\Delta t}$:

$$dion_{\Delta t} = \Delta d_{ion;m+1} - \Delta d_{ion;m}$$

$$= (C^i_{k;m+1} - C^i_{k;m} - \Delta\Phi^i_{k;\Delta t})/2 \qquad (3\text{-}21)$$

The accuracy is of course given by the accuracy of the code observations!

c) In a next step the differences $dion_{\Delta t}$ are integrated over 24 hours and fitted with a polynomial. The initial value of the electron content (value for 2:00 a.m.) is taken from a standard prediction like e.g. the Klobuchar model (see section 3.4), which is not a very satisfactory aspect of the method.

3.4 Ionosphere Models

We distinguish two types of ionosphere models, theoretical and empirical ones.

Theoretical models are based on physical laws or assumptions concerning the structure and the variations of the ionosphere. Theoretical models will not be discussed in this context here.

Empirical models are based on observations of the ionosphere. We have to distinguish between global, regional and local models. Empirical models exist (with a few exceptions, see e.g. Royden and Green, 1986) only as global models. Three models are well known and of practical interest:

- the Bent model
- Empirical model for single-frequency GPS users (Klobuchar model)
- the International Reference Ionosphere (IRI)

The **Bent model** (Bent and Llewellyn, 1973) is used to compute profiles of the electron content from 0 to 1000 km. Input parameters are the date, the time (in UT), the position of the observer, the solar flux and the sunspot number. In addition the orbit parameters and the transmitting frequencies of the satellite(s) may be specified. From the height profile of the electron content all relevant parameters for geodesy (like e.g. refraction corrections) may be obtained.

Based on the Bent model an **empirical model for single-frequency GPS users** has been developed by (Klobuchar, 1986). This model essentially consists of a cosine function plus a constant for day-time and a constant for night-time observations. Figure 3-11 shows the typical shape:

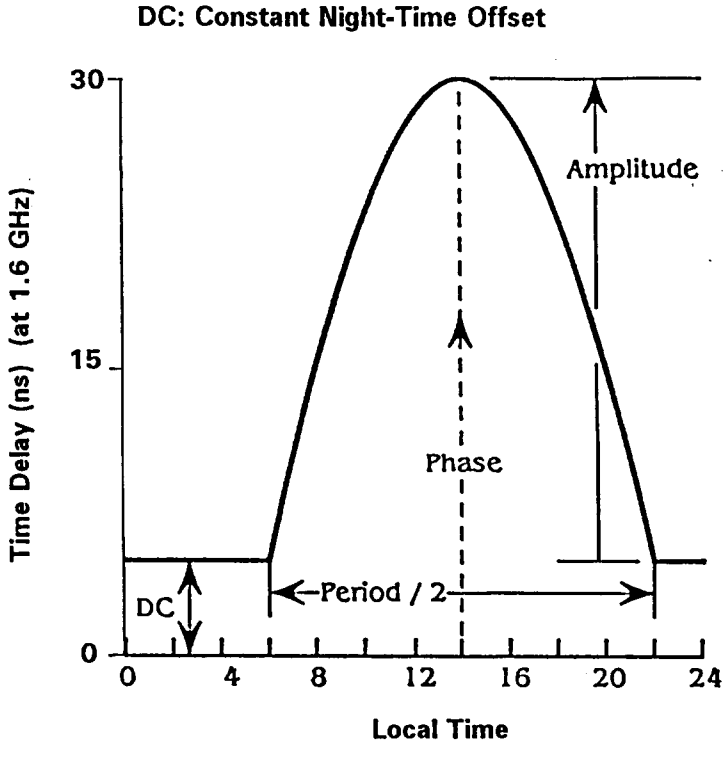

Figure 3-11
Klobuchar Model of the Ionosphere

The model parameters (amplitude A, period P) may be reconstructed using the ionosphere parameters α_i and β_i (i=0,1,2,3) given in the GPS broadcast message:

$$A = \sum_{i=0}^{3} \alpha_i \cdot \left(\phi_m\right)^i \qquad \text{(ns)} \qquad (3\text{-}22)$$

$$P = \sum_{i=0}^{3} \beta_i \cdot \left(\phi_m\right)^i \qquad \text{(seconds)} \qquad (3\text{-}23)$$

with A : Amplitude
P : Period
α_i, β_i : broadcast ionosphere coefficients
ϕ_m : geomagnetic latitude of sub-ionospheric point
The sub-ionospheric point is the projection of the ionospheric point (=intersection of the line of sight receiver-satellite and the ionosphere) to the surface of the earth

The maximum of the cosine function is set to 14:00 local time.

It is said that the Klobuchar model eliminates about 50 % of the systematic ionospheric effect on GPS satellite signals.

The third model of practical interest is the **International Reference Ionosphere (IRI)** (Rawer et al., 1981). The IRI model provides monthly median vertical profiles of electron and ion densities, electron and ion temperatures. The input parameters are the position of the observer, the sunspot number, date and time (in UT).

Several authors have tested the reliability of these empirical models comparing the electron contents predicted by the different models with actual observations:

- (McNamara, 1983) has tested the reliability of the IRI model with data from 15 different stations. For high and mid-latitudes the differences in the electron content between the measured and the model values were reasonably small, except during the night. For stations in lower latitudes he found significant discrepancies between the model and the measured values: the model values were too small and showed wrong daily variations.

- (Royden and Green, 1986) found that the Bent model predicts average ionization parameters in mid-latitudes with an error of about 20 to 30 % of the total effect provided that the sunspot number is < 130 .

- (Newby, 1992) compared (for different levels of solar activity) the predicted values for vertical electron contents from the IRI and the Bent models with Faraday rotation measurements. For all levels of solar activity the Bent model showed a better agreement with the Faraday data than the IRI model.

These results are not too surprising because the empirical models discussed above (Bent, IRI) are global models. In addition, the IRI model provides just monthly mean values of the electron content. The real conditions in the ionosphere may completely differ from the assumed model conditions: large regional gradients of the total electron content over short distances may be observed, which are not taken into account by global models.

The ionosphere models we are now going to develop are different: they are regional models based on actual GPS observations. Such models describe the ionospheric conditions for a certain time span and a certain region. These models are capable to take into account large regional gradients of the electron content.

4. MATHEMATICAL MODELS AND SOFTWARE DEVELOPMENTS

4.1 Deterministic Model

As we have seen in section 3.2 (eqn. 3-14) the ionospheric refraction correction for GPS observations may be written as:

$$\Delta d_i^{ion} = \frac{\pm\, a \cdot TEC}{f_i^2} \quad ; \quad i=1,2 \qquad (4\text{-}1)$$

with Δd_i^{ion} : ionospheric distance correction for frequency i
TEC : Total Electron Content (Electrons/m^2)
f_i : signal frequencies, i=1,2
\+ : sign for code observations
\- : sign for phase observations
a : constant (a = 40.3 [$s^{-2}m^3$])

Eqn. (4-1) shows that ionospheric refraction for GPS observations is determined by the number of free electrons along the signal path. Eqn. (4-1) is an approximation (only first order terms of the series development for the ionospheric refraction (Brunner et al., 1990) are taken into account). For our applications this approximation was found to be adequate.

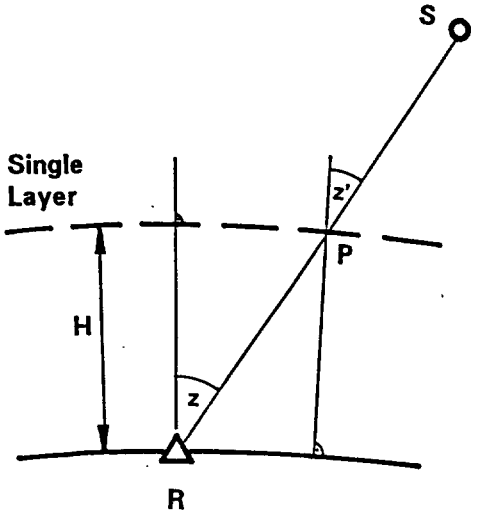

Figure 4-1
Single-layer Model of the Ionosphere

In order to model the electron content several authors have proposed the so-called **single-layer model (SLM)** of the ionosphere (see e.g. Georgiadiou and Kleusberg, 1988). The SLM is based on the assumption that all free electrons are concentrated in a spherical layer of infinitesimal thickness (single layer) at a height H above the earth surface (see Figure 4-1).

Eqn. (4-1) may then be rewritten as:

$$\Delta d_i^{ion} = \frac{\pm\ a \cdot TVEC}{f_i^2 \cdot \cos z'} \qquad (4\text{-}2)$$

where z': zenith distance at the intersection P of the actual signal with the single-layer ('ionospheric point')

TVEC : Surface density of the electrons in the single-layer at point P; TVEC is also called the total vertical electron content

The SLM reduces the complicate layer structure of the ionosphere (see section 3.1.3) to a single layer. The height of this idealized layer is usually set to about 350 km. This value corresponds approximately to the height of the peak electron density in the F-region of the ionosphere.

The functional model for the computation of single layer models may now be described in the following way:

The observation equation of a zero-difference phase observation for carriers L_1 and L_2 may be written as (see eqn. (2-2), section 2.2):

$$L_i : d + \Delta d^{trop} + \Delta d_i^{ion} + c \cdot \tau^s - c \cdot \tau_r + N_i \cdot \lambda_i - \Phi_i = v_i \qquad i=1,2 \qquad (4\text{-}3)$$

where d : geometrical distance receiver - satellite

Δd^{trop} : tropospheric refraction

Δd_i^{ion} : ionospheric refraction for carrier L_i

τ_r : receiver clock error

τ^s : satellite clock error

λ_i : wavelength of carrier L_i

N_i : ambiguity parameter
Φ_i : phase observation
v_i : residual
c : speed of light in vacuum

The observation equation for an L_4 observation (see section 2.3) is obtained by forming the difference between the carriers L_1 and L_2 both expressed in meters. Using eqn. (4-3) we may write:

$$L_4 : \left(\Delta d_1^{ion} - \Delta d_2^{ion} \right) + \left(N_1\lambda_1 - N_2\lambda_2 \right) - \Phi_4 = v_4 \qquad (4\text{-}4a)$$

where: $\Phi_4 = \Phi_1 - \Phi_2$
$v_4 = v_1 - v_2$

Because the values of the ambiguity parameters N_1 and N_2 are of no interest in this context, they may be defined as one constant C:

$$\left(\Delta d_i^{ion} - \Delta d_2^{ion} \right) + C - \Phi_4 = v_4 \qquad (4\text{-}4b)$$

where $C = (N_1\lambda_1 - N_2\lambda_2)$

Introducing eqn. (4-2) in eqn. (4-4b) we obtain (for phase observations):

$$- \frac{a \cdot TVEC}{\cos z'} \left(\frac{1}{f_1^2} - \frac{1}{f_2^2} \right) + C - \Phi_4 = v_4 \qquad (4\text{-}5)$$

The total vertical electron content TVEC is modelled as a truncated Taylor Series with the geographical latitude ϕ and the hour angle s of the sun as independent variables (Georgiadiou and Kleusberg, 1988), (Wild et al., 1989):

$$TVEC\ (\phi, s) = \sum_{i=0}^{n} \sum_{k=0}^{m} E_{ik} \cdot (\phi - \phi_0)^i \cdot (s - s_0)^k \qquad (4\text{-}6a)$$

where ϕ_0, s_0 : Origin of Taylor Series Development

$$E_{ik} = \frac{1}{i!k!} \frac{\partial^{i+k} TVEC}{\partial^i \phi \partial^k s} \Bigg|_{\phi_0, s_0}, \quad i=0,1,\ldots;\ k=0,1,\ldots \qquad (4\text{-}6b)$$

The hour angle of the sun is defined as the angle between the sun and the local meridian (positive to the west). The local solar time t is related to the hour angle of the sun by:

$$t = s + 12^h \qquad (4\text{-}7)$$

In our algorithms s_0 is selected to be the hour angle corresponding to the middle of the observation interval, ϕ_0 is defined as the mean value of the latitudes of all stations used to compute the model.

Introducing eqn. (4-6a) into eqn. (4-5) leads to the observation equations in the required form. These equations are linear in the unknown parameters E_{ik} and the constant C. The unknown parameters E_{ik} and at least one constant C for each satellite and each receiver are estimated in a least squares adjustment of all observations to all satellites from one or more stations (see section 4.3.1).

The choice of the optimum degrees for the Taylor series development depends on the behaviour of the ionosphere in time and space. Too high development degrees decrease the reliability of the estimated ionosphere parameters. The best degrees of development were found to be 1 to 2 for the latitude and 2 to 4 for the hour angle if 4 hour data spans in regions smaller than a continent were used. The reason for the higher degree in the hour angle s is the fact that using data spans of several hours the region covered by the SLM in longitude is much larger than the one covered in latitude.

The SLM is not very sensitive to the choice of the height H (Figure 4-1) of the single layer. (Georgiadiou, 1990) has shwon that the changes in the length of the baselines are about 0.04 ppm per 100 km of change in the layer height H.

The SLM does not provide a real modelling of the time dependence of the ionosphere, because only the dependence of the position of the sun (local time) is taken into account. The SLM defined by eqns. (4-5) and (4-6) might be called the model of the "frozen ionosphere". The ionosphere may be thought of as a "bulge" moving over the earth synchronously to the motion of the sun. Time dependent variations of the ionosphere in this bulge are not modelled by the SLM.

4.2 Extracting Stochastic Properties of the Ionosphere from GPS Observations

When analyzing the "residuals" of L_4 observations (eqns. (4-4a) and (4-4b)) after having removed a single layer model as described in the previous section one clearly sees that they are not randomly distributed but that there are short-term irregular variations with periods of a few minutes up to about 1 hour. We call these variations the **stochastic part of the ionosphere.**

In geodesy the stochastic part of the ionosphere is of interest mainly for the preprocessing of GPS data and in the ambiguity resolution process. In both cases the stochastic part is considered as disturbing noise. For the geophysicists, however, this irregular component of ionospheric refraction is a signal to study ionospheric phenomena.

In both cases - geodesy and geophysics - the following four questions have to be answered

- What are the typical amplitudes of the stochastic part?
- What are the corresponding periods?
- When do disturbances in the stochastic part occur?
- What are the spatial and temporal extensions of these disturbances?

As a first approach (Beutler et al., 1988) proposed to compute the variance of the changes of L_4 observations in a given time interval Δt as a measure for short period variations in the ionosphere:

$$m(\Delta t;\vec{R}_i) = \frac{f_2^2}{(f_1^2-f_2^2)} \cdot \sqrt{\text{Variance of the changes of } L_4 \text{ (reduced to the zenith) per time interval } \Delta t} \qquad (4\text{-}8)$$

with m : measure for short period variations in the L_1 carrier
f_i : signal frequency of L_i, i = 1,2
$\vec{R}_i$: position of station i

The value of the variance is multiplied with the factor $f_2^2/(f_1^2-f_2^2)$ in order to get the ionospheric changes as they are seen by the L_1 carrier.

Typically Δt = 1 minute was used. The reduction to the zenith was done by multiplying the actual change by cos(z'), z' being the zenith distance in the ionospheric point of the actual observation (see Figure 4-1).

The same procedure may be applied to single differences:

$$dm(\Delta t;\vec{R}_i,\vec{R}_j) = \frac{f_2^2}{(f_1^2-f_2^2)} \cdot \sqrt{\text{Variance of the changes of differential } L_4 \text{ observations between stations i and j (reduced to the zenith) per time interval } \Delta t} \qquad (4\text{-}9)$$

where $\vec{R}_i$, $\vec{R}_j$: Positions of the stations i and j

The L_4 observations in eqns. (4-8),(4-9) were previously corrected for the model part (single layer model). If this model correction is applied the measures m and dm are of the order of one centimeter per minute or less, whereas without model correction they would be of the order of several centimeters per minute.

The differential measure dm was used to study the spatial decorrelation of the ionosphere: for a baseline of a few meters the ionospheric refraction cancels out completely when the single differences between the observations of the two stations are formed. With increasing baseline length the ionospheric conditions at the two

end points of the baseline differ more and more. For a certain baseline length the conditions are no longer correlated and the measures m at the two end points of the baseline have to be added quadratically to obtain dm.

Figure 4-2 shows the expected ratio f=dm/m as a function of the baseline length d.

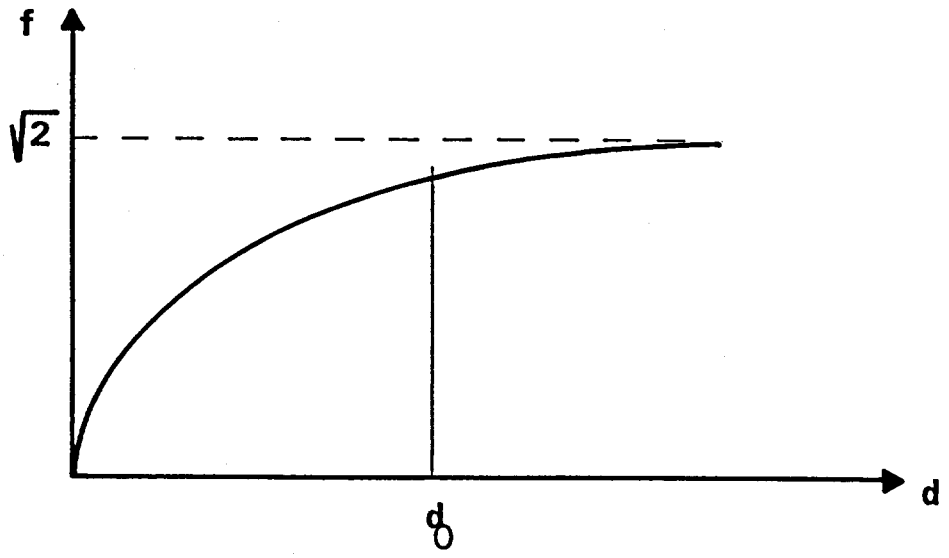

Figure 4-2
Spatial Decorrelation of the Ionosphere

d denotes the baseline length, d_0 the decorrelation distance, which corresponds to a value for f of 1.2 (80 %).

These measures were used in the processing of the 1987 Greenland campaign (Beutler et al., 1988). A good correlation with the geophysical K_p-index was observed (Beutler et al., 1988).

It is clear that the measures m and dm are only very crude measures for the stochastical part of the ionosphere. The next step was to apply the method of spectral analysis to the L_4 residuals v_4 of the single layer model. The main steps are:

1) Computation of the auto-covariance function C of the L_4 residuals v_4 of the single-layer model, where we assumed that the epochs of the residuals are equidistant (= observation interval Δt).

$$C(n\cdot\Delta t) = \frac{1}{m-n} \sum_{i=0}^{i=m-n} v_4(t_i)\cdot v_4(t_i+n\cdot\Delta t) \qquad (4\text{-}10)$$

for $n=0,1,2,\ldots,n_{max}$

where $C(n\cdot\Delta t)$: value of the auto-covariance function C for the time lag $n\cdot\Delta t$
n_{max} : $n_{max}\cdot\Delta t$ = maximum time lag (user definable)
m : number of L_4 residuals to be analyzed
$v_4(t_i)$: L_4 residual at time t_i
$v_4(t_i+n\cdot\Delta t)$: L_4 residual at time $t_i+n\cdot\Delta t$

2) Computation of the power spectrum S of the residuals v_4 by forming the Fourier transform of the auto-covariance function C:

$$S(k\cdot\Delta\omega) = \frac{1}{n_{max}\cdot\Delta t} \sum_{n=0}^{n=n_{max}} C(n\cdot\Delta t)\cdot\cos(n\cdot\Delta t\cdot k\cdot\Delta\omega) \qquad (4\text{-}11)$$

for $k=0,1,\ldots,k_{max}$

where $S(k\cdot\Delta\omega)$: power spectrum for the frequency $k\cdot\Delta\omega$
$\Delta\omega$: increment of frequency ω
k_{max} : $k_{max}\cdot\Delta\omega$ = maximum frequency (user definable)
$C(n\cdot\Delta t)$: auto-covariance function (see eqn. 4-10)

4.3 Program Developments

4.3.1 Program IONEST

For the computation of single-layer models the program IONEST (IONosphere parameter ESTimation) has been developed (Wild et al., 1989).

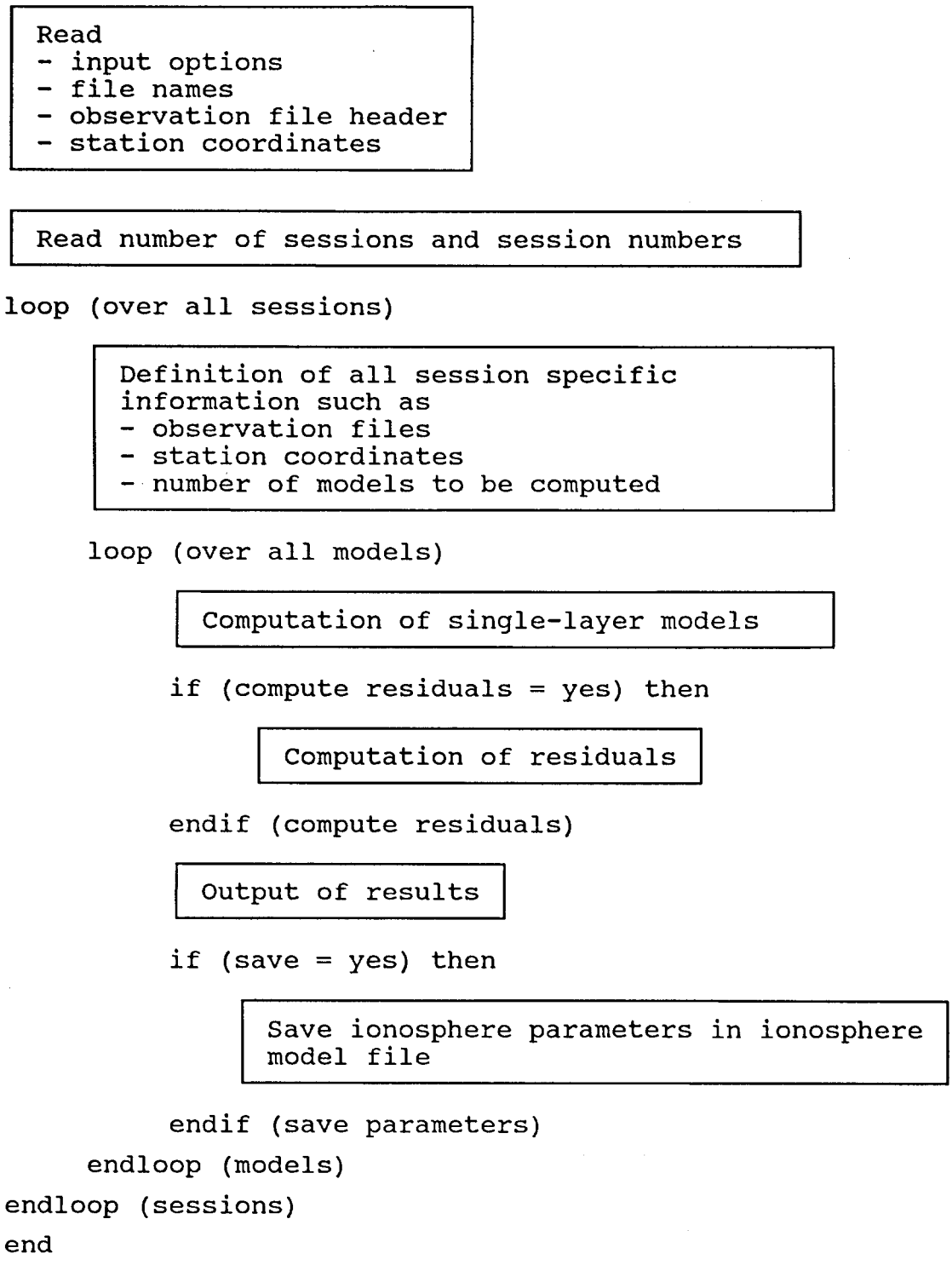

Figure 4-3
Block Diagram of the Program IONEST

IONEST is a program designed for use on permanent GPS tracking stations. It is a batch program which computes without any interaction ionosphere models using dual-frequency data. The emphasis was put on a high degree of automation. IONEST processes L_4 data (the difference between L_1 and L_2 both expressed in meters) from one or more stations. For each set of zero-difference files one or more ionosphere models are computed.

Figure 4-3 shows a block diagram of the program IONEST.

```
IONEST: OPTION INPUT FILE                                  25-JAN-93 18:21
-------------------------------------------------------------------------

(REMARK: YES=1,NO=0)

TITLE:
------

************************************************************

--> : IONOSPHERE MODEL SESSION 302

PRE-PROCESSING:                                                    *
---------------

PRINT PREPROCESSING MESSAGES (SR CHKOBS)                 --> :  0
USE CARRIER I TO DETECT BREAKS, GAPS I=3,I=4:            --> :  4
DEGREE Q OF POLYNOMIAL (Q < 4)                           --> :  1
MAX. INTERVAL LENGTH FOR TEST (MINUTES)                  --> :  4
                                                              ***.***
RMS OF ONE OBSERVATION (M)                               --> :  0.050

PROCESSING OPTIONS:
-------------------                                           *****

MINIMAL ELEVATION (DEGREES)                              --> :   20
RESIDUALS                                                --> :    0

SINGLE LAYER MODEL:
-------------------

      MODEL  DEGREE OF DEVELOPMENT IN    MAX. DEGREE OF
                LATITUDE  HOUR ANGLE      MIXED COEFF.
F      ***        **          **              **

-->:     1         1           2               2

HEIGHT OF IONOSPHERIC LAYER  (KM)
---------------------------------

     *****
-->:   350
```

Table 4-1
Example of an Input Option File for Program IONEST

The functional model used by the program IONEST was described in section 4.1.

The input option file of the program IONEST is shown in Table 4-1.

The input options of the program IONEST may be grouped into

(1) *Preprocessing options*
(2) *Processing options*

(1) Preprocessing options:
The preprocessing in the program IONEST is done on the zero-difference level. It is checked whether the observations may "locally" be represented by a low degree ($q <= 2$) polynomial. By "local" we understand an interval containing (q+2) observation epochs. It is checked whether the (q+1)th derivative of the interpolation polynomial of degree q+1 of the q+2 observations is zero (within the confidence interval given by the observation noise) or not. If this is the case the observations are accepted and the test interval is shifted by one epoch. If the (q+1)th derivative is not in agreement with the observation noise the last observation in the interval is marked and is replaced by the subsequent observation. This step may be repeated until the size of the interval with (q+2) valid observations exceeds a user defined maximum length. If this happens a new set of (q+2) observations to the right of the "old" interval is chosen and the described procedure is performed again.

For code observations the marked measurements are interpreted as outliers and left out, in the case of phase observations for each discontinuity detected in the preprocessing step a new ambiguity parameter for the satellite under consideration is introduced.

This preprocessing procedure may operate on the ionosphere-free linear combination L_3 or on L_4. Normally L_4 is used, because (after all) the model parameters will be computed using L_4 too. If rapid variations due to extreme ionospheric conditions occur it may be preferable to use L_3.

(2) Processing options:

There are two options to define the observation scenario: the minimum elevation and the sampling rate. The degrees of the Taylor series development for latitude, hour angle and for the terms containing both partial derivatives (mixed terms) may be specified as well as the height H of the single layer above the Earth's surface (see Figure 4-1). For all applications presented here this heigth H was set to 350 km. (Georgiadiou, 1990) showed that the SLM's are not very sensitive to the value of this parameter.

The computed ionosphere parameters may be stored in an ionosphere model file, which then may be used by the programs of the Bernese GPS Software Version 3 (preprocessing- and parameter estimation programs). An example of an ionosphere model file is given in Table 4-2.

TEST TURT89 **10-MAY-91 09:30**

```
IONOSPHERE MODEL NUMBER                              :    1
TYPE OF IONOSPHERE MODEL                             :    1
ORIGIN OF DELEVOPMENT: TIME (UT)   (Y M D H)         : 1989  7  5  9.5
                       LATITUDE    (DEGREES)         :   46.3049
                       LONGITUDE   (DEGREES)         :    7.6735
                       HEIGHT OF LAYER (KM)          :  350
DEGREE OF DEVELOPMENT: TIME                          :    2
                       LATITUDE                      :    2
                       MIXED                         :    2
NORMALIZATION FACTORS: LATITUDE (DEGREES)            :   6.00
                       TIME (HOURS)                  :   2.00
                       ELECTRON CONTENT              :        1.0E+16
APPLICABILITY          FROM EPOCH                    : 1989  7  5  7.0
                       TO EPOCH                      : 1989  7  5 12.0

COEFFICIENTS:
DEG. LAT   DEG. TIME  COEFFICIENT        RMS
    0          0       55.3083700    0.20041950E-00
    0          1        2.8553350    0.52978370E-01
    0          2       -5.8404520    0.58169490E-01
    1          0       -1.4306010    0.13799130E-00
    1          1       -6.8968340    0.21521420E-00
    2          0       -9.7648740    0.11498560E-00
   -1
```

Table 4-2
Example of Ionosphere Model File

4.3.2 Program IONMAP

The program IONMAP was developed for automatic processing of the data of the International GPS Service for Geodynamics (IGS) (results see section 5.2).

The program is based on the program IONEST. Whereas IONEST uses all the input and output file formats of the Bernese GPS Software (Rothacher et al., 1993), IONMAP uses the RINEX observation and navigation format (Gurtner et al., 1989) and may therefore be used outside the environment of the Bernese GPS Software as a stand-alone program.

IONMAP has the following new options

- one or more RINEX 24-hour files (= stations) of one day may be processed in one program run. Each file is treated separately.

- for each station n models of m hours duration may be computed

- different development degrees may be chosen for each model

Three different output files are generated by the program IONMAP:

(1) The output **summary file**, containing for each station and for each model the station name, the time interval, the number of observations, the rms of a single L_4 observation, the mean electron content (in TECU's, see section 3.3) and its corresponding rms. Table 4-3 shows such a summary file for 3 different stations.

(2) The **single layer model result file** contains all the single layer models of one day and for all stations. This output file has the format of the ionosphere model file used by the Bernese GPS software. The same file format is also used in the program TECVAL (see section 4.3.3).

(3) The **residual files** contain all the L_4 residuals for one station and one day. The residual files are used as input files for the program SPARES (see section 4.3.4).

IGS: AUTOMATIC IONOSPHERE MODEL PROCESSING

STATION	TIME (UT)	DATE	NOBS	RMS (M)	TVEC (TECU)
ALGO 40104M002	00 - 04	1992-10-16	1874	0.18	12.286 +0.153
ALGO 40104M002	04 - 08	1992-10-16	1828	0.09	5.644 ±0.089
ALGO 40104M002	08 - 12	1992-10-16	1329	0.05	3.633 ±0.083
ALGO 40104M002	12 - 16	1992-10-16	1953	0.07	14.614 ±0.072
ALGO 40104M002	16 - 20	1992-10-16	945	0.08	23.675 ±0.164
ALGO 40104M002	20 - 24	1992-10-16	2506	0.06	16.472 ±0.047
DRAO 40105M002	00 - 04	1992-10-16	1866	0.18	11.993 ±0.179
DRAO 40105M002	04 - 08	1992-10-16	1797	0.07	6.283 ±0.101
DRAO 40105M002	08 - 12	1992-10-16	1639	0.09	5.544 ±0.081
DRAO 40105M002	12 - 16	1992-10-16	1825	0.11	7.342 ±0.089
DRAO 40105M002	16 - 20	1992-10-16	2437	0.09	18.220 ±0.075
DRAO 40105M002	20 - 24	1992-10-16	2636	0.08	18.688 ±0.061
FAIR 40408M001	00 - 04	1992-10-16	2238	0.32	20.005 ±0.331
FAIR 40408M001	04 - 08	1992-10-16	1882	0.13	4.288 ±0.165
FAIR 40408M001	08 - 12	1992-10-16	1872	0.12	5.403 ±0.156
FAIR 40408M001	12 - 16	1992-10-16	1939	0.14	3.797 ±0.114
FAIR 40408M001	16 - 20	1992-10-16	2223	0.06	7.776 ±0.062
FAIR 40408M001	20 - 24	1992-10-16	2363	0.10	13.450 ±0.090

Table 4-3
Output Summary File of Program IONMAP

4.3.3 Program TECVAL

The program TECVAL is an auxiliary program to compute TEC values (in TECU) using as input files the ionosphere model files generated by the programs IONEST or IONMAP.

TECVAL may either be used to compute single TEC values for a given point in the ionosphere (defined by ellipsoidal or Cartesian coordinates) or to compute profiles of TEC values in

- latitude (for a given longitude and local time)
- longitude (" " " latitude " " ")
- local time (" " " longitude and latitude)

The increments for the profiles may be defined by the program user.

TECVAL is the interface between the internal file formats of the Bernese GPS Software and other users (like e.g. geophysicists) who

are just interested in the programs IONMAP and SPARES for ionospheric research.

4.3.4 Program SPARES

The program SPARES processes one or more residual files generated by the program IONMAP. These residual files contain all residuals of one station and one day (6 ionosphere models).

The kernel of the program SPARES has been taken from (Schuh, 1978; Brockmann, 1991). The theory of the spectral analysis was outlined in section 4.2.

For our application the original algorithm was simplified: only one iteration is executed and only the power spectrum of the residuals is computed, the Fourier adjustement is skipped. The program SPARES generates for each model and for each satellite two different plot files containing the L_4 residuals and the corresponding power spectrum.

The flow diagram of the program SPARES is given in Table 4-4.

loop (over all residual files)

Read Residual File Header

loop (over all models)

loop (over all satellites)

Read Residuals

Check Residuals for Equidistant Time Arguments

Compute Auto-covariance Function of the Residuals

Compute Power Spectrum of the Residuals

Generate Plot Files

endloop (satellites)

endloop (models)

endloop (residual files)

Table 4-4

Flow Diagram of the Program SPARES

5. APPLICATIONS

Permanent GPS tracking stations will become more and more important in the next years. The main purpose of these stations is the contribution to the determination of GPS orbits, the monitoring of displacements between the stations of the tracking network and the definition of a reference frame for regional/local surveys. A large number of such stations has been established in the past two years for the International GPS Service for Geodynamics (IGS).

The data collected by these stations may well be used to compute (in a highly automated way) simple ionosphere models, describing the ionospheric properties above the station area. These models are of interest for different user groups, in particular for geodesists and geophysicists.

In this chapter we present typical applications for ionosphere modelling and mapping techniques using the data collected by permanent GPS tracking stations. The following topics will be addressed:

- The elimination of ionosphere biases (scale factors) in geodetic networks,
- the contribution of ionosphere models to ambiguity resolution,

  and

- the global description of the ionosphere.

The first two applications are examples for the use of ionosphere models in geodesy, the last one is a pure geophysical application.

Based on the results and experiences obtained in this section we will propose a concept for a future "Ionosphere Service" for permanent GPS tracking stations.

5.1 Geodetic Applications of Ionosphere Modelling

Three applications are presented: The first demonstrates the elimination of ionospheric biases (like scale factors) in geodetic networks, the second is a special application of the program IONEST for the calibration of the radar altimeter of the European Space Agency's ERS-1, and the third illustrates the use of ionosphere models for ambiguity resolution.

5.1.1 Elimination of Ionosphere Biases in Geodetic Networks

We first study the use of a single layer model in the well known test network Turtmann in the Swiss Alps (see e.g. (Schneider, 1992), (Gurtner et al., 1987)), then we demonstrate that the method works also under different ionospheric conditions, and finally we illustrate the concept of regional ionosphere modelling applying the models generated with the data of only one dual frequency reference receiver.

The Turtmann test network is a high precision terrestrial 3D network (9 stations, 5 km x 6 km x 1 km) located in the Swiss Alps (see Figures 5-1 and 5-2). The standard deviations of the station coordinates are of the order of 1 mm for the position and of a few mm for the height.

Different GPS campaigns have been organized in the network in the years 1985-1992. From the point of view of ionosphere modelling the first three campaigns were similar: they took place in October (1985, 1986, and 1987). Since in these days only the 5-7 satellite test configuration of the GPS was available, very similar daily observation sessions (early morning) were the result. In addition the solar activity in these years was low.

This situation changed for the campaigns in the following years, as the two following examples show:

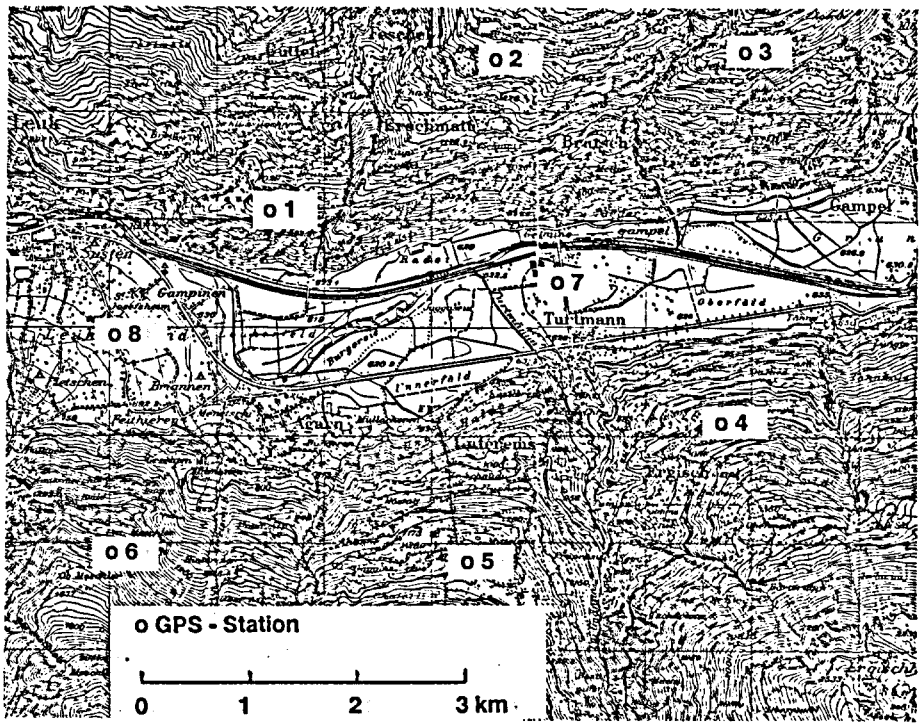

Figure 5-1

Turtmann Test Network

(Reproduziert mit Bewilligung des Bundesamtes für Landestopographie vom 7.4.1994)

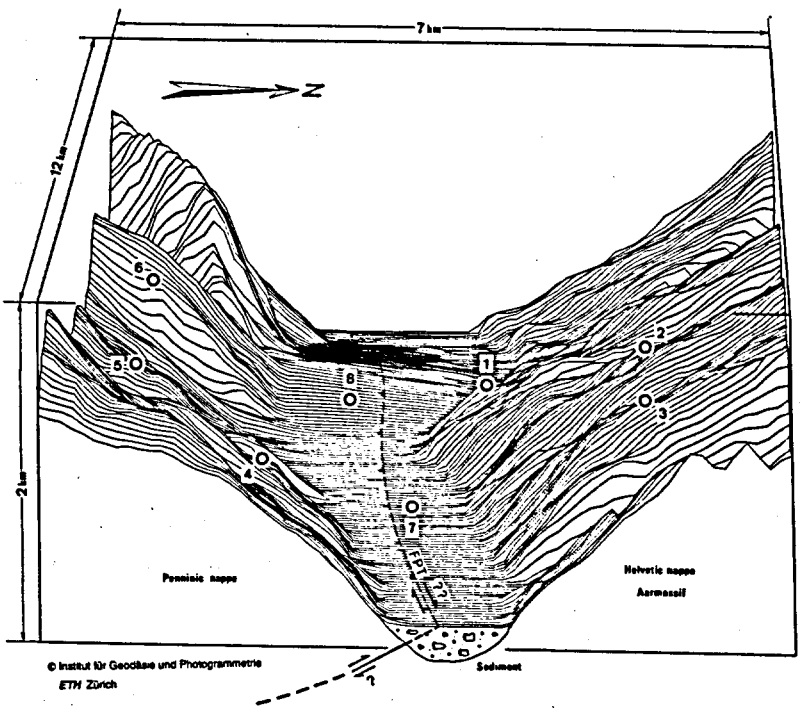

Figure 5-2

Turtmann Test Network

Perspective Drawing

In 1989 the campaign took place from July 5 - July 7, the daily observation time lasted from 8 a.m. to 1 p.m. (local time). A total of 16 receivers (10 WM-102 and 6 Trimble 4000ST) were operated in the network. The solar activity in 1989 was more pronounced than in the preceeding years, higher electron contents and stronger gradients of the electron density between sunrise and noon were the consequence. The GPS observations were therefore more biased by the ionosphere.

In 1992 the GPS campaign was observed in October. The daily observation window lasted from 2 p.m. to 5 p.m. local time. A total of 10 receivers (4 LEICA SR299, 3 Trimble 4000SSE, and 3 Ashtech XII-P) were operated in the network. The level of solar activity in 1992 was lower than in 1989.

In order to get a first impression of the ionospheric conditions for the 1989 and the 1992 campaign plots of the L_4 observable and its time derivative were generated. It should be mentioned that the origins of the curves are arbitrary (actually the first observation was set to zero). For each campaign very similar plots result for all sites and all days. Figure 5-3 and Figure 5-4 show the results of the 1989 campaign, Figure 5-5 and Figure 5-6 those of the campaign in 1992.

For both campaigns single layer ionosphere models were estimated using the data of one station (Turtmann 7.0) in the network. The development degrees for all models were selected as follows: latitude = 1, hour angle of the sun = 2, and mixed terms = 2. The results of the ionosphere model estimation for the 1989 campaign are given in Table 5-1, those for the 1992 campaign in Table 5-2.

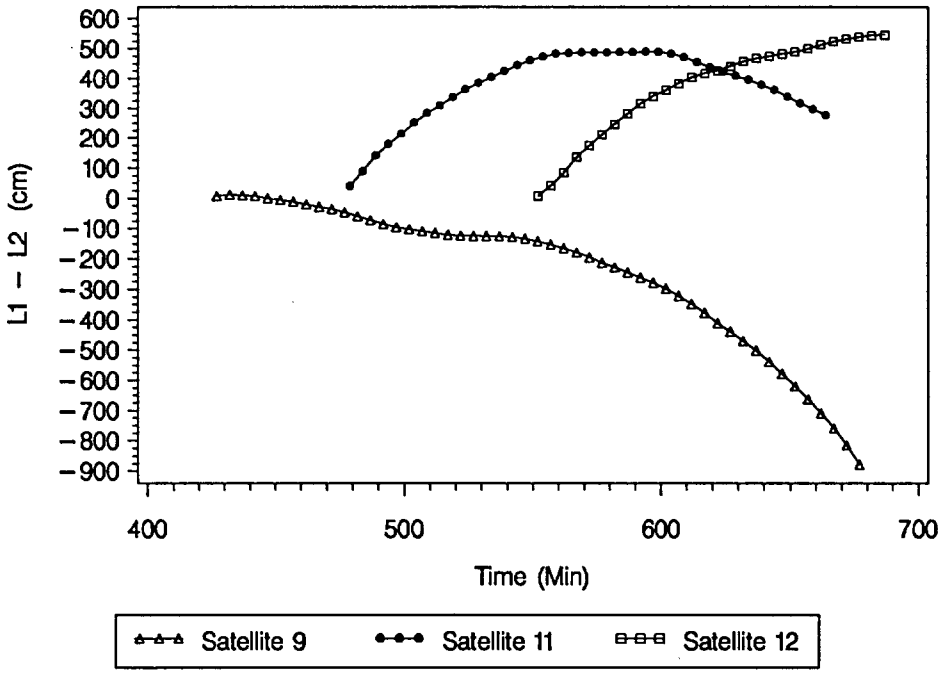

Figure 5-3
Station: Turtmann 7.0; Satellites 9, 11, 12
$L_1 - L_2$ (in cm)
Turtmann 1989 Campaign (5 July)

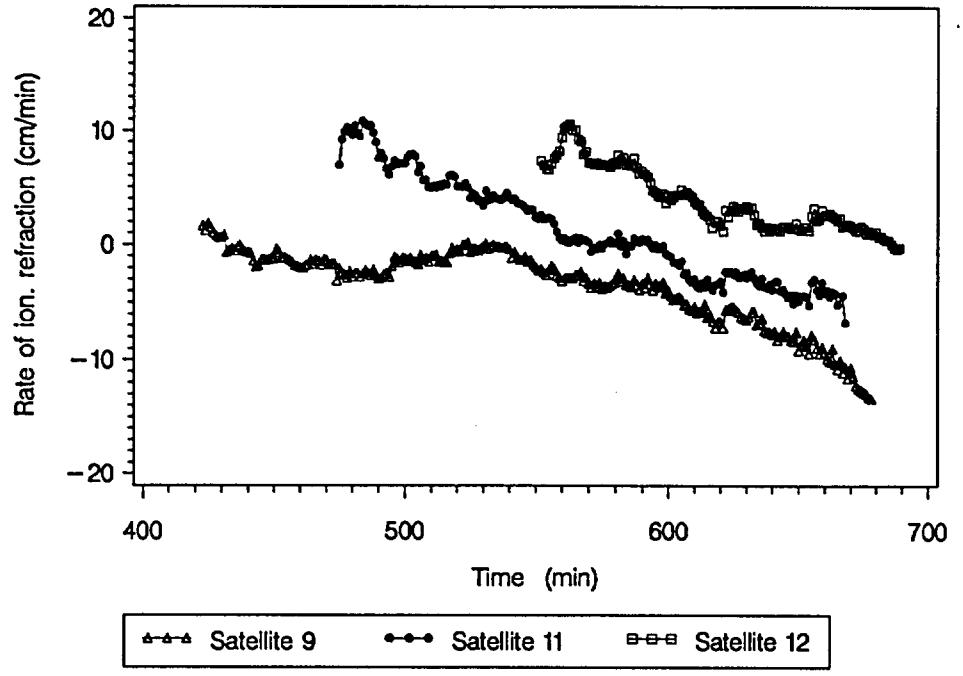

Figure 5-4
Station: Turtmann 7.0; Satellites 9, 11, 12
Rate of Ionospheric Refraction (L_1-L_2)/min
Turtmann 1989 Campaign (5 July)

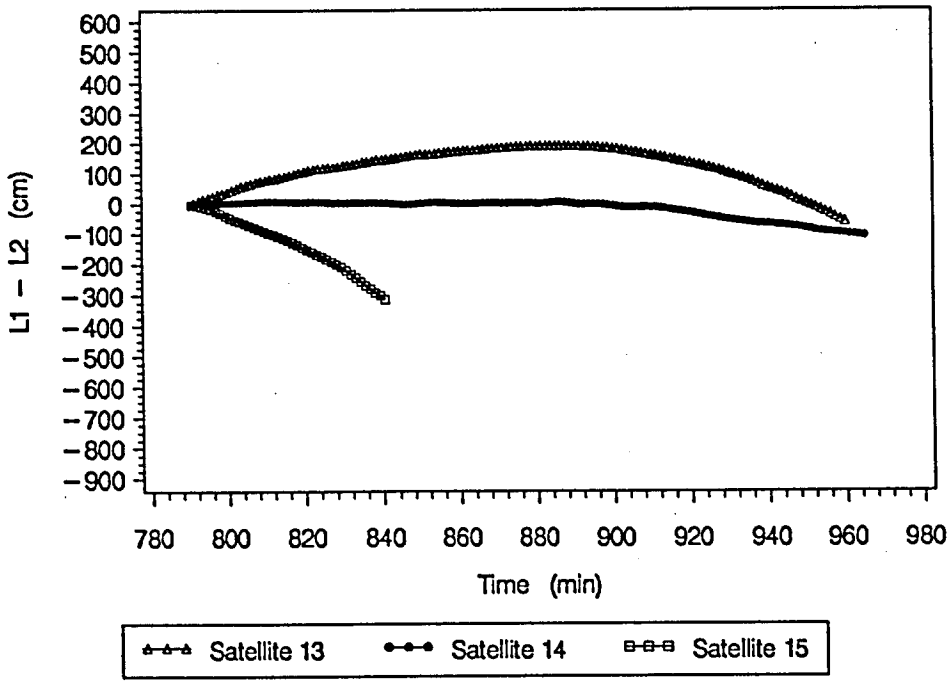

Figure 5-5

Station: Turtmann 7.0; Satellites 13, 14, 15

$L_1 - L_2$ (in cm)

Turtmann 1992 Campaign (28 October)

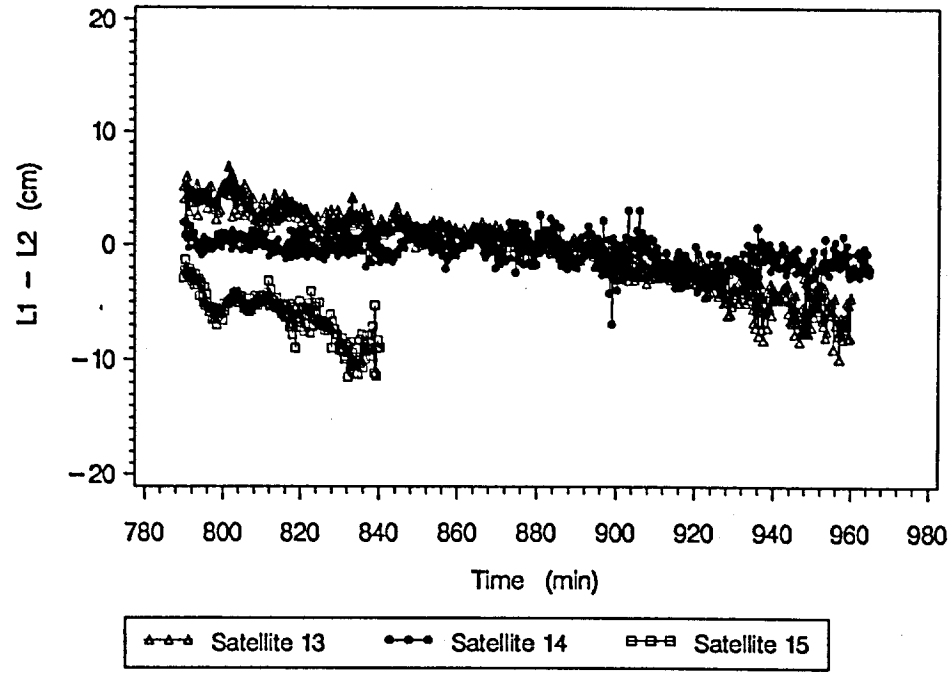

Figure 5-6

Station: Turtmann 7.0; Satellites 13, 14, 15

Rate of Ionospheric Refraction (L_1-L_2)/min

Turtmann 1992 Campaign (28 October)

RESULTS OF SINGLE LAYER MODEL:

CAMPAIGN: TURT89

STATION	TURT 7.0	TURT 7.0	TURT 7.0
DATE	1989-07-05	1989-07-06	1989-07-07
NUM OF OBS	1207	1191	1127
RMS (M)	0.191	0.233	0.174

LAT	HOUR A.	TEC	RMS	TEC	RMS	TEC	RMS
0	0	52.172 ±	0.354	49.352 ±	0.334	33.768 ±	0.432
0	1	-4.206 ±	0.113	-0.101 ±	0.096	3.885 ±	0.112
0	2	-4.716 ±	0.082	-7.802 ±	0.106	-4.506 ±	0.125
1	0	-1.242 ±	0.244	-8.413 ±	0.216	-5.254 ±	0.280
1	1	-5.657 ±	0.273	-0.486 ±	0.283	0.516 ±	0.278

Table 5-1
Single-layer Ionosphere Models for the Turtmann 1989 Campaign
(July 5 - July 8 1989)
Total Electron Content (TEC) in TECU

RESULTS OF SINGLE LAYER MODEL:

CAMPAIGN: TURT92

STATION	TURT 7.0	TURT 7.0
DATE	1992-10-28	1992-10-29
NUM OF OBS	3301	3440
RMS (M)	0.165	0.233

LAT	HOUR A.	TEC	RMS	TEC	RMS
0	0	26.750 ±	0.144	25.525 ±	0.077
0	1	-12.739 ±	0.062	-4.710 ±	0.034
0	2	0.480 ±	0.080	0.293 ±	0.043
1	0	-5.966 ±	0.080	-2.802 ±	0.045
1	1	0.245 ±	0.134	4.880 ±	0.070

Table 5-2
Single-layer Ionosphere Models for the Turtmann 1992 Campaign
(October 28 and 29, 1992)
Total Electron Content (TEC) in TECU

The scale factor expected in a geodetic network using L_1 phase observations (with a minimum elevation of 20°) is related to the total electron content of the ionosphere (Beutler et al., 1987b) by:

$$d\ell / \ell \approx - 0.07 \cdot TVEC \quad (ppm) \qquad (5\text{-}1)$$

with $d\ell$: change in baseline length due to the ionosphere
ℓ : baseline length
TVEC: total vertical electron content (in TECU)

The values in Table 5-1 and 5-2 let us expect scale factors (between a single-frequency solution and the ground truth) of about 3.7 ppm for the Turtmann 1989 Campaign and 1.9 ppm for the 1992 Campaign.

In order to get an impression of the efficiency of the single layer models we computed (for both campaigns) two different single frequency (L_1) solutions:

- Solution 1: L_1 without ionosphere model
- Solution 2: L_1 with ionosphere model

In all solutions one troposphere parameter per station was estimated (apart from the stations Turmann 7.0, Turtmann 7.1 and Turtmann 7.2) in order to eliminate the systematic influence of the troposphere. The minimum elevation was set to 20° for all solutions.

The result of the 7 parameter Helmert transformations between the two solutions (without and with ionosphere model) and the reference solution of the Swiss Federal Office of Topography (L+T) are shown in Tables 5-3 and 5-4.

HELMERT TRANSFORMATION

RESIDUALS IN LOCAL SYSTEM (NORTH, EAST, UP)

NAME	RESIDUALS IN METERS North	East	Up
BRUN	-0.0012	0.0002	-0.0104
BRAE	-0.0064	0.0014	0.0203
BRAE GPS	-0.0043	0.0013	0.0051
JEIZ	0.0011	-0.0030	0.0059
JEIZ GPS	-0.0021	0.0002	-0.0090
JEIZ GPS E	0.0010	-0.0015	-0.0088
ERGI	0.0057	-0.0017	0.0078
OEMS	0.0034	0.0019	0.0002
AGAR GPS	0.0018	0.0002	0.0063
TURT 7.0	0.0010	-0.0025	-0.0115
SUST 8.0	0.0000	0.0034	-0.0059

NUMBER OF PARAMETERS : 7
NUMBER OF COORDINATES : 33
RMS OF TRANSFORMATION : 0.0067 M

PARAMETERS:

TRANSLATION IN X :	-0.006	±	0.002	M
TRANSLATION IN Y :	-0.002	±	0.002	M
TRANSLATION IN Z :	0.013	±	0.002	M
ROTATION AROUND X-AXIS:	-0.91	±	0.22	"
ROTATION AROUND Y-AXIS:	0.77	±	0.26	"
ROTATION AROUND Z-AXIS:	-0.34	±	0.15	"
SCALE FACTOR :	-3.59	±	0.71	MM/KM

Table 5-3a
Helmert Transformation Between L_1 Solution
(3 Days, Without Ionosphere Model) and Ground Truth
Turtmann 1989 Campaign (July 5 - July 8, 1989)

HELMERT TRANSFORMATION

RESIDUALS IN LOCAL SYSTEM (NORTH, EAST, UP)

NAME	RESIDUALS IN METERS North	East	Up
BRUN	0.0003	0.0009	-0.0101
BRAE	-0.0069	0.0007	0.0195
BRAE GPS	-0.0056	0.0008	0.0044
JEIZ	0.0001	-0.0033	0.0059
JEIZ GPS	-0.0026	0.0009	-0.0103
JEIZ GPS E	-0.0004	-0.0019	-0.0088
ERGI	0.0068	-0.0021	0.0079
OEMS	0.0013	0.0006	0.0026
AGAR GPS	-0.0007	-0.0017	0.0040
TURT 7.0	0.0050	-0.0008	-0.0097
SUST 8.0	0.0026	0.0059	-0.0054

NUMBER OF PARAMETERS : 7
NUMBER OF COORDINATES : 33
RMS OF TRANSFORMATION : 0.0067 M

PARAMETERS:

TRANSLATION IN X :	-0.007	±	0.002	M
TRANSLATION IN Y :	-0.001	±	0.002	M
TRANSLATION IN Z :	0.011	±	0.002	M
ROTATION AROUND X-AXIS:	-0.48	±	0.22	"
ROTATION AROUND Y-AXIS:	0.23	±	0.25	"
ROTATION AROUND Z-AXIS:	-0.26	±	0.15	"
SCALE FACTOR :	-1.16	±	0.71	MM/KM

Table 5-3b
Helmert Transformation Between L_1 Solution
(3 Days, With Ionosphere Model) and Ground Truth
Turtmann 1989 Campaign (July 5 - July 8, 1989)

HELMERT TRANSFORMATION

RESIDUALS IN LOCAL SYSTEM (NORTH, EAST, UP)

NAME	RESIDUALS IN METERS North	East	Up
BRUN 1	-0.0010	0.0017	0.0034
BRAE 2	-0.0027	-0.0001	0.0050
JEIZ GPS	-0.0011	-0.0014	0.0012
ERGI 4	-0.0011	0.0016	0.0087
OEMS 5	0.0009	-0.0003	-0.0042
AGAR GPS	0.0038	-0.0033	0.0072
TURT 7	0.0014	-0.0005	-0.0050
TURT 7.1	0.0013	-0.0005	-0.0049
TURT 7.2	0.0014	-0.0005	-0.0050
SUST 8	-0.0029	0.0032	-0.0064

NUMBER OF PARAMETERS : 7
NUMBER OF COORDINATES : 30
RMS OF TRANSFORMATION : 0.0040 M

PARAMETERS:

TRANSLATION IN X	:	-0.003	±	0.001 M
TRANSLATION IN Y	:	-0.004	±	0.001 M
TRANSLATION IN Z	:	0.009	±	0.001 M
ROTATION AROUND X-AXIS	:	-1.110	±	0.140 "
ROTATION AROUND Y-AXIS	:	0.233	±	0.171 "
ROTATION AROUND Z-AXIS	:	-0.352	±	0.104 "
SCALE FACTOR	:	-2.135	±	0.498 MM/KM

Table 5-4a

Helmert Transformation Between L_1 Solution (2 Days, Without Ionosphere Model) and Ground Truth Turtmann 1992 Campaign (October 28 - October 29, 1992)

HELMERT TRANSFORMATION

RESIDUALS IN LOCAL SYSTEM (NORTH, EAST, UP)

NAME	RESIDUALS IN METERS North	East	Up
BRUN 1	-0.0004	0.0016	0.0030
BRAE 2	-0.0034	0.0010	0.0028
JEIZ GPS	-0.0018	-0.0007	-0.0016
ERGI 4	-0.0021	0.0018	0.0076
OEMS 5	-0.0012	0.0004	-0.0037
AGAR GPS	0.0019	-0.0027	0.0043
TURT 7	0.0028	-0.0013	-0.0028
TURT 7.1	0.0028	-0.0013	-0.0028
TURT 7.2	0.0028	-0.0013	-0.0029
SUST 8	-0.0013	0.0026	-0.0039

NUMBER OF PARAMETERS : 7
NUMBER OF COORDINATES : 30
RMS OF TRANSFORMATION : 0.0031 M

PARAMETERS:

TRANSLATION IN X	:	-0.004	±	0.001 M
TRANSLATION IN Y	:	-0.002	±	0.001 M
TRANSLATION IN Z	:	0.008	±	0.001 M
ROTATION AROUND X-AXIS	:	-1.262	±	0.110 "
ROTATION AROUND Y-AXIS	:	0.010	±	0.134 "
ROTATION AROUND Z-AXIS	:	-0.362	±	0.081 "
SCALE FACTOR	:	-0.672	±	0.389 MM/KM

Table 5-4b

Helmert Transformation Between L_1 Solution (2 Days, With Ionosphere Model) and Ground Truth Turtmann 1992 Campaign (October 28 - October 29, 1992)

The scale factors of the L_1 solutions without ionosphere models in Tables 5-3 and 5-4 show a good agreement with the theoretically expected values (see eqn. (5-1)): for the Turtmann 1989 Campaign a scale factor of 3.5 ppm was expected (estimated: 3.6 ppm), for the 1992 campaign the expected scale factor was 1.8 ppm (estimated: 2.1 ppm).

By introducing single-layer ionosphere models the scale factor could be reduced significantly. The reduction of the scale factor to the 0.5-1 ppm level in small networks has been demonstrated in many other examples and seems to be the state of the art. In a different context we will present below also the transformation between the GPS solution using the ionosphere-free linear combination and the ground truth (Tables 5-10 and 5-11). It is interesting to note that this solution, unbiased by the ionosphere, gives (within the error bars) the same scale factor as the pure L_1 solution, indicating that the remaining bias has nothing to do with the ionosphere.

In a next step the question whether the same results could also be obtained if the single layer ionosphere models are estimated using the data of a permanent GPS tracking station in the vicinity of the network was addressed. In our case we used the data of the permanent GPS tracking station in Zimmerwald (at a distance of about 70 km from the Turtmann area). Since this station has been built up for the IGS in spring 1992, the test could be performed for the Turtmann 1992 campaign only.

Table 5-5 shows the result of the single layer model estimation using the data of the station Zimmerwald. One may note, that the differences in the total vertical electron content are marginal compared to the values for the model estimation using the data of a receiver in the Turtmann network (Table 5-2).

RESULTS OF SINGLE LAYER MODEL:

CAMPAIGN: TURT92

STATION	ZIMMERWALD	ZIMMERWALD
DATE	1992-10-28	1992-10-29
NUM OF OBS	1932	1952
RMS (M)	0.189	0.114

LAT	**HOUR A.**	**TEC**	**RMS**	**TEC**	**RMS**
0	0	26.314	± 0.190	25.439	± 0.115
0	1	-11.227	± 0.083	-4.073	± 0.050
0	2	0.091	± 0.105	-0.696	± 0.065
1	0	- 5.307	± 0.107	-2.594	± 0.064
1	1	0.881	± 0.160	4.836	± 0.104

Table 5-5
Single-layer Ionosphere Models for the Turtmann 1992 Campaign
(October 28 and 29, 1992)
Total Electron Content (TEC) in TECU

Table 5-6 shows the Helmert transformation between an L_1 solution for the Turtmann network (using the ionosphere model of the permanent tracking station Zimmerwald) and the ground truth.

It is interesting to note that practically the same residual scale factor (-0.61 instead of -0.67) remains when using the ionosphere model stemming from the Zimmerwald and not from the Turtmann receiver. This is another hint that the remaining scale factor has nothing to do with the ionosphere.

HELMERT TRANSFORMATION

RESIDUALS IN LOCAL SYSTEM (NORTH, EAST, UP)

NAME	RESIDUALS IN METERS North	East	Up
BRUN 1	-0.0004	0.0018	0.0031
BRAE 2	-0.0034	0.0010	0.0027
JEIZ GPS	-0.0019	-0.0007	-0.0017
ERGI 4	-0.0021	0.0017	0.0078
OEMS 5	-0.0011	0.0003	-0.0037
AGAR GPS	0.0020	-0.0028	0.0041
TURT 7	0.0028	-0.0014	-0.0028
TURT 7.1	0.0027	-0.0013	-0.0028
TURT 7.2	0.0028	-0.0013	-0.0029
SUST 8	-0.0013	0.0027	-0.0038

NUMBER OF PARAMETERS : 7
NUMBER OF COORDINATES : 30
RMS OF TRANSFORMATION : 0.0031 M

PARAMETERS:

TRANSLATION IN X	:	-0.004	±	0.001 M
TRANSLATION IN Y	:	-0.002	±	0.001 M
TRANSLATION IN Z	:	0.008	±	0.001 M
ROTATION AROUND X-AXIS:		-1.266	±	0.110 "
ROTATION AROUND Y-AXIS:		0.019	±	0.135 "
ROTATION AROUND Z-AXIS:		-0.362	±	0.082 "
SCALE FACTOR	:	-0.611	±	0.392 MM/KM

Table 5-6

Helmert Transformation Between L_1 Solution (2 Days, With Ionosphere Model) and Ground Truth Turtmann 1992 Campaign (October 28 - October 29, 1992)

No significant differences between the results in Table 5-6 and Table 5-4b may be observed, which indicates that for networks in the vicinity (up to 100 km) of permanent GPS tracking stations the ionosphere models distributed by the permanent station are sufficient for the elimination of ionosphere biases.

As we have seen in section 3.1.3 at least three different ionospheric regions have to be distinguished in latitude. We therefore include results for three campaigns processed in the past:

- Hawaii 1988 (equatorial region)
  From April 14 to April 28 10 points were measured by the U.S. National Geodetic Survey (NGS) with TI-4100 receivers. One station (Kokee GPS) was operated as a permanent station. On the other sites one session per day was observed (0-6 UT). The size of the network is 500 x 300 km. The baseline lengths vary between 20 km and 150 km.

- Granit 1987 (mid-latitude region)
  From June 16 to June 18 12 sites were measured in Switzerland with 7 TI-4100 receivers. One session per day was observed from 12:30-16:30 local time. The network size was roughly 200 x 200 km.

- Greenland 1987 (auroral zone)
  14 sites were observed from July 17 to July 26 by TI-4100 receivers. The baseline lengths varied between 500 m and 32 km. One session of six hours (starting in the afternoon) per day was observed.

For more detailed information about the campaigns and the results see (Wild et al., 1989), (Beutler et al., 1988). Let us summarize the most important results:

For all campaigns ionosphere models were computed using different development degrees (corresponding to the strength and the variability of the ionosphere for the region in concern). The benefit of ionosphere modelling has been tested by computing single frequency solutions (L_1, L_2 or L_5 solutions) without and with ionosphere mo-

dels and comparing them (using 7 parameter Helmert transformations) to the corresponding ionosphere-free solution (L_3), which was considered as the "truth" in all cases (no reliable independent solutions were available).

Table 5-8 shows the characteristics of the different solutions:

Campaign	Ionosphere Model (SLM) Development Degrees Lat/Hour Angle/Mixed	Solution Type to Test the Model
Hawaii 1988	2/5/5	L_5, amb. fixed
Granit 1987	1/2/2	L_1, amb. fixed
Greenland 1987	1/1/1	L_5, amb. fixed

Table 5-8
Development Degrees of the Ionosphere Models and Types of Solutions to be Compared to the L_3 Solutions

The results of the Helmert transformations (7 parameters) between the solutions without and with ionosphere model and the reference solutions (L_3 solutions) are given in Table 5-9:

Campaign	Scale Factor (mm/km) Without Ionosphere Model	With Ionosphere Model
Hawaii 1988	-2.417 ± 0.231	-0.104 ± 0.225
Granit 1987	0.597 ± 0.084	-0.121 ± 0.082
Greenland 1987	-0.914 ± 0.256	0.002 ± 0.218

Table 5-9
Comparison between Single Frequency Solutions (Without and With Ionosphere Models) and Ionosphere Free Solutions

These results show that ionosphere modelling using regional single-layer models is successful for networks of a size of a few kilometers up to 200 x 300 km. Ionospheric modelling techniques were successfully used even under very difficult ionospheric conditions. More material, e.g. the results of surveys made by the Swiss Federal Office of Topography (Wiget et al., 1990), points into the same direction.

In the past the program IONEST was mainly used to provide ionosphere models to single frequency GPS users. Today it seems that single frequency receivers are no longer popular in geodesy mainly because the prices for dual frequency receivers are rapidly decreasing and because new observation and computing techniques like the rapid static positioning (Frei, 1991) may only be used if dual frequency receivers are available.

There still remains an application of ionosphere models for dual-frequency receivers, however: usually the systematic influence of the ionosphere (= scale factor) in geodetic networks is eliminated (in the case of dual-frequency data) by forming the ionosphere-free linear combination L_3. The disadvantage of this linear combination is the amplification of the observation noise by a factor of about 3 compared to the noise of a L_1 or L_2 observation. For medium size or large networks this is generally no problem, but for small networks (< 1-2 km) the higher noise may directly cause a degradation of the precision of the network. Examples for such small networks are e.g. dam control networks.

In order to illustrate this fact we used again observations of the Turtmann 1989 and 1992 campaigns and we compared the residuals and the rms of the Helmert transformations of

- a transformation between the L_3 solutions and the terrestrial ground truth

and

- a transformation between the L_1 solutions and the ground truth.

The results of these comparisons are given in Tables 5-10 and 5-11.

HELMERT TRANSFORMATION

RESIDUALS IN LOCAL SYSTEM (NORTH, EAST, UP)

NAME	RESIDUALS IN METERS					
	L_3			L_1 + Ion. model		
	North	East	Up	North	East	Up
BRUN	0.0001	-0.0104	-0.0135	0.0003	0.0009	-0.0101
BRAE	-0.0107	0.0053	0.0243	-0.0069	0.0007	0.0195
JEIZ	0.0004	-0.0089	0.0099	0.0001	-0.0033	0.0059
JEIZ GPS	-0.0035	0.0020	-0.0205	-0.0026	0.0009	-0.0103
ERGI	0.0071	-0.0002	0.0127	0.0068	-0.0021	0.0079
OEMS	0.0026	0.0009	0.0041	0.0013	0.0006	0.0026
AGAR GPS	-0.0049	-0.0006	0.0006	-0.0007	-0.0017	0.0040
TURT 7.0	0.0055	0.0040	-0.0198	0.0050	-0.0008	-0.0097
SUST 8.0	0.0034	0.0080	0.0022	0.0026	0.0059	-0.0054

NUMBER OF PARAMETERS	: 7	7
NUMBER OF COORDINATES	: 27	33
RMS OF TRANSFORMATION	: 0.0110	0.0067

PARAMETERS:

TRANSLATION IN X	: -0.007	±	0.004	-0.007	±	0.002	M
TRANSLATION IN Y	: -0.004	±	0.004	-0.001	±	0.002	M
TRANSLATION IN Z	: 0.017	±	0.004	0.011	±	0.002	M
ROTATION AROUND X-AXIS:	0.42	±	0.38	-0.48	±	0.22	M
ROTATION AROUND Y-AXIS:	0.17	±	0.46	0.23	±	0.25	M
ROTATION AROUND Z-AXIS:	-0.17	±	0.27	-0.26	±	0.15	M
SCALE FACTOR	: -1.58	±	1.28	-1.16	±	0.71	MM/KM

Table 5-10

Comparison of Helmert Transformations Between L_3 (3 Days), resp. L_1 (3 Days, With Ionosphere Model) and Ground Truth Turtmann 1989 Campaign (5 July - 7 July 1989)

HELMERT TRANSFORMATION

RESIDUALS IN LOCAL SYSTEM (NORTH, EAST, UP)

NAME	RESIDUALS IN METERS					
	L_3			L_1 + Ion. model		
	North	East	Up	North	East	Up
BRUN 1	-0.0015	0.0030	0.0102	-0.0004	0.0016	0.0030
BRAE 2	-0.0031	-0.0014	-0.0230	-0.0034	0.0010	0.0028
JEIZ GPS	-0.0029	-0.0022	-0.0007	-0.0018	-0.0007	-0.0016
ERGI 4	-0.0037	0.0009	0.0055	-0.0021	0.0018	0.0076
OEMS 5	-0.0020	-0.0006	-0.0263	-0.0012	0.0004	-0.0037
AGAR GPS	-0.0019	-0.0027	0.0127	0.0019	-0.0027	0.0043
TURT 7	0.0047	-0.0010	0.0104	0.0028	-0.0013	-0.0028
TURT 7.1	0.0047	-0.0010	0.0104	0.0028	-0.0013	-0.0028
TURT 7.2	0.0048	-0.0010	0.0103	0.0028	-0.0013	-0.0029
SUST 8	0.0010	0.0060	-0.0096	-0.0013	0.0026	-0.0039

NUMBER OF PARAMETERS	: 7	7
NUMBER OF COORDINATES	: 30	30
RMS OF TRANSFORMATION	: 0.0096 M	0.0031 M

PARAMETERS:

TRANSLATION IN X	: -0.004	± 0.003	-0.004	± 0.001 M
TRANSLATION IN Y	: -0.002	± 0.003	-0.002	± 0.001 M
TRANSLATION IN Z	: -0.006	± 0.003	0.008	± 0.001 M
ROTATION AROUND X-AXIS	: -0.834	± 0.335	1.262	± 0.110 M
ROTATION AROUND Y-AXIS	: -0.992	± 0.409	0.010	± 0.134 M
ROTATION AROUND Z-AXIS	: -0.320	± 0.248	0.362	± 0.081 M
SCALE FACTOR	: -1.140	± 1.190	-0.672	± 0.389 MM/KM

Table 5-11

Comparison of Helmert Transformations Between L_3 (2 Days), resp. L_1 (2 Days, With Ionosphere Model) and Ground Truth Turtmann 1992 Campaign (28 October - 29 October 1992)

The rms values of the transformations reveal the amplification of the errors for the L_3 solution. Comparing the residuals there is no significant difference for the North-component, whereas the East-component of the L_3 solution shows a slight tendency for greater residuals. The main difference of the two solutions may be observed in the Up-component, where the L_3 solution shows significantly higher residuals. For a discussion of the scale factor see the comments after Table 5-4.

5.1.2 Special Application of the Program IONEST: Calibration of the ERS-1 Altimeter

The first ESA (European Space Agency) European Remote Sensing satellite ERS-1 was launched in July 1991. The orbit of ERS-1 has an inclination of 98° and an altitude of 780 km. The primary goal of the ERS-1 mission is to map the earth's surface by means of different sensors, namely a Synthetic Aperture Radar (SAR), a Wind Scatterometer (SCAT), an Along-Track Scanning Radiometer and Microwave Sounder (ATSR/M), and a Radar Altimeter (RA).

Figure 5-7 shows the satellite and Table 5-12 gives an overview over the technical characteristics of ERS-1 and the Radar Altimeter (RA) (this information is relevant for the following discussion).

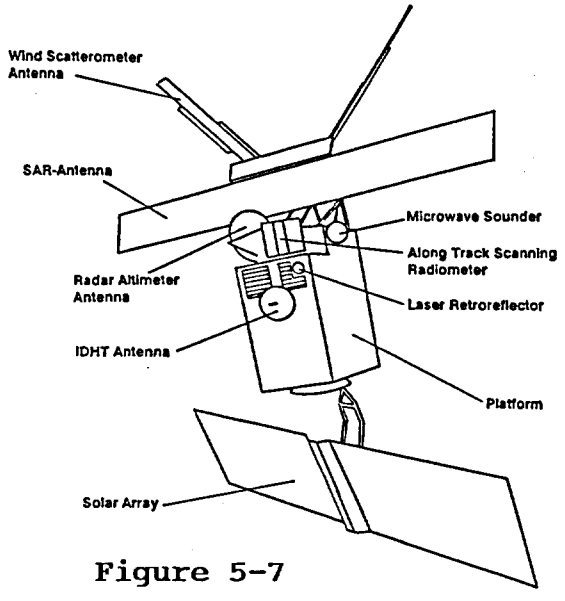

Figure 5-7
ERS-1

Orbit	Inclination	: 98 Degrees
	Nominal Height	: 780 km
	Total Weight	: 1356 kg
RA	Frequency:	13.8 GHz
	Accuracy :	± 10 m
	Resolution:	1-2 km / every 6 km
	Significant wave height:	1 - 20 m
	Accuracy:	± 0.5 m or 10 %

Table 5-12
Technical Characteristics of ERS-1 and the Radar Altimeter RA

As shown in Table 5-12 the altimeter works at 13.8 GHz. The distances between the satellite and the sea surface are measured by run-time measurements of the radar signal, which is affected by the troposphere and the ionosphere. The signal has to be corrected for tropospheric and ionospheric refraction in order to get the geometric distance satellite - surface which is of primary interest for the mission.

The effects of the troposhere are not discussed here; for more information see e.g. (Francis et al., 1992).

The high inclination of ERS-1 causes a north-south satellite ground-track which from time to time passes at a few kilometers distance from the research platform of the Istituto delle Grande Masse (IDGM, Venice) in the Adriatic Sea. These satellite passes over the research platform were used for the **absolute calibration of the radar altimeter** of ERS-1 combining measurements of the RA, of GPS, and of SLR (Satellite Laser Ranging). The principle is shown in Figure 5-8.

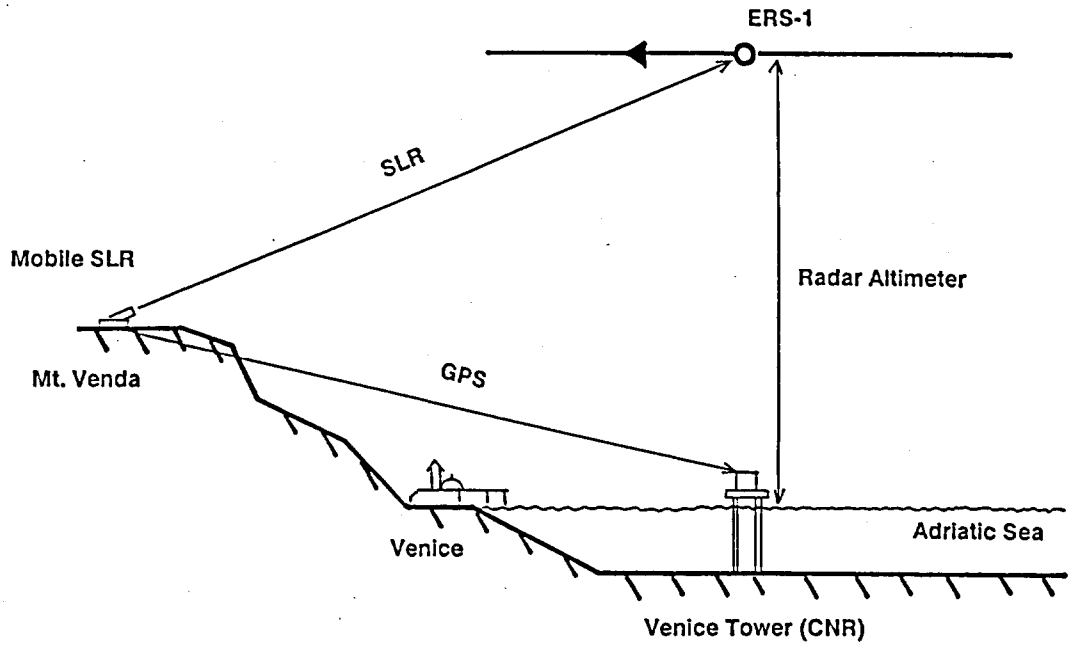

Figure 5-8
Concept of the Absolute Calibration of the Radar Altimeter

The distance between Monte Venda and the satellite ERS-1 was continuously measured by the Dutch mobile SLR system. In addition ERS-1 was tracked by all European SLR stations in the vicinity (see Figure 5-8). The relative position of Monte Venda with respect to the platform was determined in a GPS campaign in 1990 (see below) and is therefore known. Using this information it was possible to compute the "true distance" between ERS-1 and the sea surface. Because this height was also continiously measured by means of the ERS-1 radar altimeter, the latter measurements could be directly compared to the "true" values.

The actual procedure was the following:

In a first step the position of the research platform was determined in a GPS campaign. This campaign took place in October 1990. The goal of the campaign was to determine the position of the platform with respect to the SLR stations in the vicinity (Graz, Wettzell, Grasse, Zimmerwald, and Matera). In addition the position for a mobile laser system on the Monte Venda was determined. Figure 5-9 shows the research platform in the Adriatic Sea and the locations

of the SLR stations. A detailled description of the campaign and of the results may be found in (Gurtner and Overgaauw, 1991). The formal errors of all three coordinates of the research platform were found to be approximately 1 cm.

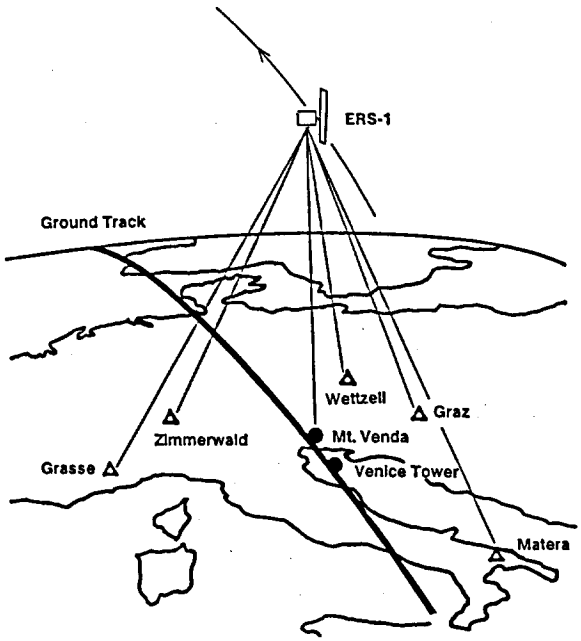

Figure 5-9
Locations of SLR Sites and Platform

In a second step the calibration of the ERS-1 altimeter took place in 1991. From July 31 to September 17 every 3 days a pass of ERS-1 could be used as a calibration pass.

For all these passes different ionospheric observation techniques were used in order to determine the total electron content during the pass and to correct the altimeter measurements for ionospheric refraction:

- *Faraday Rotation Measurements*

The Istituto di Ricerca sulle Onde Elettromagnetiche (IROE) performs TEC determinations on a routine basis using the method of Faraday rotation, providing (vertical) TEC data above the sub-ionospheric point. During the ERS-1 calibration campaign the sub-ionospheric point of the satellite METEOSAT 2 was located at 40.2° North and 8.5° East. The TEC values used for the altimeter calibration were extrapolated from these values using the information

about TEC gradients from GPS and DORIS (see below).

The data of Faraday rotation measurements were not available for the entire ERS-1 altimeter calibration campaign: on August 7 no data were available due to a receiver failure. From August 19 to October 5 METEOSAT 2 underwent equinoctial eclipse producing gaps in the data during the night. During these gaps TEC values have been extrapolated using special methods (for details see Francis et al., 1992).

- ***DORIS (Doppler Orbitography and Radiopositioning Integrated by Satellite)***

DORIS (Lefevbre, 1989; Willis et al., 1990) is a radio-navigation system, which has primarily been designed for precise orbit determination for earth-observation missions like e.g. TOPEX/POSEIDON. DORIS operates on two frequencies (2 GHz and 400 MHz), the signals being sent to the satellite from about 50 ground stations. In the onboard receivers the Doppler shift is integrated over a period of 10 seconds.

Using the two carriers (similar to GPS) a linear combination may be formed which is related to the slant electron content of the ionosphere. This slant electron content is then transformed into the total electron content TEC by multiplication with the cosine of the zenith distance of the signal path at the ionospheric point (assuming a single layer at a height H = 350 km).

The DORIS TEC model consists of a longitude/latitude grid of TEC values and a corresponding interpolation algorithm.

- ***GPS***

During the entire ERS-1 calibration campaign GPS derived ionosphere models have been computed using the program IONEST (see section 4.3).

For the model computations only the data of the receiver on the platform were processed. Two different receiver types were used: during a first period a WM-102 was installed, which had to be replaced by a TRIMBLE ST due to a failure. This explains the short

gap in the availability of the GPS data.

The origin of the development for the ionosphere models was set to the longitude and latitude of the platform, the time origins were always set to 21:00 UT, aproximately the middle of the observation interval. The following development degrees were used for the latitude, the hour angle, and the mixed terms (see section 4.3.1):

- latitude : 1
- hour angle : 2
- mixed terms : 2

The TEC estimates were transformed to ionospheric path delays (in cm) using eqn. (4-1).

Table 5-13 gives an overview over all ionospheric path delays available from the different observation techniques. Figure 5-10 shows a plot of the observed ionospheric path delays as a function of time, and Figure 5-11 shows the sunspot numbers and the solar 10.7 cm flux during the corresponding period.

An interesting result of Table 5-13 is the fact that the path delays determined with the TRIMBLE ST receiver show a better correspondence with the ones of the Faraday rotation technique. This may be due to inter-channel calibration problems of the WM-102 introducing biases in the TEC estimation.

Figure 5-10 shows the ionospheric path delays (cm) as a function of time. The two levels of accuracy become obvious also in this plot. For days 210 - 240 the GPS derived path delays seem to be (in most cases) higher than the values of the other observation techniques. The discrepancy between the values increases with increasing level of solar activity (days 225-240). After day 242 (1 September 1991) the path delays resulting from the different techniques are in agreement on the 1 cm level, an encouraging result indeed.

Date	Day	Faraday Rotation cm	RMS	Instr.	GPS cm	RMS	DORIS cm	cm	Total error
31 Jul	211	3.91	0.6					3.9	1.0
3 Aug	214	1.35	0.6	WM102	2.05	0.1	3.1	2.1	1.0
6 Aug	217			WM102	2.83	0.1	2.2	2.5	0.5
9 Aug	220	3.25	0.5	WM102	4.43	0.1	3.2	3.6	0.8
12 Aug	223	2.08	0.5	WM102	4.29	0.1	1.5	2.6	1.5
15 Aug	226	2.61	0.5	WM102	2.48	0.2	2.6	2.6	0.4
18 Aug	229	4.62	0.5	WM102	3.03	0.1	3.9	3.9	0.8
21 Aug	232	2.50	3.0	WM102	6.43	0.2	3.3	4.1	2.0
24 Aug	235	4.91	3.0	WM102	5.36	0.1	4.9	5.0	0.2
27 Aug	238	4.22	3.0	WM102	7.22	0.2	5.1	5.5	1.5
30 Aug	241	1.89	1.3	WM102	2.65	0.1	2.5	2.3	0.4
2 Sep	244	2.94	1.3					2.9	0.2
5 Sep	247	3.30	1.3					3.3	0.2
8 Sep	250	3.95	2.8	TRIM.ST	3.68	0.1		3.8	0.2
11 Sep	253	2.60	2.8	TRIM.ST	3.40	0.1		3.0	0.4
14 Sep	256	4.37	1.3	TRIM.ST	4.55	0.1		4.5	0.2
17 Sep	259	5.38	1.3	TRIM.ST	4.30	0.1		4.8	0.4

Table 5-13
Ionospheric Measurements and Results Using the Different Techniques for the ERS-1 Calibration (from (Francis et al., 1992))

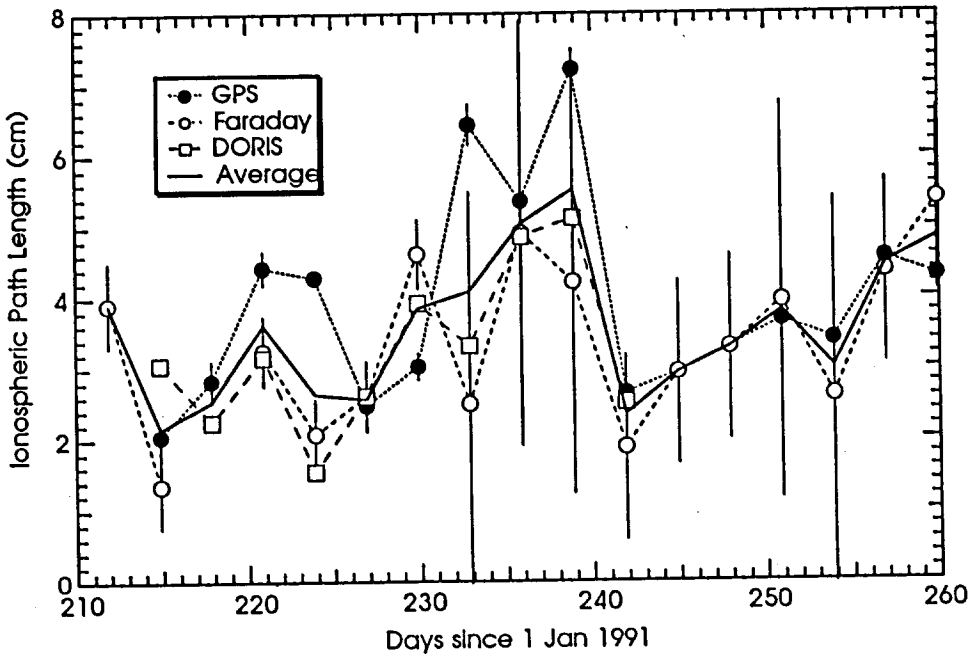

Figure 5-10
Ionospheric Path Delays (cm)
Determined using Different Observation Techniques
Days 210 - 260, 1991

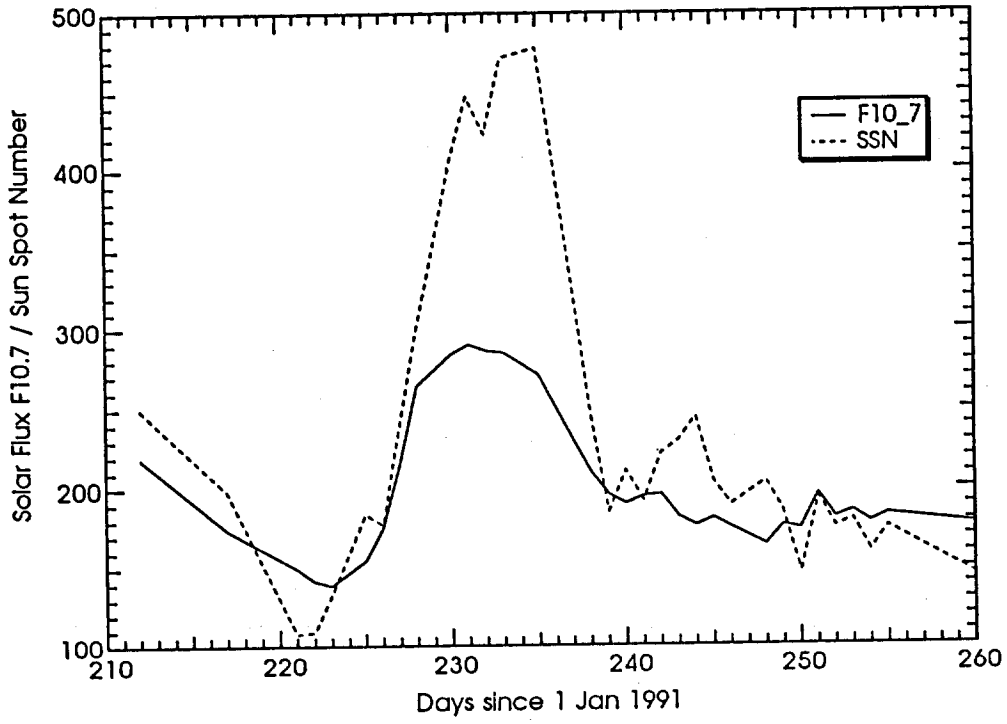

Figure 5-11
Solar Flux (F107) and Sunspot Number (SSN)
Days 210 - 260, 1991

5.1.3 Ionosphere and Ambiguity Resolution

In two cases the ionosphere plays an important role for the ambiguity resolution:

- for long baselines (> 20 km)

- for short baselines (< 5 km) and short observation times (< 5 minutes) (Rapid Static Processing Techniques)

For long baselines the direct resolution for the original L_1 and L_2 ambiguities is usually not possible because of the increasing systematic effects (orbit errors and atmospheric influences). Several authors have proposed methods to solve this problem. An overview over different techniques is given in (Blewitt, 1990).

If dual-frequency P-code receivers are available the best way to resolve the wide-lane ambiguities is to compute the so-called Wübbena-Melbourne observable (a combination of phase and P-code of the two carriers L_1 and L_2) (Melbourne, 1985; Wübbena, 1985), which directly gives the wide-lane ambiguity.

If no dual-frequency P-code receivers are available (as in our case) or if the P-code is not available due to AS then in the Bernese GPS Software Version 3.4 the following procedure is suggested (Rothacher et al., 1993):

(1) If no good a priori coordinates are available:
compute a solution without resolving ambiguities using the ionosphere-free linear combination L_3. This solution will provide good a priori station coordinates.

(2) Compute an L_5 solution (= "wide-lane" linear combination) fixing all stations on the coordinates computed in step (1) (or given by an independent source) and solve for the L_5 ambiguities (differences between the L_1 and L_2 ambiguities). Because of the wavelength of 86 cm (43 cm resp. for squaring type receivers) the ambiguity resolution on L_5 is easier than for the original carriers L_1 and L_2.

(3) Introduce the L_5 ambiguities (= difference between the L_1 and L_2 ambiguities) as known values into an L_3 solution and solve for the remaining L_1 ambiguities.

The problem is the influence of the ionosphere on the L_5 linear combination, although the remaining ionospheric effect in L_5 (if measured in units of the wavelength of L_5) is only -0.28 times the corresponding effect in L_1.

In this chapter we analyze a medium size GPS network and try to answer the following questions:

- Do the computed ionosphere models improve the ambiguity resolution in L_5?

- Is it possible to predict problems in ambiguity resolution on L_5 for baselines of different length using the ionosphere models generated with the data of a permanent tracking station?

In August 1992 the five Swiss stations of the EUREF-89 network were remeasured in a special GPS campaign, called the EUREF-CH-92 campaign (Wiget et al., 1993). The campaign was performed during the EPOCH'92 campaign of IGS (Mueller and Beutler, 1992) in order to benefit from the highest possible orbit accuracy. The main goal of the campaign was to improve the accuracy of the geometry of the five EUREF points in Switzerland. In the final solution of EUREF-89 the ionosphere-free linear combination L3 was used and the ambiguities were not fixed. The overall accuracy of EUREF-89 is reported to be of the order of 3-5 cm (Gurtner et al., 1992). Fixing the ambiguities for all baselines between the EUREF points in Switzerland in the 1992 campaign and using high-accuracy orbits should increase the accuracy to within the 1 cm level. The new Swiss first order GPS network (LV95) (see e.g. (Schneider, 1993)) will be transformed into this improved reference frame.

Figure 5-12 shows the LV95 network and the 5 EUREF stations (bold). A total of 6 Trimble receivers was used in the EUREF-CH-92 campaign:

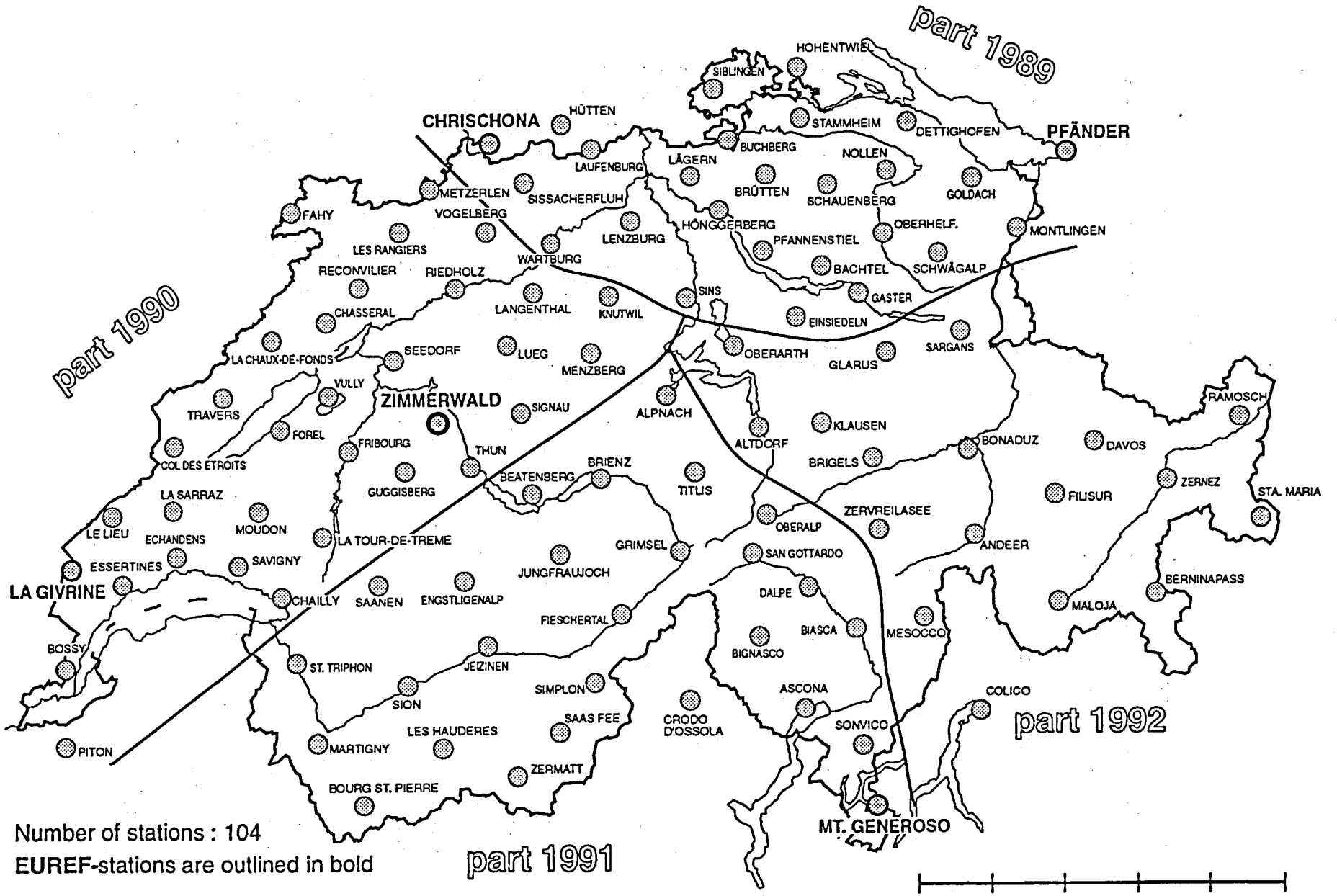

Figure 5-12

The New GPS Network in Switzerland

4 Trimble 4000SLD (operating in the old so-called 'Standard Format', where the observation epochs may differ from the full second by up to 256 milliseconds) and two Trimble 4000SST (observing in the 'Compact Format', where the observation epoch corresponds to full GPS seconds). Under SA (see section 2.1.3) data from two receivers measuring in different observation formats may no longer be combined because the behaviour of the satellite clock may not be modelled accurately enough between the two observation epochs. This problem could be resolved by operating two receivers of the two types at the SLR site Zimmerwald. We then formed the baselines of Table 5-14:

Station 1	Station 2	Receiver 1	Receiver 2	Length (km)
Zimmerwald	Mt. Generoso	4000SST	4000SST	185
Zimmerwald	Chrischona	4000SLD	4000SLD	78
Zimmerwald	Pfänder	4000SLD	4000SLD	232
Zimmerwald	La Givrine	4000SLD	4000SLD	114

Table 5-14
Baselines of the EUREF-CH-92 Campaign

Two sessions per day were scheduled and observed: session 1 from 08:15-19:45 (local time) and session 2 from 20:00-08:00. The elevation mask was set to 15°, the observation interval to 30 seconds.

For all days of the EUREF-CH-92 campaign the program IONMAP (see section 4.4) has been used to generate 6 single-layer ionosphere models per day (each of them valid for 4 hours). Two variants of ionosphere models were computed: the first one using the data of the permanent GPS tracking station Zimmerwald only and a second one using the data of all 5 stations in the network.

To describe the ionospheric conditions during the EUREF-CH-92 campaign the TEC values for 02:00, 06:00, 10:00, 14:00, 18:00, 22:00 UT (interval mids of the 6 daily models) for each of the 5 days (computed from the data of the station Zimmerwald) are given in Table 5-15.

Day	TEC values (in TECU)					
	02:00	06:00	10:00	14:00	18:00	22:00
216	5.5	15.1	14.8	18.8	22.5	13.1
217	8.0	14.3	17.8	24.0	27.2	14.8
218	10.0	14.3	15.9	19.4	17.9	11.8
219	9.4	17.8	26.1	27.1	21.0	13.1
220	6.4	12.9	19.6	20.0	18.4	11.3
221	5.5	4.5	98.3	20.1	21.6	17.8

Table 5-15
TEC Values
EUREF-CH Campaign (3 - 8 August 1992)

The TEC values show a very regular daily pattern for all days (minimum during the night and a maximum between 14:00 and 18:00). The TEC value for day 221 at 10:00 is an outlier caused by a very small number of observations. The overall behaviour may be considered as typical for mid-latitude ionospheric conditions.

The irregular part of the ionosphere has been visualized by showing the L_4 residuals of the modelling step and the changes in the residuals per 30 seconds (see Figures 5-13a and 5-13b).

The irregular part of the ionosphere shows the same homogeneous behaviour for all days as the regular part. The amplitude of the L_4 residuals is of the order of 15-20 cm (with maximum values of 30 cm). Since the stochastic part of the ionosphere is not very critical for longer observation sessions we will now focus on the systematic part.

For the ambiguity resolution on L_5 all unmodelled systematic influences (like orbits, clocks, and ionosphere) will result in increased fractional parts of the ambiguities. In our case the syste-

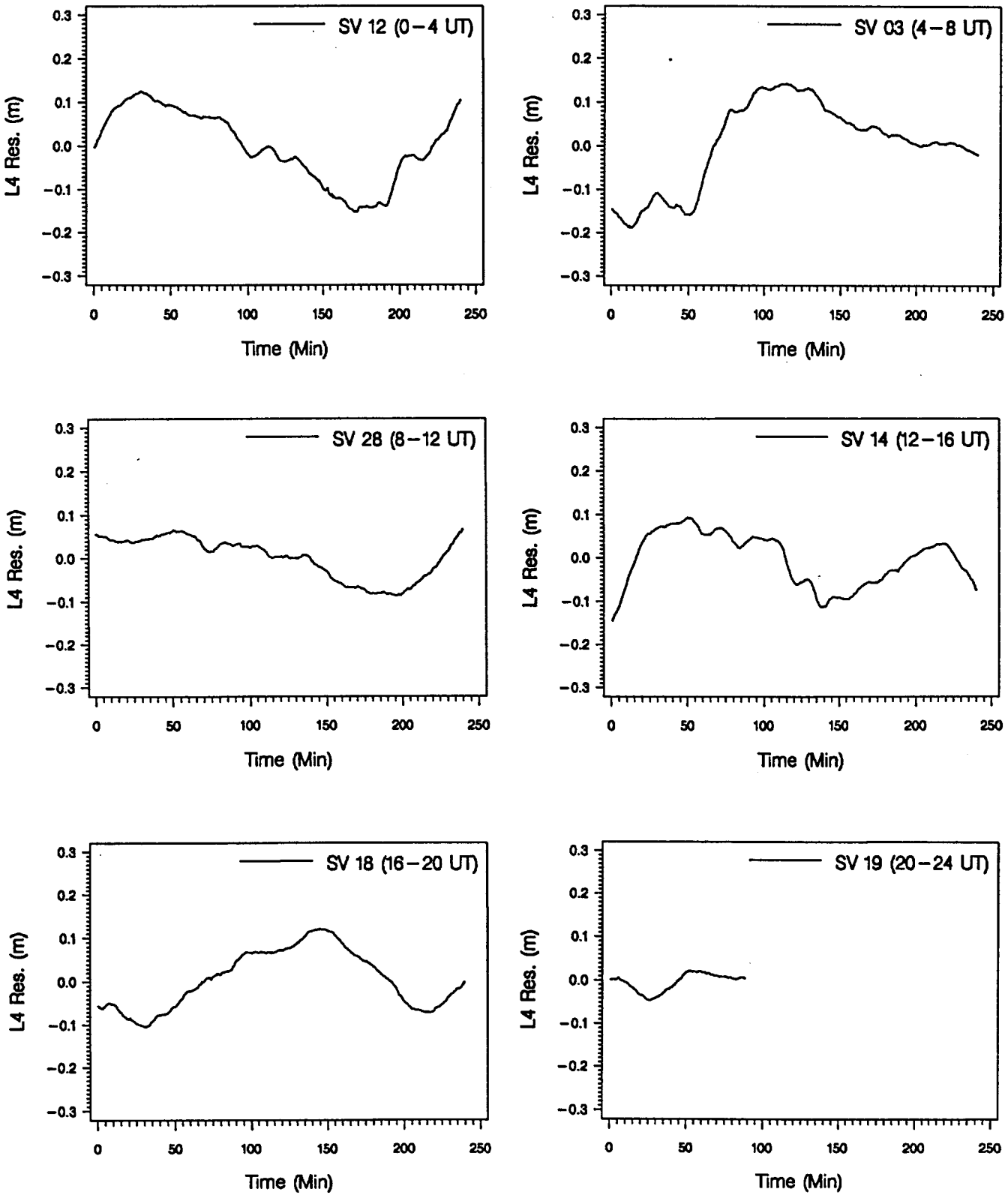

Figure 5-13a

L_4 Residuals for Different Satellites

EUREF-CH-92 Campaign, 4 August 1992 (Day 217)

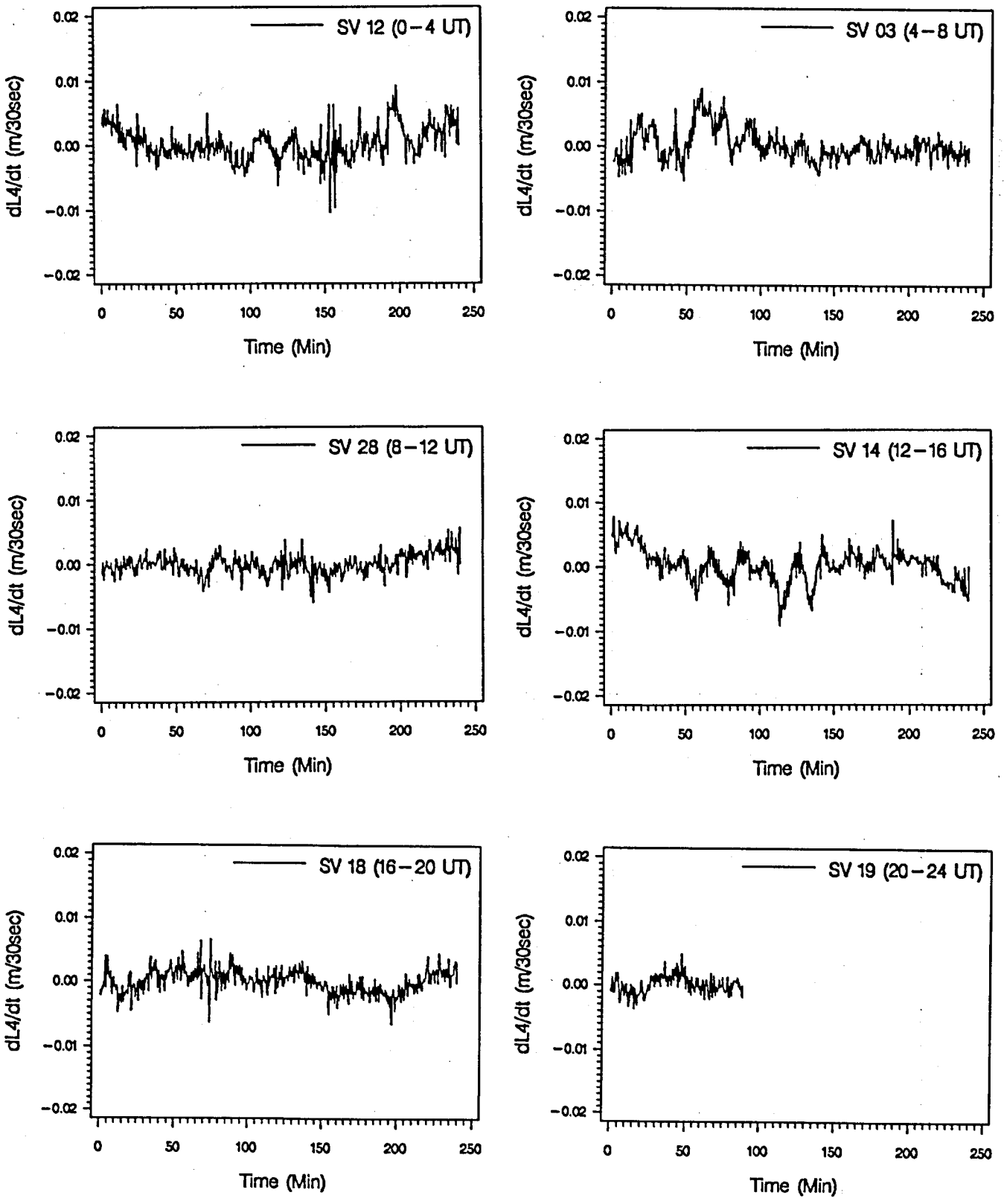

Figure 5-13b

Changes in L_4 Residuals per 30 Seconds

EUREF-CH-92 Campaign, 4 August 1992 (Day 217)

matic influence of orbit errors may be considered neglectible, since we are using very accurate IGS orbits. In order to test the efficiency of the ionosphere models we therefore directly compare the fractional parts of the L_5 ambiguities computed without and with ionosphere models.

We compared the fractional parts using different minimum elevation angles (15°, 20°, 25°, and 30°) in order to study at the same time the elevation dependency of the ambiguity resolution on L_5. In the comparison we made the distinction between the full wavelength receivers (Trimble 4000SST) and the squaring type receivers (Trimble 4000SLD). In addition two types of ionosphere models were applied: a first type based only on the data from the permanent GPS tracking station Zimmerwald and a second type based on the data of all stations in the network.

Figures 5-14 - 5-17 show the histograms of the fractional parts of the L_5 ambiguities of all days for the squaring type receivers (for different elevations and using two types of ionosphere models), Figures 5-18 - 5-21 the corresponding fractional parts for the full wavelength receiver.

We first note that the fractional parts of the L_5 ambiguities are significantly smaller when ionosphere models are used. No significant differences between the two types of ionosphere models could be observed. This indicates that the data of one permanent tracking station are sufficient to compute ionosphere models which can be used (at least over distances of 200-300 km) to improve the ambiguity resolution on L_5. It becomes obvious that the best value for the elevation for the ambiguity resolution on L_5 is 20°, whereas higher minimum elevations do no longer improve the ambiguity resolution. The major part of the histograms in Figures 5-14 to 5-21 show an asymmetry with respect to zero, which is caused by the ar-

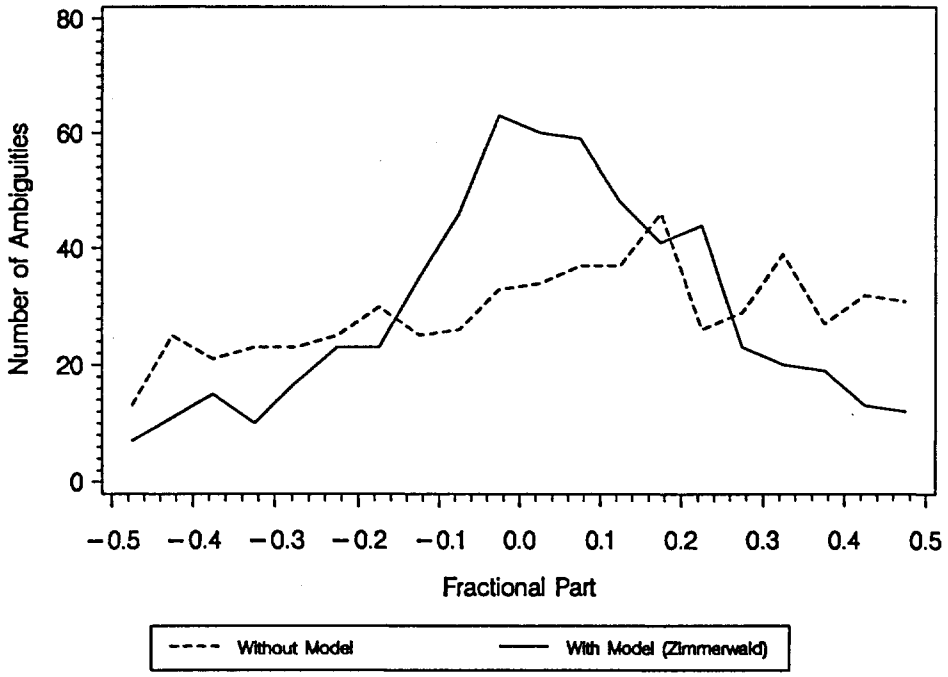

Figure 5-14a

Fractional Parts of L_5 Ambiguities, Elevation = 15°

Ionosphere Model: Zimmerwald, Half Wavelength on L_5

EUREF-CH-92 Campaign (3 - 8 August 1992)

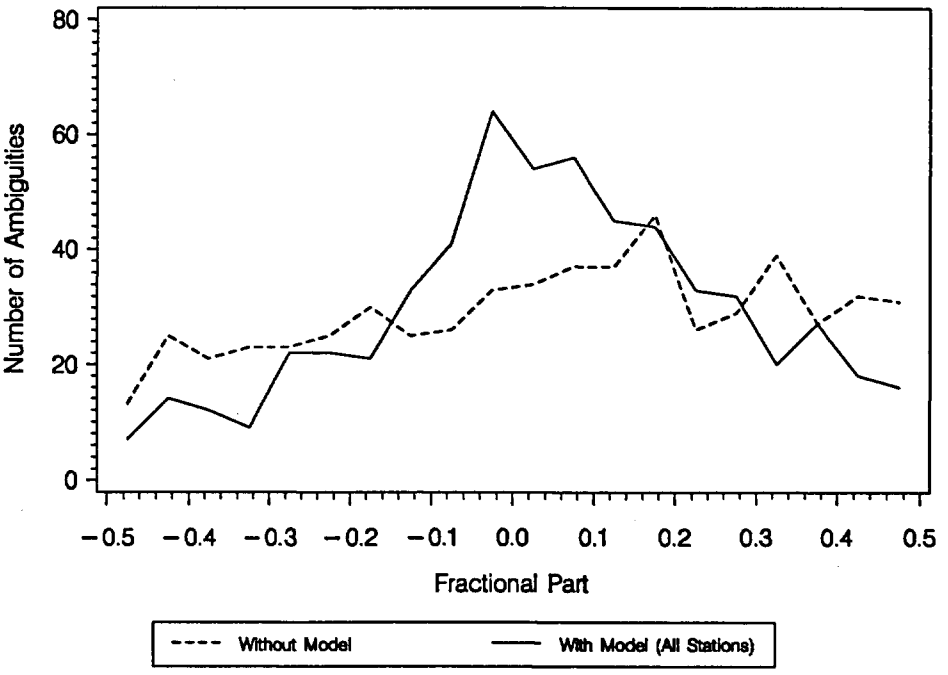

Figure 5-14b

Fractional Parts of L_5 Ambiguities, Elevation = 15°

Ionosphere Model: All Stations, Half Wavelength on L_5

EUREF-CH-92 Campaign (3 - 8 August 1992)

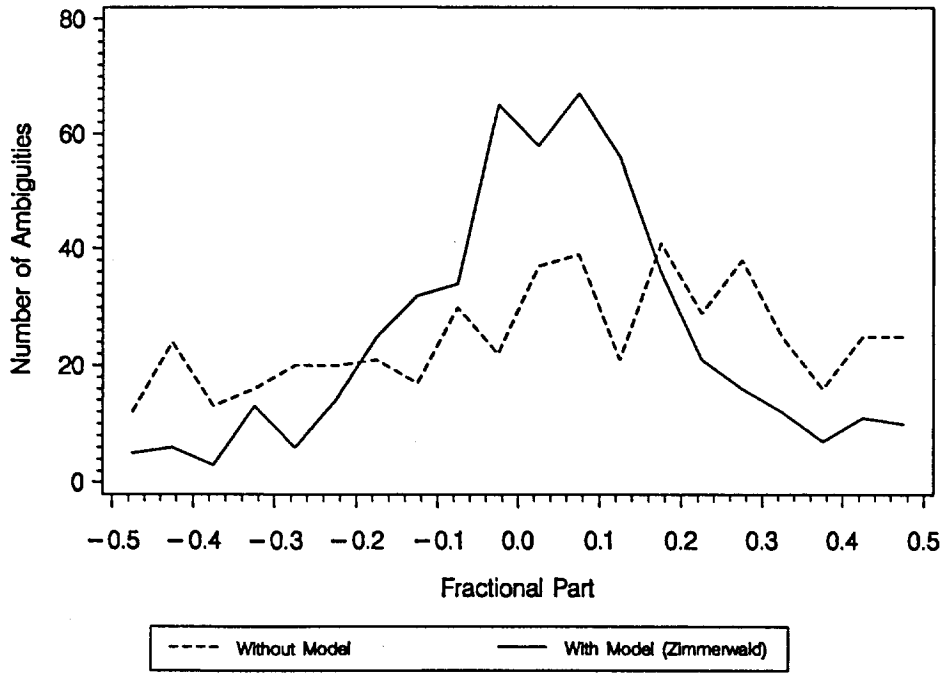

Figure 5-15a

Fractional Parts of L_5 Ambiguities, Elevation = 20°

Ionosphere Model: Zimmerwald, Half Wavelength on L_5

EUREF-CH-92 Campaign (3 - 8 August 1992)

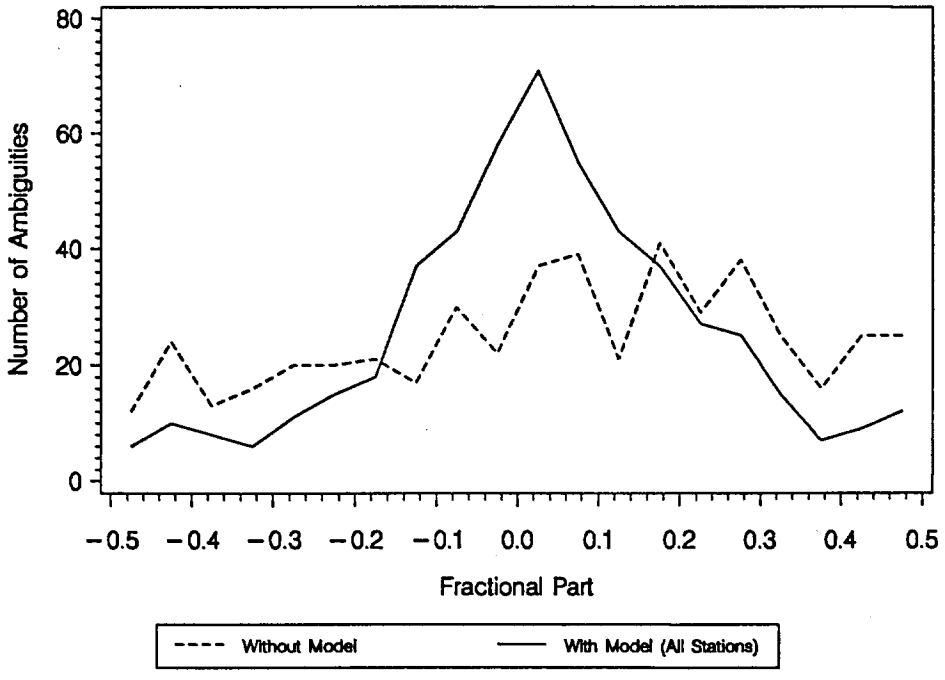

Figure 5-15b

Fractional Parts of L_5 Ambiguities, Elevation = 20°

Ionosphere Model: All Stations, Half Wavelength on L_5

EUREF-CH-92 Campaign (3 - 8 August 1992)

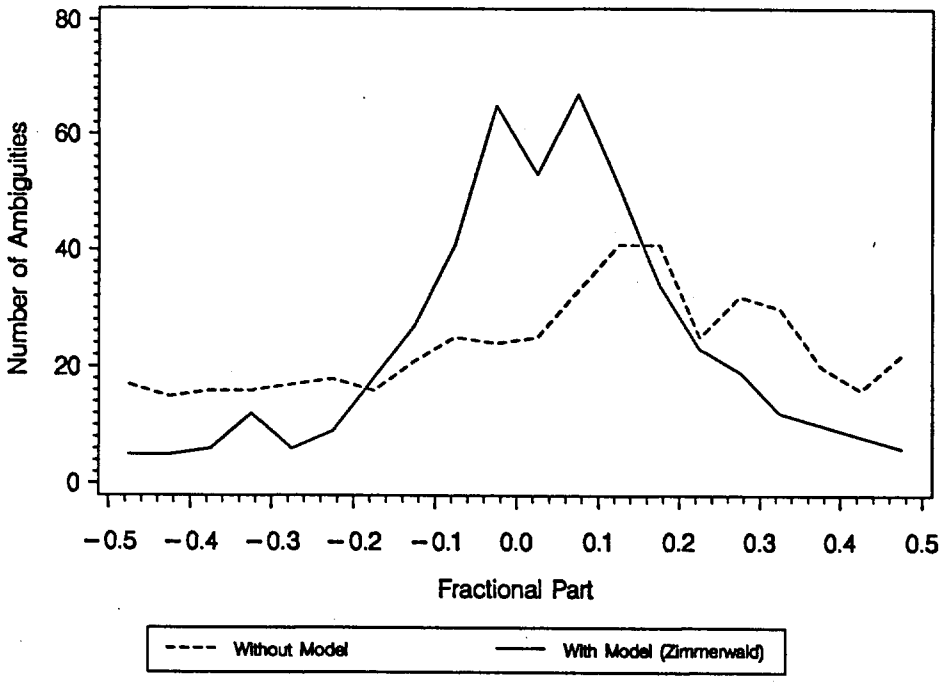

Figure 5-16a

Fractional Parts of L_5 Ambiguities, Elevation = 25°
Ionosphere Model: Zimmerwald, Half Wavelength on L_5
EUREF-CH-92 Campaign (3 - 8 August 1992)

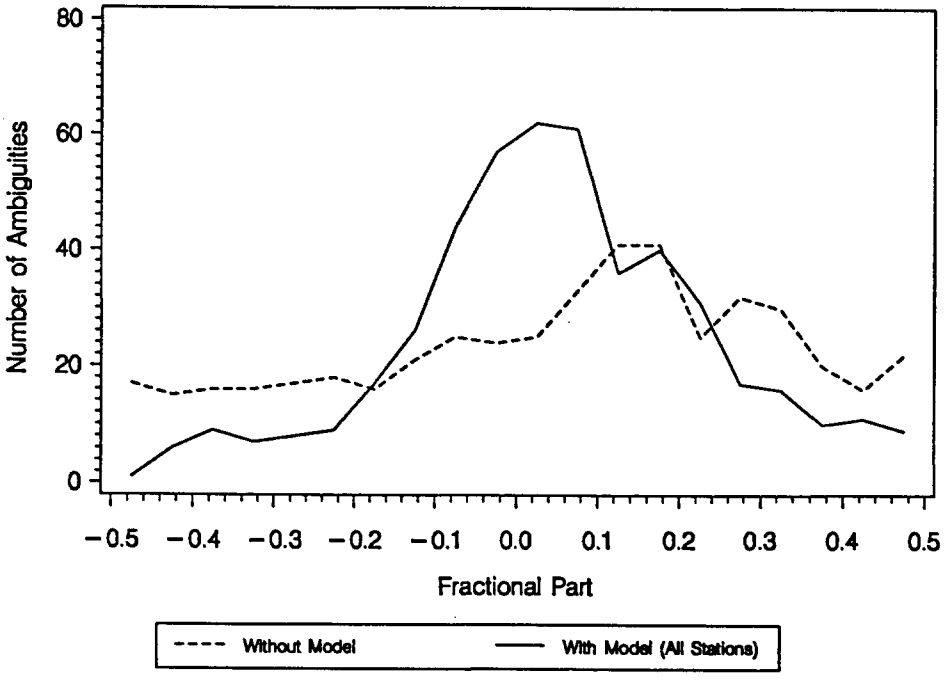

Figure 5-16b

Fractional Parts of L_5 Ambiguities, Elevation = 25°
Ionosphere Model: All Stations, Half Wavelength on L_5
EUREF-CH-92 Campaign (3 - 8 August 1992)

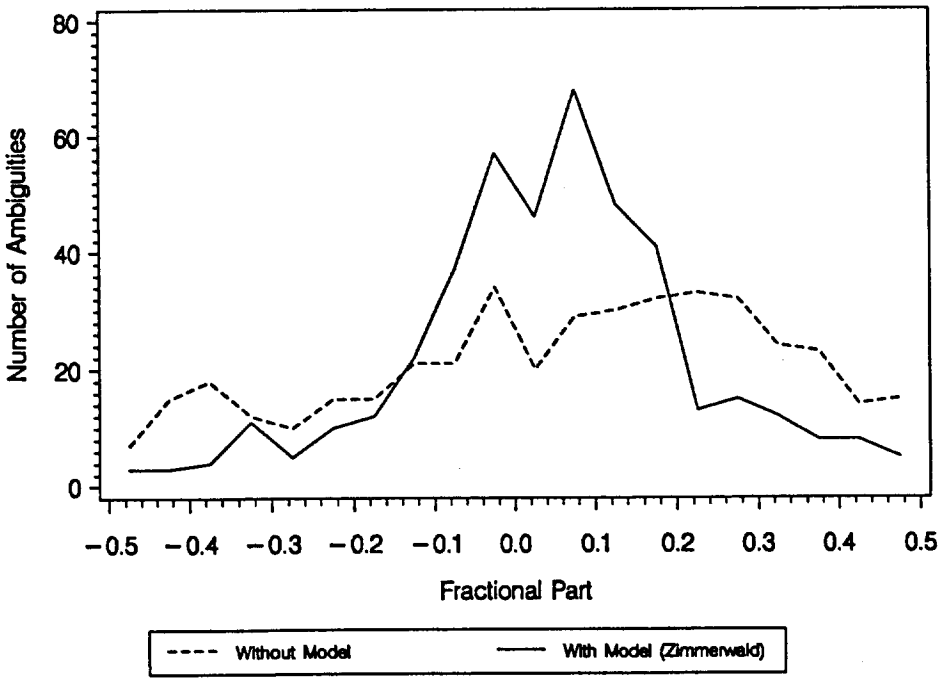

Figure 5-17a

Fractional Parts of L_5 Ambiguities, Elevation = 30°

Ionosphere Model: Zimmerwald, Half Wavelength on L_5

EUREF-CH-92 Campaign (3 - 8 August 1992)

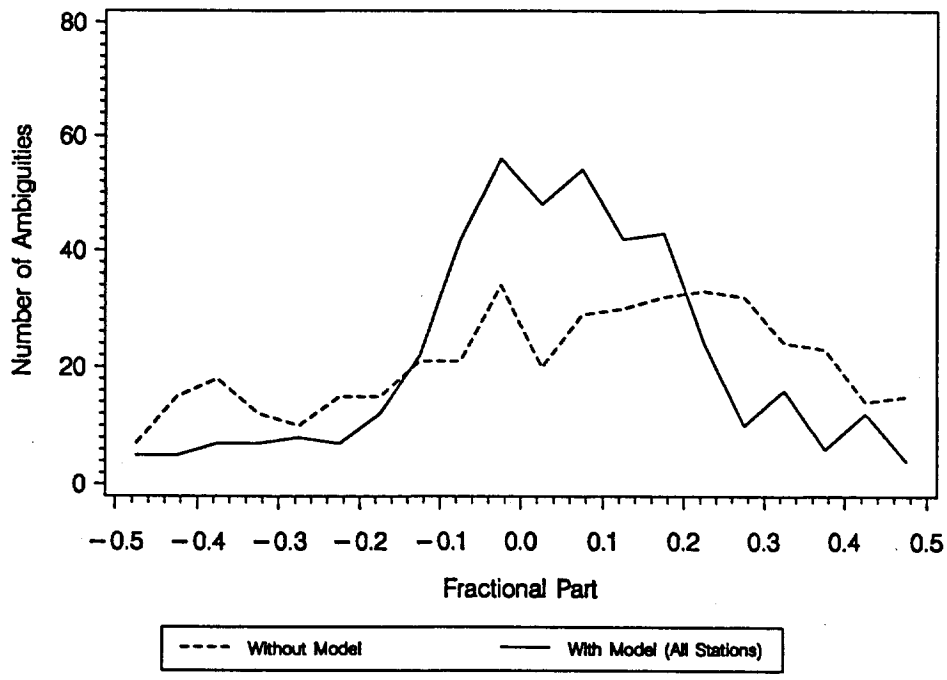

Figure 5-17b

Fractional Parts of L_5 Ambiguities, Elevation = 30°

Ionosphere Model: All Stations, Half Wavelength on L_5

EUREF-CH-92 Campaign (3 - 8 August 1992)

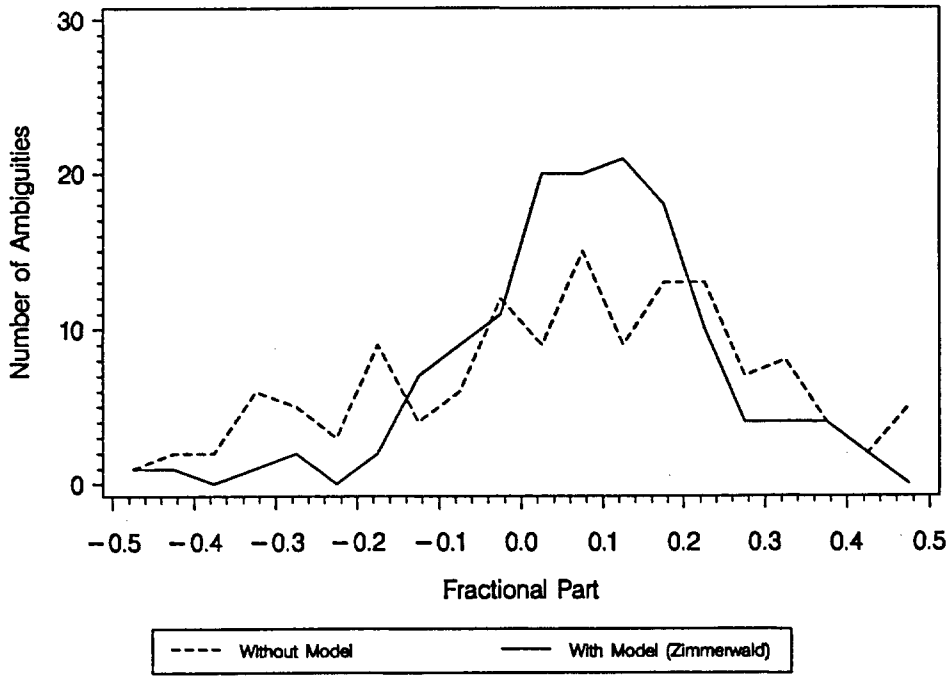

Figure 5-18a

Fractional Parts of L_5 Ambiguities, Elevation = 15°
Ionosphere Model: Zimmerwald, Full Wavelength on L_5
EUREF-CH-92 Campaign (3 - 8 August 1992)

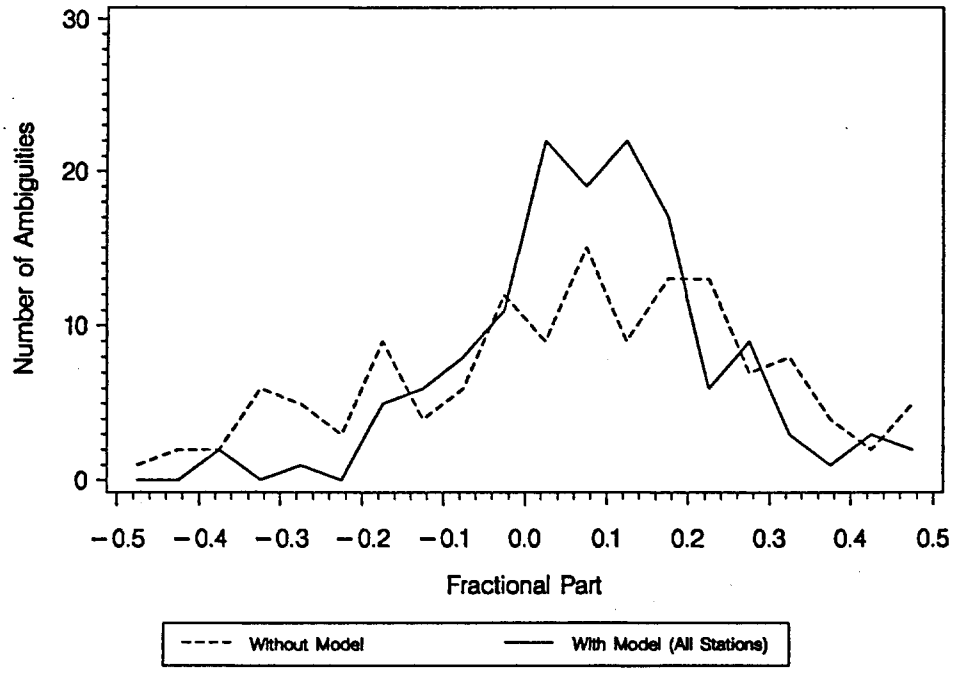

Figure 5-18b

Fractional Parts of L_5 Ambiguities, Elevation = 15°
Ionosphere Model: All Stations, Full Wavelength on L_5
EUREF-CH-92 Campaign (3 - 8 August 1992)

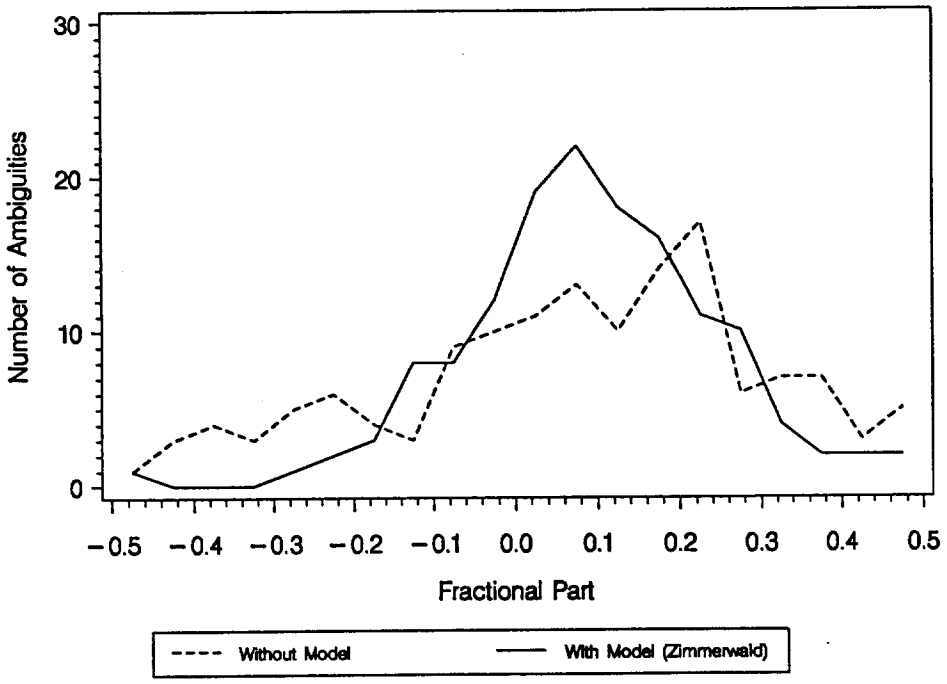

Figure 5-19a

Fractional Parts of L_5 Ambiguities, Elevation = 20°
Ionosphere Model: Zimmerwald, Full Wavelength on L_5
EUREF-CH-92 Campaign (3 - 8 August 1992)

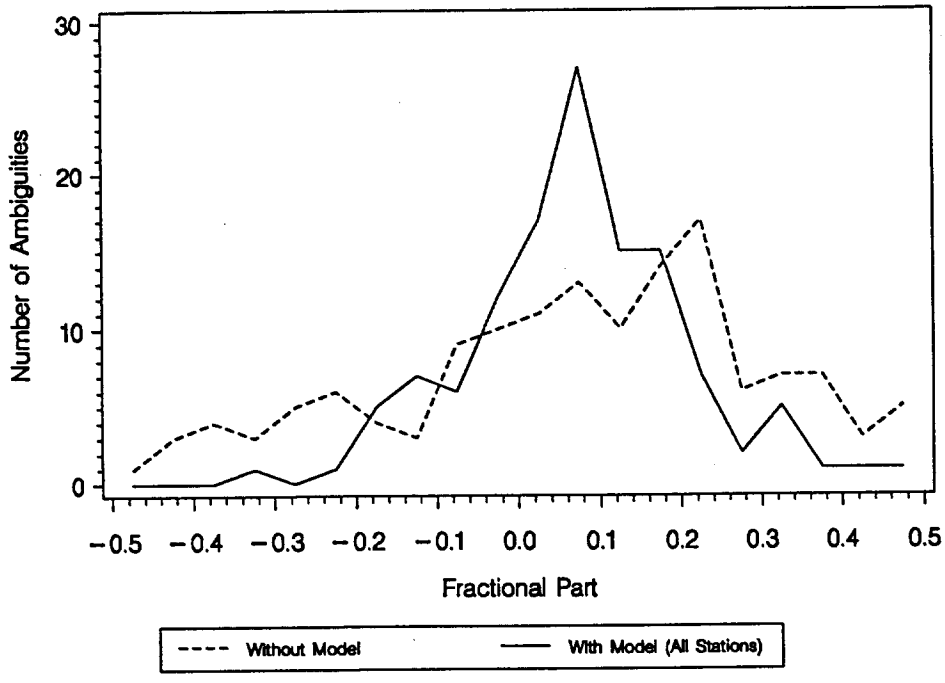

Figure 5-19b

Fractional Parts of L_5 Ambiguities, Elevation = 20°
Ionosphere Model: All Stations, Full Wavelength on L_5
EUREF-CH-92 Campaign (3 - 8 August 1992)

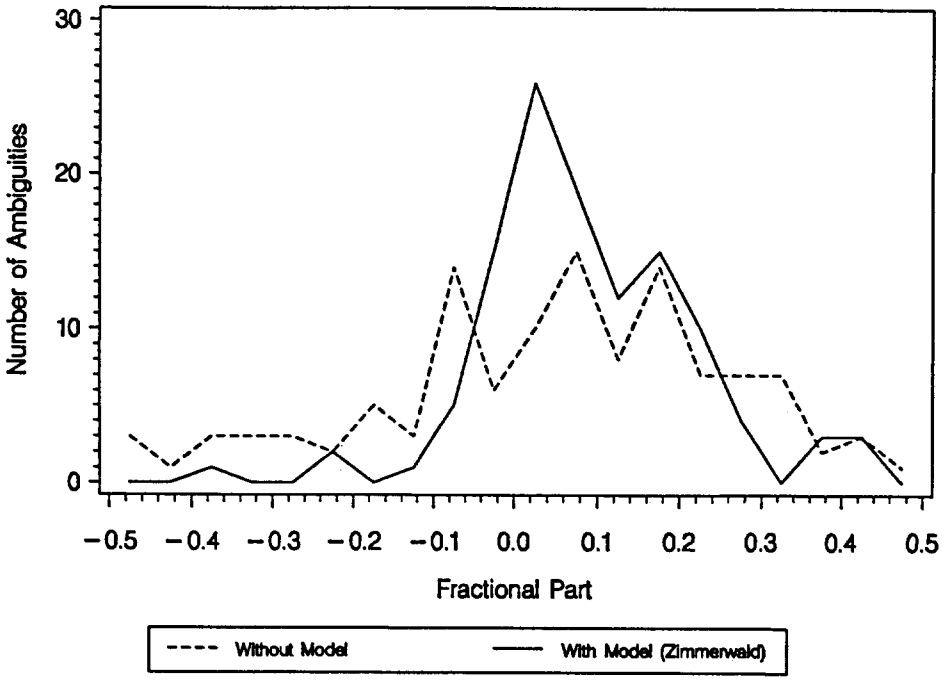

Figure 5-20a

Fractional Parts of L_5 Ambiguities, Elevation = 25°
Ionosphere Model: Zimmerwald, Full Wavelength on L_5
EUREF-CH-92 Campaign (3 - 8 August 1992)

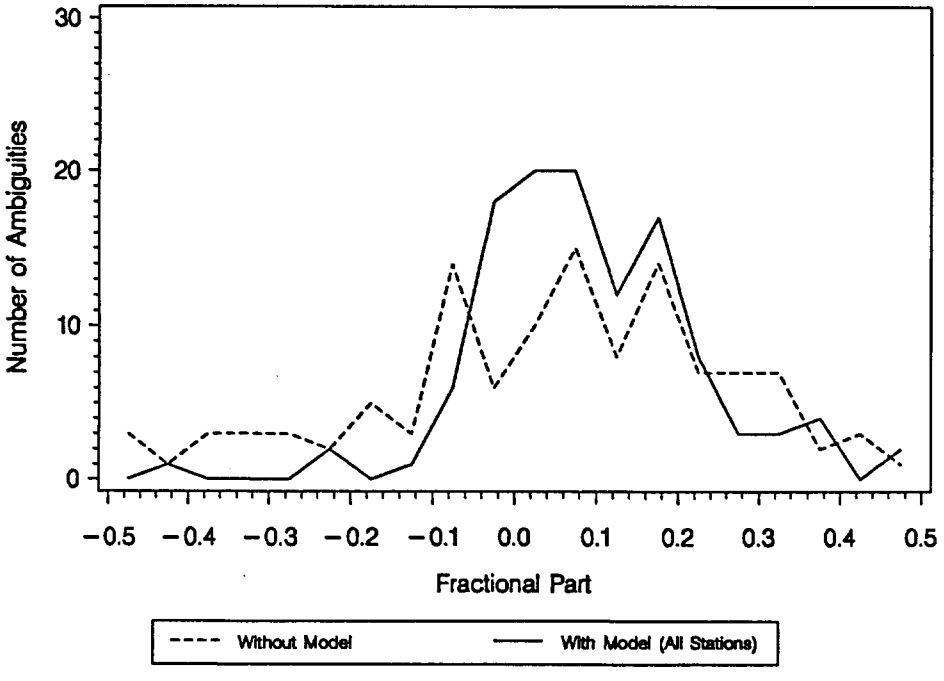

Figure 5-20b

Fractional Parts of L_5 Ambiguities, Elevation = 25°
Ionosphere Model: All Stations, Full Wavelength on L_5
EUREF-CH-92 Campaign (3 - 8 August 1992)

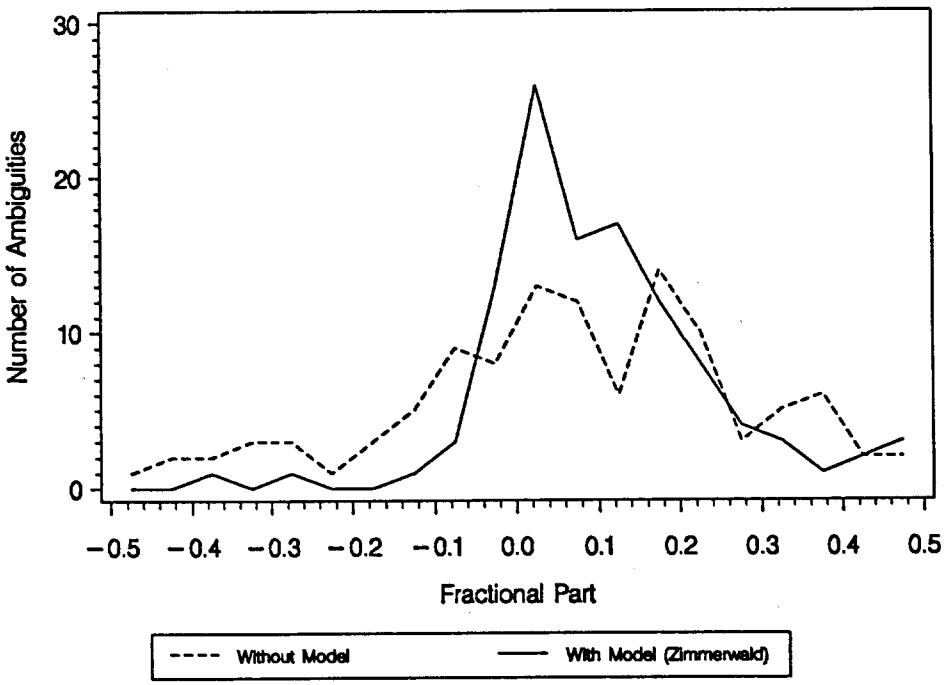

Figure 5-21a

Fractional Parts of L_5 Ambiguities, Elevation = 30°
Ionosphere Model: Zimmerwald, Full Wavelength on L_5
EUREF-CH-92 Campaign (3 - 8 August 1992)

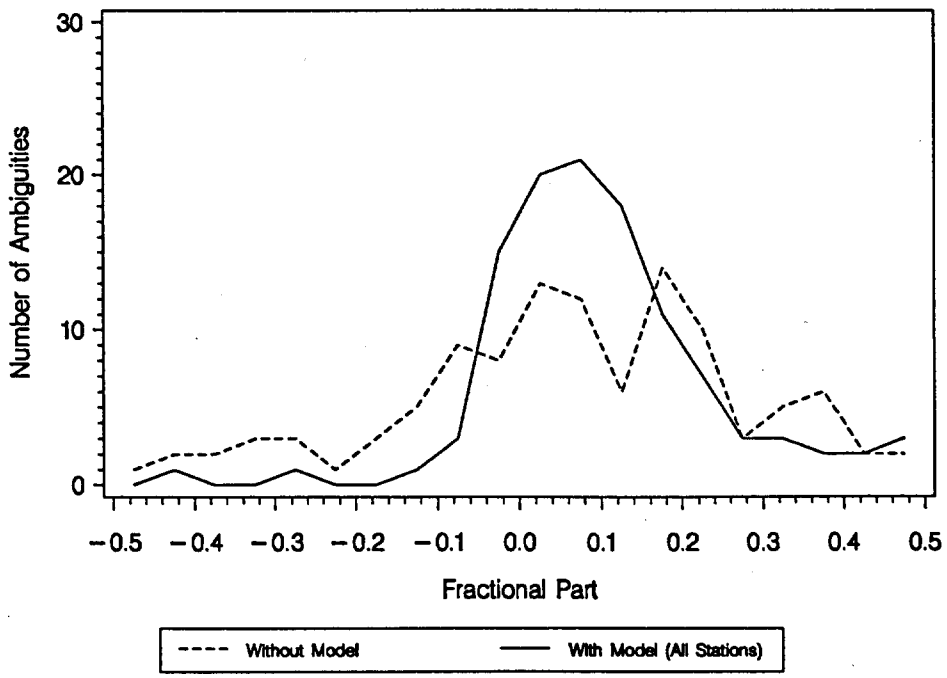

Figure 5-21b

Fractional Parts of L_5 Ambiguities, Elevation = 30°
Ionosphere Model: All Stations, Full Wavelength on L_5
EUREF-CH-92 Campaign (3 - 8 August 1992)

bitrary choice of a reference satellite in the ambiguity definition. This reference satellite may be biased by different error sources (troposphere or residual ionospheric effects).

Different ambiguity resolution strategies were developped and tested at the AIUB (Mervart et al., 1993). In the "classical" ambiguity resolution approach (used at the AIUB) all ambiguities are estimated as real values in a first step and then set to integers using a 3-sigma criterion in a second step. A new method (called the iterative approach) also estimates the ambiguities as real values first, but then, in a first iteration step, just resolves the n ambiguities (where n is an input option) with the smallest rms. Then the procedure is repeated with the previously solved n ambiguities introduced as integer numbers.

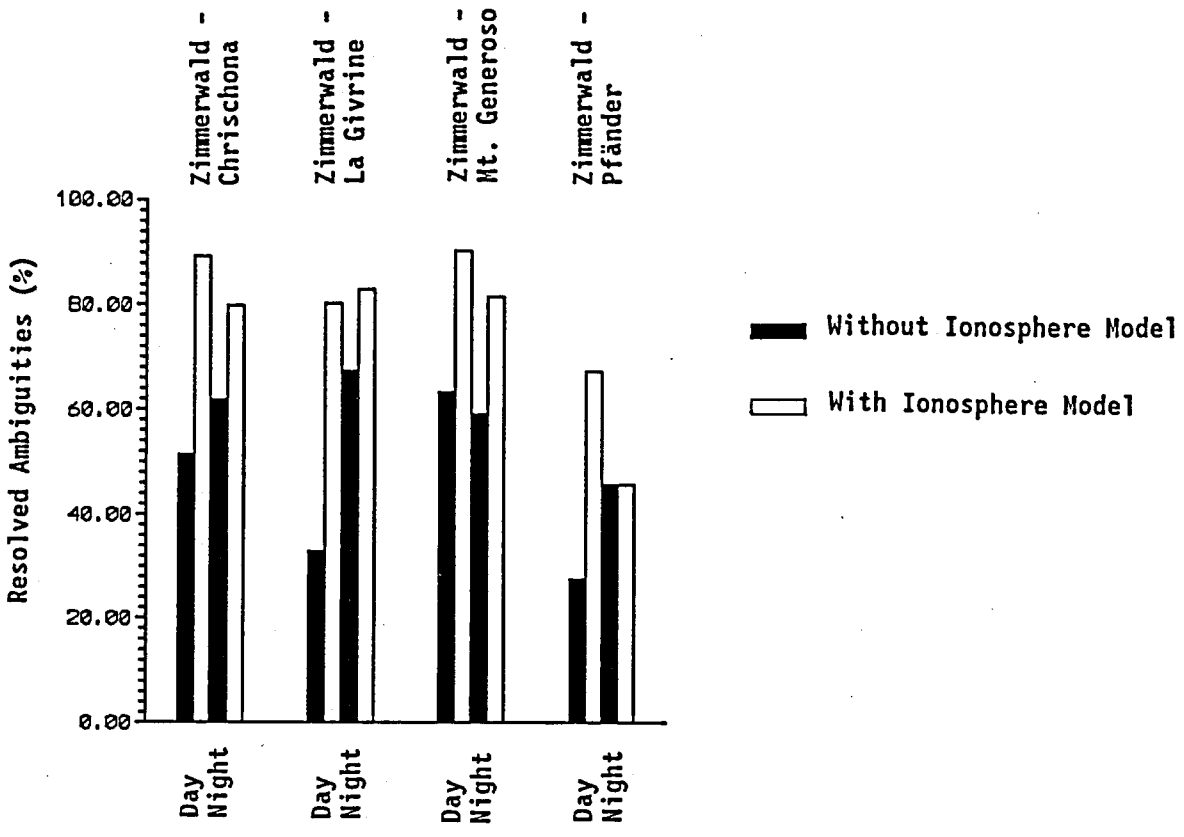

Figure 5-22

L_5 Ambiguity Resolution ("Classical" Approach)

EUREF-CH-92 Campaign (3 - 8 August 1992)

Both techniques have been tested for the EUREF-CH-92 campaign. No major difference between the two strategies could be observed, which indicates that the problems in the ambiguity resolution are caused by the systematic influences of the ionosphere and not by the resolution method. Figure 5-22 shows the benefit of ionosphere models for the L_5 ambiguity resolution (using the "classical" approach) for all baselines and all days (splitted up in day and night sessions). For the 3-sigma criterion a sigma value of 0.08 has been used, the minimum elevation was set to 20°. As ionosphere models the models with the data of the station Zimmerwald were used.

One may note that the ionosphere models considerably improve the wide-lane ambiguity resolution during the day, whereas the benefit is less pronounced during the night (in some cases even more ambiguities are resolved without ionosphere models). It is also obvious that the percentage of resolved ambiguities decreases with increasing baseline length.

In a next step we tried to answer the question whether problems in the ambiguity resolution may be predicted using single-layer ionosphere models.

The most important influence of the ionosphere on the ambiguity resolution are the unmodelled gradients of the total electron content between the two end points of the baseline. The total vertical electron contents are again computed using the program TECVAL (see section 4.5), which needs as input an ionosphere model and the coordinates of the involved stations. The gradients may roughly be approximated by the difference of the total electron contents (in the zenith direction) above the considered stations. We then may compute the influence of the ionosphere on a single-difference L_5 observation as follows:

$$I_5 = \varkappa \cdot (dI_1 - dI_2) \qquad (5\text{-}2)$$

where I_5: Influence of unmodelled gradients in the total electron content on an L_5 single-difference L_5 observation

x : Factor to transform from L_4 to L_5

$$x = \frac{f_1 \cdot f_2}{f_1^2 - f_2^2}$$

$$dI_1 = -40.3 \cdot 10^{16} \cdot TVEC_1 \cdot \left(\frac{1}{f_1^2} - \frac{1}{f_2^2} \right) :$$

Influence of the ionosphere on an L_4 (zero-difference) observation from station 1

$$dI_2 = -40.3 \cdot 10^{16} \cdot TVEC_2 \cdot \left(\frac{1}{f_1^2} - \frac{1}{f_2^2} \right) :$$

Influence of the ionosphere on an L_4 (zero-difference) observation from station 2

$TVEC_1$: Total vertical electron content above station 1 (in TECU)
$TVEC_2$: Total vertical electron content above station 2 (in TECU)
f_1 : Frequency of carrier L_1
f_2 : Frequency of carrier L_2

Table 5-16 shows the estimated influences of the ionosphere (I_5) on a single-difference L_5 observation for a satellite with an elevation of 45°, i.e. the zenith values have been divided by the cosine of 45°. In order to give an impression of the time dependency (difference between day and night) the values are given for different times of the day (interval mids in UT of the 4 hour ionosphere models).

The order of magnitude for the influence of the ionosphere on single-difference L_5 observations seems to be 10-15 cm during the night and 15-30 cm during the day. The effect on a double-difference L_5 observation results from an arbitrary superposition of two satellites, which may have opposite signs for their single-difference ionospheric corrections, i.e. by forming the double-diffe-

rence the influence of the ionosphere may either be subtracted or added. The noise of the double-difference will be amplified by a factor of 1.4 with respect to the corresponding single-difference observation. Looking at the values in Table 5-16 we may therefore expect problems in ambiguity resolution specially for the sessions during the day, whereas during the night more ambiguities should be resolvable. The size of the I_5 values is about 50-60 % of an L_5

Day	Station 1	Station 2	I_5 (in m) 02:00	06:00	10:00	14:00	18:00	22:00
216	Z'wald	Mt. Generoso	-0.09	-0.23	-0.13	-0.28	-0.09	-0.03
		Chrischona	0.07	0.10	0.10	0.18	-0.08	0.07
		Pfänder	0.06	0.00	0.11	0.13	0.10	0.14
		La Givrine	-0.04	-0.01	-0.07	-0.09	-0.07	-0.09
217	Z'wald	Mt. Generoso	-0.06	-0.17	-0.17	-0.31	-0.14	-0.05
		Chrischona	0.06	0.05	0.10	0.22	0.11	0.10
		Pfänder	0.06	-0.06	0.06	0.19	0.11	0.18
		La Givrine	-0.05	0.04	-0.04	-0.13	-0.07	-0.11
218	Z'wald	Mt. Generoso	-0.08	-0.25	-0.34	-0.30	-0.12	-0.15
		Chrischona	0.10	0.13	0.22	0.24	0.12	0.13
		Pfänder	0.14	0.06	0.14	0.24	0.16	0.16
		La Givrine	-0.09	-0.03	-0.11	-0.16	-0.11	-0.10
219	Z'wald	Mt. Generoso	-0.15	-0.08	-0.13	-0.26	-0.11	-0.08
		Chrischona	0.12	-0.04	0.04	0.22	0.14	0.11
		Pfänder	0.11	-0.20	-0.05	0.26	0.23	0.17
		La Givrine	-0.08	0.12	0.03	-0.17	-0.14	-0.11
220	Z'wald	Mt. Generoso	-0.15	-0.15	-0.30	-0.31	-0.13	-0.13
		Chrischona	0.14	0.05	0.16	0.26	0.12	0.15
		Pfänder	0.15	-0.04	0.05	0.27	0.14	0.21
		La Givrine	-0.11	0.03	-0.03	-0.18	-0.09	-0.13

Table 5-16
Influence of the Ionosphere on Single-Sifference Observations in L_5 (For a Mean Elevation of 45°)

cycle in the present case, where squaring type receivers have been used reducing the wavelength of the L_5 linear combination to 43 cm.

Comparing the quadratic mean of the I_5 values in Table 5-16 with the quadratic mean (over all satellites) of the fractional parts of the L_5 ambiguities (see Table 5-17) one may note that the order of magnitude of these fractional parts may be predicted by using one single-layer ionosphere model.

Day	Session	RMS of Fractional Parts of L_5 Ambiguities (in cm)	Predicted I_5 Values (Mean Elevation = 45°) (in cm)
216	1	9.4	12.8
	2	9.6	6.3
217	1	11.1	13.8
	2	12.6	11.0
218	1	13.0	18.8
	2	12.6	12.0
219	1	13.1	14.8
	2	8.2	10.7
220	1	11.5	17.0
	2	10.3	15.5

Table 5-17
Comparison Between RMS of the Fractional Parts of the L_5 Ambiguities and the Predicted Influence I_5 of the Ionosphere

There is no strong correlation between the two columns in Table 5-17. However, one may note that the orders of magnitude for the influence of the ionosphere on a double-difference L_5 observation may be predicted well using single-layer ionosphere models and the procedure described above.

A second application of ionosphere models for ambiguity resolution is given when resolving ambiguities using short observation intervals (Fast Ambiguity Resolution Approach (FARA), see (Frei, 1991)). For the applications discussed above (long observation time spans) the main influence of the ionosphere are the gradients of the total electron contents, whereas the short period variations of the ionosphere do not affect the ambiguity resolution. This situation is different for FARA applications where short period variations of the ionosphere affect the ambiguity resolution because of the short observation intervals of up to several minutes only.

The application of ionosphere models for the FARA method is a current research topic of the AIUB and is not discussed in this context.

5.2. Monitoring the Ionosphere using GPS

5.2.1 The Test Data Set

The **International GPS Service for Geodynamics (IGS)** (Mueller and Beutler, 1992) has been organized by the International Association of Geodesy (IAG). The main goals of the IGS are

- the generation of precise ephemerides for the GPS satellites,
- the determination of earth rotation parameters,
- the determination of GPS clock information,
- to establish standards for GPS equipment, site selection, data analysis etc. for the increasing number of scientists using GPS, and
- to investigate the behaviour of the ionosphere.

We will address this last point only which so far was not yet studied in detail.

The data acquisition network of the IGS is divided into two categories, namely

a) the **Core Network**, comprising about 30 globally distributed sites which are permanently operated

and

b) the **Fiducial Network**, consisting of about 100-200 stations. These fiducial stations are not operated permanently, but only during special campaigns (so-called Epoch Campaigns, for about 2 weeks per year).

Figure 5-23 shows the Core Network as it was realized in 1992. All stations which are automatically processed for the ionosphere models (see below) are underlined.

The data collected at the observatories (core or fiducial stations) are transmitted to the so-called **operational data centers**, where the data are transferred into the receiver-independent exchange format RINEX (Gurtner et al., 1989), then they are passed to the

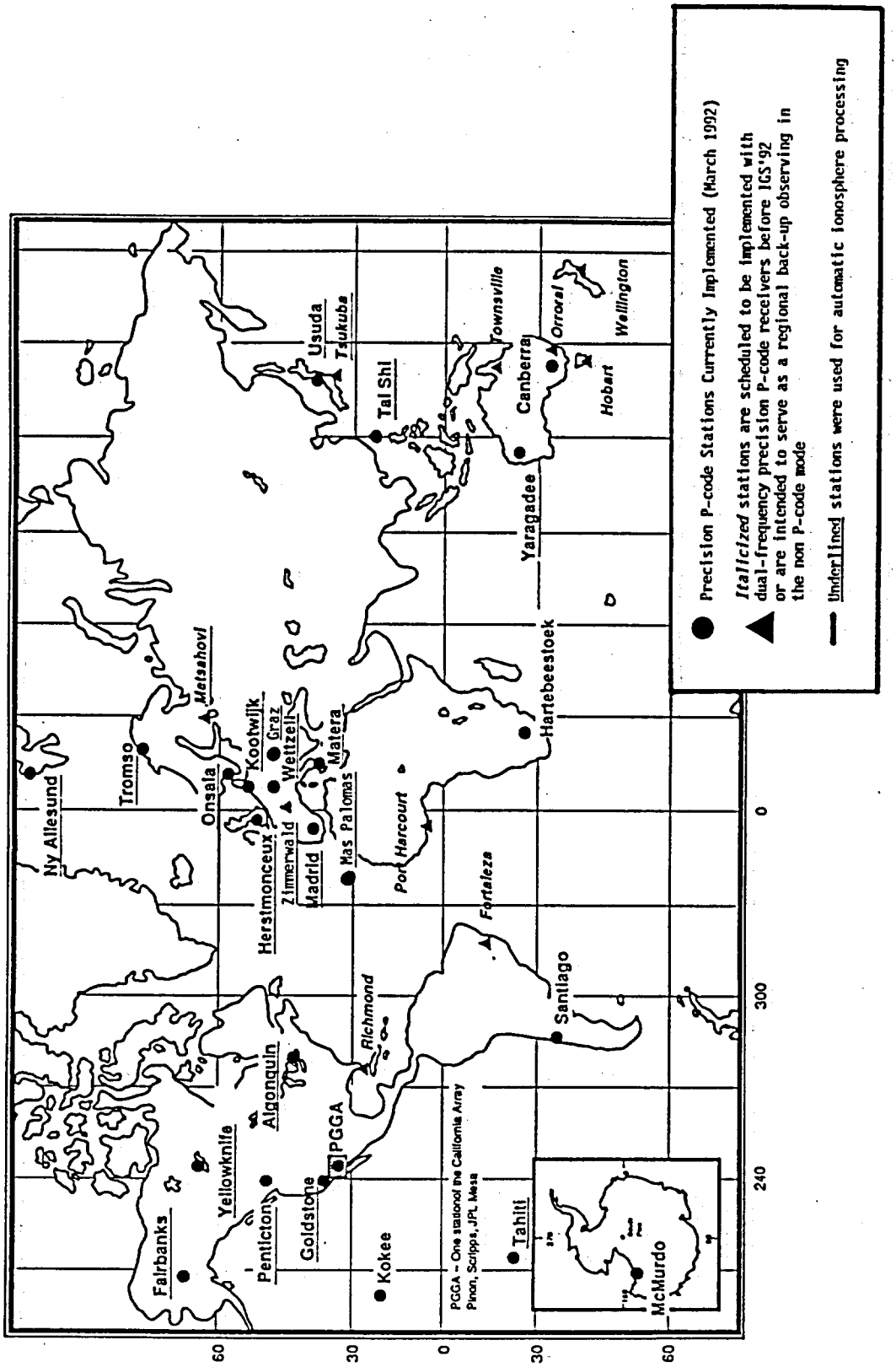

Figure 5-23

Core Network of the IGS (Status: 1992)

network centers (or global data centers), from where they may be retrieved by the **analysis centers.**

The main task of the **analysis centers** is to provide the daily analysis of the incoming data and to derive products such as orbits and earth rotation parameters.

One of the analysis centers of the IGS has been established in collaboration with IfAG (Institute for Applied Geodesy, Germany), IGN (Institut Géographique National, France) and L+T (Swiss Federal Office of Topography) under the acronym **CODE (= Center for Orbit Determination in Europe)** at the Astronomical Institute of the University of Berne (AIUB).

In the CODE computing environment the automatic ionosphere analysis program IONMAP (see section 4.4) has been set up. Figure 5-23 shows the stations which are automatically processed, Table 5-18 gives additional information about the stations. The stations were selected in order to cover the three different regions which have to be distinguished for ionospheric monitoring purposes:

- the polar / auroral region (A),
- the mid-latitude region (ML), and
- the equatorial region (E).

The test data set covers 60 days, namely the time span between day 245 (September 1) and day 305 (October 31) of the year 1992. For all the stations given in Table 5-18 six ionosphere models per day (valid for four hours each) were computed automatically, using the program IONMAP (see section 4.3.2) with the input options given in Table 5-19.

Station Name	Abbreviation	Latitude	Longitude	Type
Fairbanks	FAIR	65.0	-147.5	A
Metsahovi	METS	60.2	24.4	A
Ny Allesund	NYAL	78.9	11.7	A
Onsala	ONSA	57.4	11.9	A
Tromsoe	TROM	69.7	18.9	A
Yellowknife	YELL	62.5	-114.5	A
Algonquin	ALGO	46.0	-78.1	ML
Penticton	DRAO	49.3	-119.6	ML
Goldstone	GOLD	35.3	-116.9	ML
Graz	GRAZ	47.1	15.5	ML
Herstmonceux	HERS	50.9	0.3	ML
Kootwijk	KOSG	52.2	5.8	ML
Madrid	MADR	40.4	-4.3	ML
Matera	MATE	40.7	16.7	ML
Tsukuba	TSUK	36.1	140.1	ML
Usuda	USUD	36.1	138.4	ML
Wettzell	WETT	49.1	12.9	ML
Zimmerwald	ZIMA	46.9	7.5	ML
Mas Palomas	MASP	27.8	-15.6	E
Tahiti	PAMA	-17.6	-149.6	E
Taiwan	TAIW	25.0	121.5	E
Yaragadee	YAR1	-29.0	115.3	E

A: Auroral Region, ML: Mid-latitude Region, E: Equatorial Region

Table 5-18

IGS Stations Used for Automatic Ionosphere Processing

IONMAP: OPTION INPUT FILE **19-MAR-91 17:48**

```
(REMARK: YES=1,NO=0)

TITLE:

**********************************************************************

--> : IGS: AUTOMATIC IONOSPHERE PROCESSING

PRE-PROCESSING:                                                    *

PRINT PREPROCESSING MESSAGES (SR CHKOBS)                --> :   0
USE CARRIER I TO DETECT BREAKS, GAPS I=3,I=4:           --> :   4
DEGREE Q OF POLYNOMIAL (Q < 4)                          --> :   1
MAX. INTERVAL LENGTH FOR TEST (MINUTES)                 --> :   4
                                                             ***.***
RMS OF ONE OBSERVATION (M)                              --> :   0.050

PROCESSING OPTIONS:
                                                                *****

TYPE OF IONOSPHERE MODELING     (SINGLE LAYER=1)        --> :     1
MINIMAL ELEVATION (DEGREES)                             --> :    15
RESIDUALS                                               --> :     1

SINGLE LAYER MODEL:

                    FROM                TO              DEG. OF DEVELOPMENT
      MOD# YYYY MM DD HH.H YYYY MM DD HH.H    LAT  HA  MIXED

F      *** **** ** ** **.* **** ** ** **.*     **   **  **
-->:     1 1992 09 28 00.0 1992 09 28 04.0      1   2   2
-->:     2 1992 09 28 04.0 1992 09 28 08.0      1   2   2
-->:     3 1992 09 28 08.0 1992 09 28 12.0      1   2   2
-->:     4 1992 09 28 12.0 1992 09 28 16.0      1   2   2
-->:     5 1992 09 28 16.0 1992 09 28 20.0      1   2   2
-->:     6 1992 09 28 20.0 1992 09 28 24.0      1   2   2

HEIGHT OF IONOSPHERIC LAYER  (KM)

     *****
-->:   350
```

Table 5-19
Input Option File for Automatic Ionosphere Processing

Remarks:

- *Preprocessing options:*

  The rms error of an L_4 observation has been set to 5 cm, in order to be sure that data taken under disturbed ionospheric conditions may be processed in an automatic way too.

- *Development degrees:*
  For reasons of computing simplicity the same development degrees were used for all models, i.e. no distinction was made between an equatorial and a mid-latitude station. With the options of Table 5-19 5 parameters have to be estimated per model.

The following questions were addressed:
- What is the performance of such a routine service (do the data arrive in time, what is the quality of the data)?

- What are the accuracies of the TEC values estimated using GPS phase observations compared to other observation techniques?

- How well is the GPS derived information about ionospheric conditions correlated with other geophysical parameters, like e.g. the sunspot numbers, the solar flux (S10.7) or the geomagnetic K_p-index?

5.2.2 Results

In order to simulate a routine service the program IONMAP was operated in a completely automatic way, i.e. just the stations which were available and offered no problems were processed. The delay between observation and computation was set to 2 days, i.e. the data of the different stations had to be available at the CODE analysis center within 2 days. No attempt was made to correct erroneous files or to reprocess certain days when delayed data files arrived in the processing center. Table 5-20 gives an overview over the processing statistic for the test period.

There are two major gaps in the test data: the first from day 251 (7 September 1992) until day 256 (12 September 1992), the second from day 301 (27 October 1992) until day 305 (31 October 1992). These gaps were caused by software problems in the VMS environment of the program IONMAP. For three stations (Mas Palomas, Wettzell, and Ny Allesund) the data were retrieved later on from the database at the Scripps Institute of Oceanography (SIO) (one of the three IGS network centers).

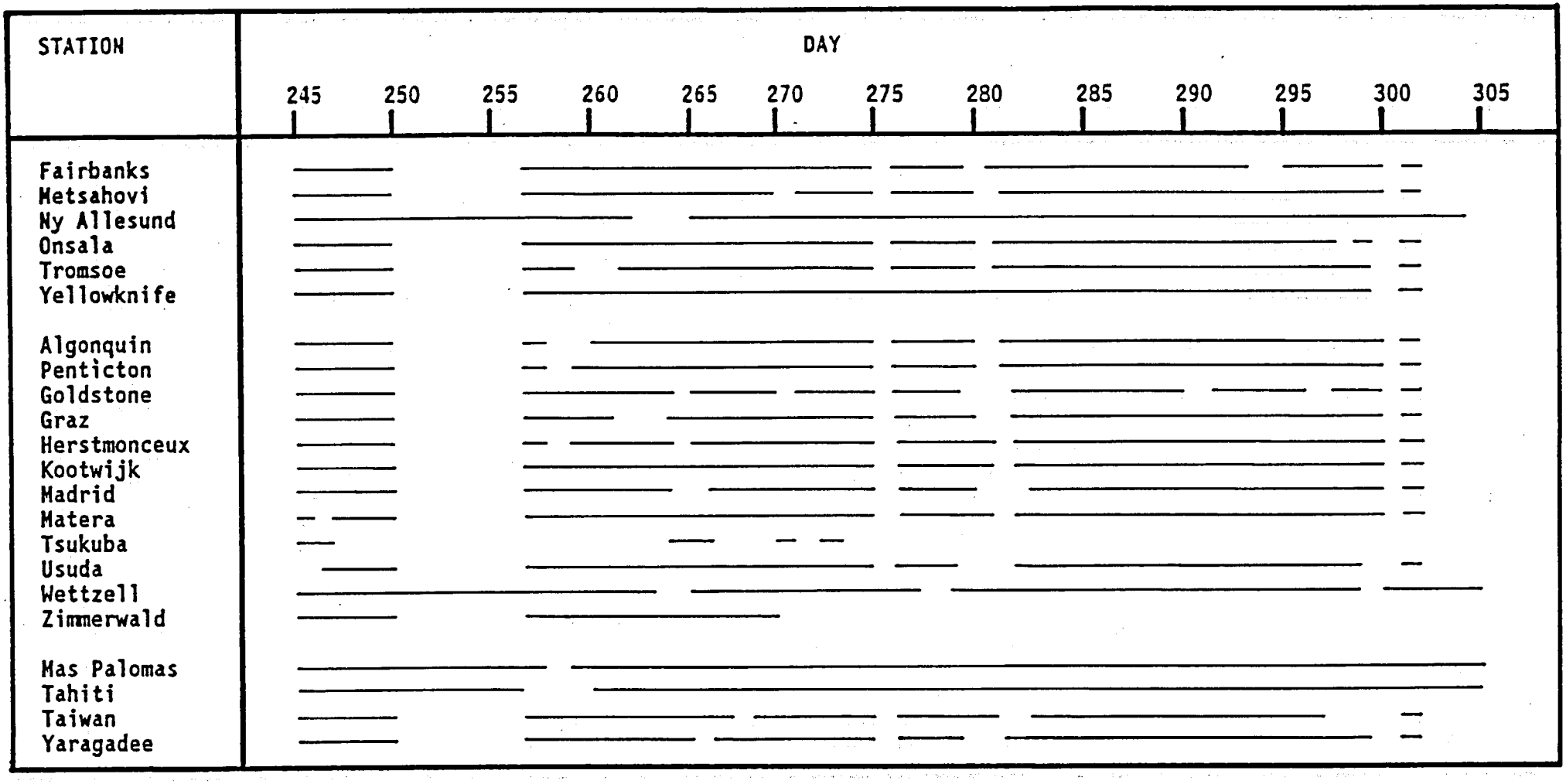

Figure 5-20

Processing Statistic for Days 245 - 305

For a considerable part of the 1992 IGS Test Campaign the station Zimmerwald was equipped with an ASHTECH dual-frequency P-code receiver. When the ASHTECH receiver was removed the station Zimmerwald was no longer used for ionosphere model computations.

All other gaps in the data were caused by the fact, that the data from the corresponding station was not available in time (i.e. within 2 days) at the analysis center, or that there were other problems with the automatic processing (like changed station names, wrong file types and so on).

A serious problem during the test period was the fact that AS (= Anti-Spoofing, see section 2.1.3) was turned on during all the weekends (from Saturday 1:00 UT until Monday 10:00 UT). Due to AS most of the receivers in the IGS network had problems to track the Block II satellites on L_2, or, if the data was collected, the noise level was extremely high. The receiver performance on the L_2 carrier influences directly the program IONMAP, where the L_4 linear combination (= the difference between L_1 and L_2, both expressed in meters) is used to estimate the total electron content. The difference between a day without AS (Day 262, Friday 18 September) and with AS (Day 263, Saturday 19 September) for the station Usuda (ROGUE receiver) is shown in Table 5-21.

Day	AS	Mod#	Time (UT)	# of Obs	RMS (m) of L_4 Obs.	TEC (in TECU)
262	Off	1	00:00-04:00	1854	0.09	10.296 ± 0.076
		2	04:00-08:00	2096	0.10	14.559 ± 0.077
		3	08:00-12:00	2283	0.05	08.827 ± 0.051
		4	12:00-16:00	2203	0.07	07.018 ± 0.056
		5	16:00-20:00	1648	0.05	04.723 ± 0.056
		6	20:00-24:00	2094	0.11	11.913 ± 0.100
263	On	1	00:00-04:00	1145	0.04	18.560 ± 0.065
		2	04:00-08:00	1172	0.13	19.347 ± 0.215
		3	08:00-12:00	567	0.12	30.355 ± 1.116
		4	12:00-16:00	426	0.01	0.727 ± 0.419
		5	16:00-20:00	468	0.03	0.875 ± 0.313
		6	20:00-24:00	1008	0.06	6.724 ± 0.166

Table 5-21
Performance of IONMAP With/Without AS

The results in Table 5-21 are typical for the entire test period. The first impression of the results of day 263 may be misleading: the rms error of the L_4 observations has decreased and the coefficients look reasonable. The drastically reduced number of observations makes the results far less reliable, because the single layer model is very sensitive to the satellite distribution. This circumstance is also illustrated by the mean errors of the Total Electron Content (TEC).

The test data set offered a good opportunity to assess the accuracy of the computed ionosphere models. In a first step the following test was carried out: 15 days with different ionospheric conditions were selected as a test data set (day 272 to day 286). In order to take into account the latitude dependence of ionospheric conditions three stations with different geographical latitudes were selected:

- Mas Palomas (equatorial)
- Wettzell (mid-latitude)
- Yellowknife (auroral)

For each station two TEC values were computed at the boundary between the domains of two (four-hours) ionosphere models (i.e. for 00:00, 04:00, 08:00, 12:00, 16:00 and 20:00 UT) using the two neighbouring models. In principle the two TEC values should be identical. The differences ΔTEC_i (i=1,...,6) between the two TEC values are realistic (or even worst case) measures for the accuracy of the single layer models.

The results are given in Table 5-22 (all values in TECU).

Day	Station	ΔTEC_1	ΔTEC_2	ΔTEC_3	ΔTEC_4	ΔTEC_5	ΔTEC_6	Mean Value
272	MASP	---	18.6	55.1	76.7	22.4	11.7	36.9
	WETT	---	---	---	2.1	2.4	6.6	3.7
	YELL	---	1.4	3.8	2.4	0.6	13.9	4.4
273	MASP	9.8	8.5	2.8	3.7	0.2	3.4	4.7
	WETT	4.9	4.7	5.4	3.6	1.8	0.5	3.5
	YELL	0.6	0.6	1.9	3.8	2.4	6.4	2.6
274	MASP	1.9	0.7	3.5	3.8	28.7	4.8	7.2
	WETT	0.2	0.3	2.7	2.3	0.9	1.3	1.3
	YELL	2.9	3.1	1.1	1.2	7.7	5.5	3.6
275	MASP	18.3	11.7	12.6	22.1	1.3	5.1	11.9
	WETT	4.9	3.1	5.8	4.0	1.4	0.7	3.3
	YELL	4.3	0.9	3.4	1.0	3.0	11.0	3.9
276	MASP	22.5	3.4	5.4	15.2	0.8	9.3	9.4
	WETT	1.2	1.6	0.2	1.1	2.4	1.1	1.3
	YELL	14.3	5.9	1.1	3.4	7.1	5.5	6.2
277	MASP	13.4	4.9	32.2	27.9	50.8	5.5	23.2
	WETT	2.9	7.9	2.6	15.7	6.5	18.2	9.0
	YELL	12.5	0.8	1.1	0.4	2.9	8.8	4.4
278	MASP*)	154.1	18.6	24.3	5.5	18.6	1.8	13.8
	WETT	34.2	28.3	2.6	12.1	---	---	19.3
	YELL	18.8	9.4	6.5	5.8	1.8	7.8	8.4
279	MASP	2.9	19.2	25.2	27.4	16.6	1.1	15.4
	WETT	---	4.0	6.3	2.5	3.0	1.0	3.4
	YELL	0.7	5.0	2.3	0.1	2.0	8.5	3.1
280	MASP	5.7	2.0	2.1	0.2	1.2	12.9	4.0
	WETT	2.2	1.7	1.8	2.3	2.5	2.5	2.2
	YELL	0.7	2.5	3.9	1.0	2.0	10.7	3.5
281	MASP	20.9	2.1	5.4	1.0	0.2	23.5	8.9
	WETT	2.6	2.9	3.2	3.5	0.2	1.7	2.4
	YELL	6.6	3.5	3.2	3.6	1.4	7.0	4.2
282	MASP	31.8	3.1	6.1	9.2	8.5	13.6	12.0
	WETT	---	2.1	2.6	1.8	0.6	5.6	2.5
	YEL	0.4	0.1	2.8	3.0	1.3	6.8	2.4
283	MASP	31.7	3.7	7.3	2.0	11.3	2.7	9.8
	WETT	3.4	0.5	3.0	9.5	9.4	3.7	4.9
	YELL	4.2	6.5	2.1	8.1	13.9	8.9	7.3

Table 5-22
Accuracy of the Single Layer Models

284	MASP	7.9	5.0	4.0	10.1	10.5	197.2*)	7.5
	WETT	1.3	4.8	7.7	28.0	3.5	11.9	9.5
	YELL	4.1	3.6	2.8	2.8	2.1	2.9	3.0
285	MASP	62.9	2.4	3.7	6.0	23.8	325.5*)	19.8
	WETT	7.9	13.6	15.8	72.0	3.6	1.5	19.1
	YELL	7.4	5.0	5.2	3.8	10.1	30.8	10.4
286	MASP	132.3	31.3	14.4	16.8	7.3	10.3*)	16.0
	WETT	1.8	18.4	3.0	28.1	1.2	0.9	8.9
	YELL	4.6	5.6	4.0	0.7	0.1	0.1	2.5

*) Outliers caused by small numbers of observations (not used for computation of mean values)

Table 5-22 (Cont.)
Accuracy of the Single Layer Models

Using the daily mean values of the differences between two consecutive single layer models for the three stations the following mean values for the entire test period were computed:

Station	Mean ΔTEC of All Days (in TECU) With AS - Days	Without AS - Days
Mas Palomas (MASP):	13.4	12.4
Wettzell (WETT):	6.8	3.5
Yellowknife (YELL):	4.7	3.8

Table 5-23
Mean TEC of All Days (With and Without AS-Days)

The mean accuracy for the determination of absolute TEC values is of the order of 3-4 TECU for mid-latitude and auroral stations. The higher values for the equatorial stations may be explained by the larger gradients in the electron content which were not adequately modelled using the relatively low degrees for the Taylor series development in the program IONMAP.

A second possibility to assess the accuracy of the single layer models is to compare the computed TEC values with TEC values obtained by other observation techniques, like e.g. Faraday rotation measurements (see section 3.3.3).

Unfortunately there were no Faraday derived TEC data available for the test period because the public TEC database at the Stanford University had been inoperational after August 1992. We therefore had to establish a second test data set for the comparison of Faraday and GPS derived TEC values. As second test data set we chose the 10 days from day 190 (8 July) to day 199 (17 July) of the year 1992. As in the accuracy investigation above we also tried to cover the 3 main geographical regions (auroral, mid-latitude and equatorial). Table 5-24 gives additional information about the Faraday and GPS stations used for the comparison.

Station	Observation Technique	Country	Lat.	Long.	Satellite
Sheyma	Faraday	Alaska	52	-174	GOES-3
Fairbanks	GPS	Alaska	65	-147	--
Sagamore Hill	Faraday	USA	42	- 70	GOES-2
Westford	GPS	USA	42	- 71	--
Palahua	Faraday	Hawaii	21	-158	GOES-3
Kokee	GPS	Hawaii	21	-159	--

Table 5-24
Stations of the Test Data Set for the Comparison With GPS Derived TEC Values

The Faraday TEC data for these stations are given as hourly values (in TECU). The data are collected and distributed by the Space Environment Laboratories of the NOAA.

Figures 5-24 to 5-26 show the comparisons between the Faraday TEC values and the hourly values derived by GPS for the 6 stations of Table 5-24.

The two observation techniques (GPS and Faraday) give different kinds of results for different stations: whereas the stations Kokee (GPS) and Palahua (Faraday) show a good agreement of the observed TEC values (mean difference: 7 TECU) much worse results are observed for the stations Westford (GPS) and Sagamore Hill (Faraday). Here a shift of 20 TECU's is present which might be explained by

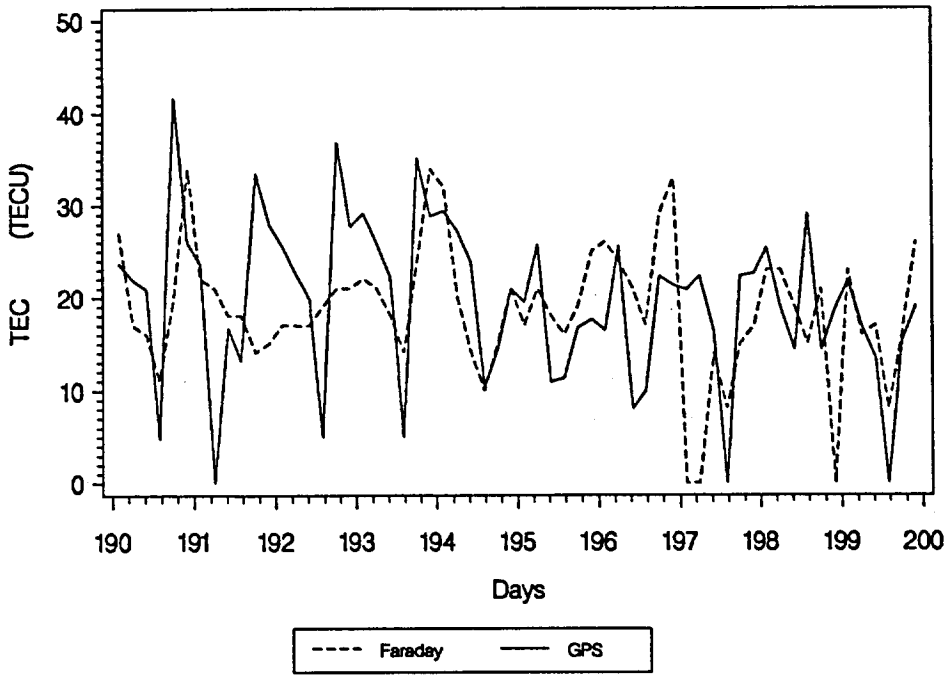

Figure 5-24

Comparison of Faraday TEC and GPS Derived TEC

GPS: Fairbanks, Faraday: Shemya

Days 190 - 199 (8-July - 17-July-1992)

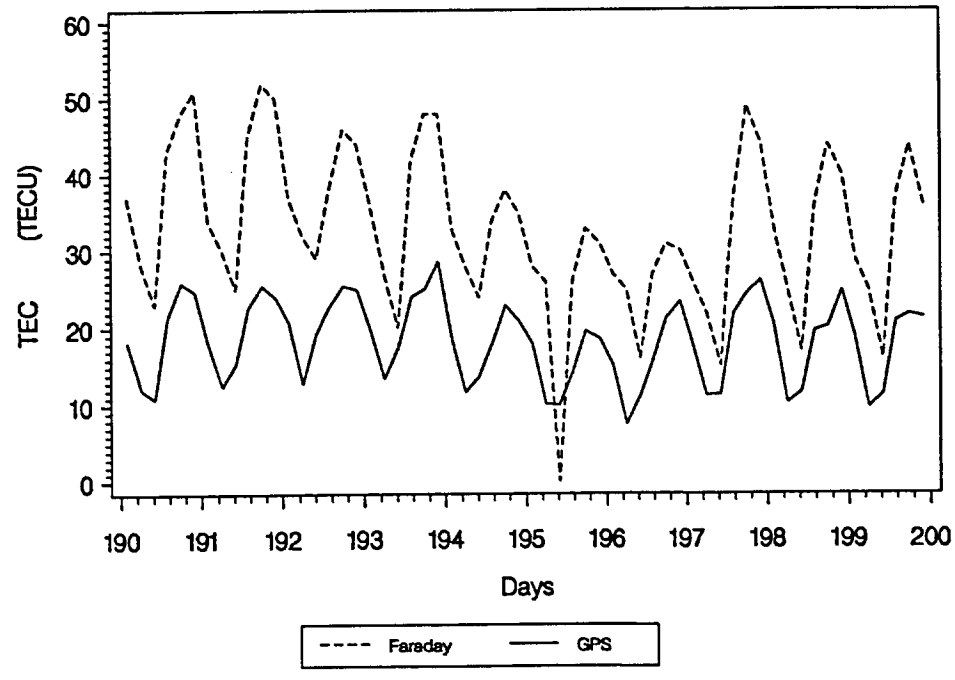

Figure 5-25

Comparison of Faraday TEC and GPS Derived TEC

GPS: Westford, Faraday: Sagamore Hill

Days 190 - 199 (8-July - 17-July-1992)

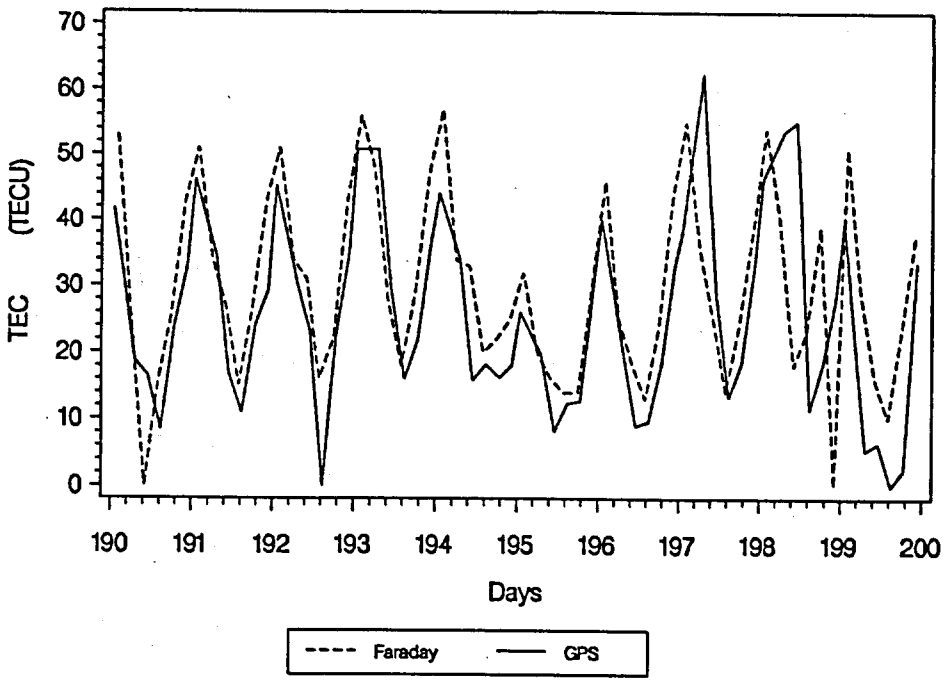

Figure 5-26
Comparison of Faraday TEC and GPS Derived TEC
GPS: Kokee, Faraday: Palahua
Days 190 - 199 (8-July - 17-July-1992)

the fact that we are using uncorrected Faraday data of the satellite GOES-2. There are several uncertainties in the Faraday measurements (see e.g. Davies and Hartmann, 1993), such as cycle ambiguities, calibration problems and so on. These problems may bias the Faraday observations by up to 5-10 TECU's. If the observed shift is removed the remaining mean difference is of the order of 15 TECU's. The mean differences for the auroral stations Fairbanks (GPS) and Shemya (Faraday) are of the order of 17 TECU. This may partly be explained by the large geographical separation of the GPS and the Faraday rotation sites.

The observed differences between the Faraday and the GPS data may be considerably reduced by forming daily mean values. When comparing these mean values the remaining difference is of the order of 3-4 TECU, which indicates that GPS is more suited for the determination of long term variations of the TEC values.

These results show the problems in the determination of absolute TEC values using GPS observations. The main problem areas are (see e.g. Wanninger, 1992):

- differential equipment group delays,
- multipath,
- phase center offsets, and
- random observation errors.

It is generally accepted that absolute TEC values determined by GPS may be biased up to 2-15 TECU's, if uncalibrated receivers are used, which is (at least for the moment) the case for all stations of the IGS.

Nevertheless it is interesting to use the data of the IGS stations (see Table 5-18) in order to get an impression of the order of magnitude of the estimated TEC values and their changes. The resulting TEC values were plotted in Figure 5-27 (auroral stations), Figure 5-28 (mid-latitude stations) and Figure 5-29 (equatorial stations).

Table 5-25 shows the mean TEC values and the mean daily TEC amplitudes of all processed stations. In the following figures the days with AS (Anti-Spoofing) turned on were excluded. The mean amplitudes were computed as the square root of the variance of the TEC values.

The mean values of the TEC estimates show for all stations a clear latitude dependence: the mean TEC for the auroral and the mid-latitude stations is about 10-15 TECU, whereas significantly higher values are observed for the equatorial stations (20-30 TECU).

The daily variations of the TEC values (the TEC amplitudes) show the same latitude dependence as the absolute TEC values: for equatorial stations they are by a factor of two higher than for mid-latitude and auroral stations.

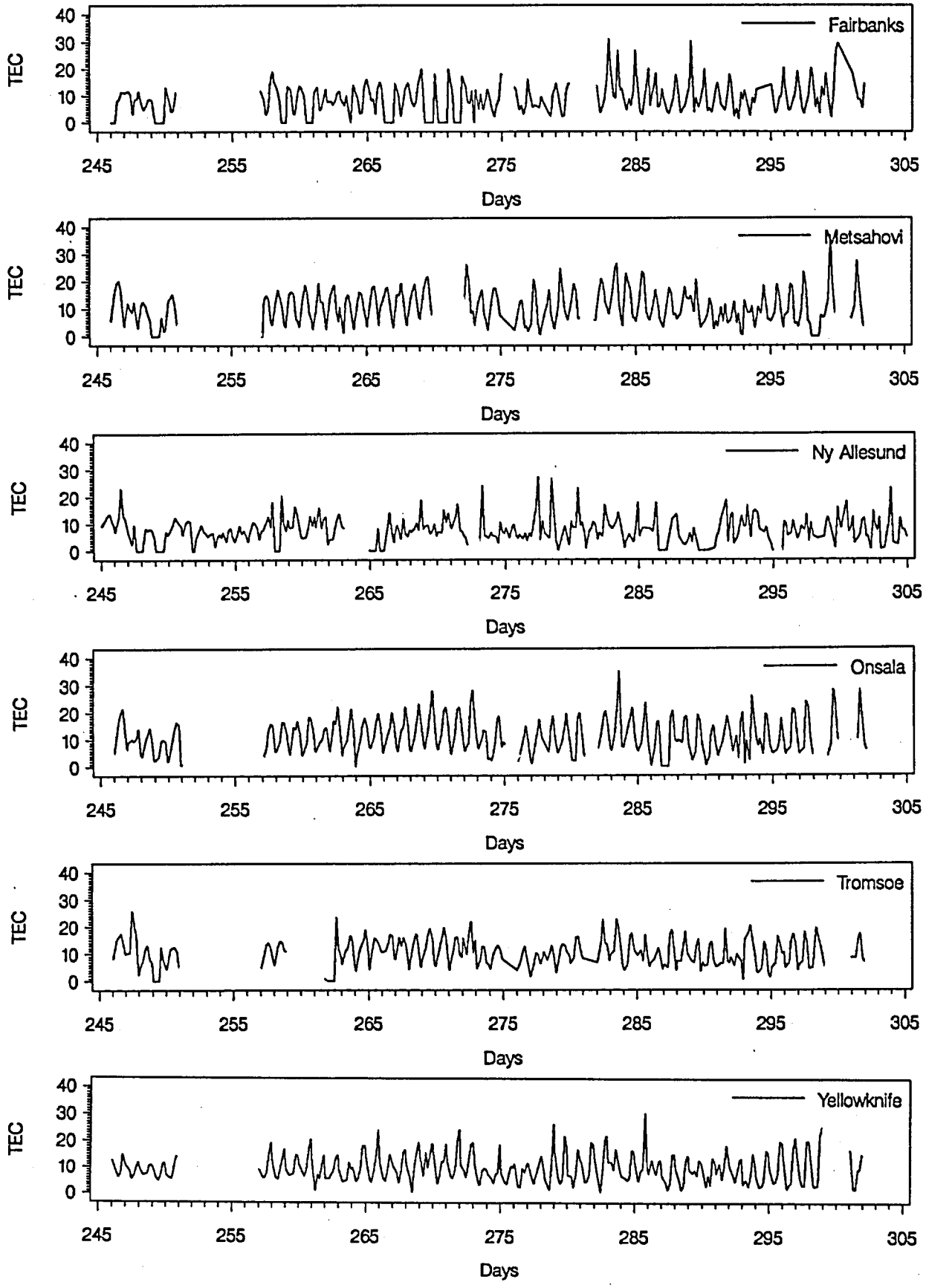

Figure 5-27

Total Electron Content (TEC) for 6 Auroral Stations from 1-Sept-92 to 31-Oct-1992 (in TECU)

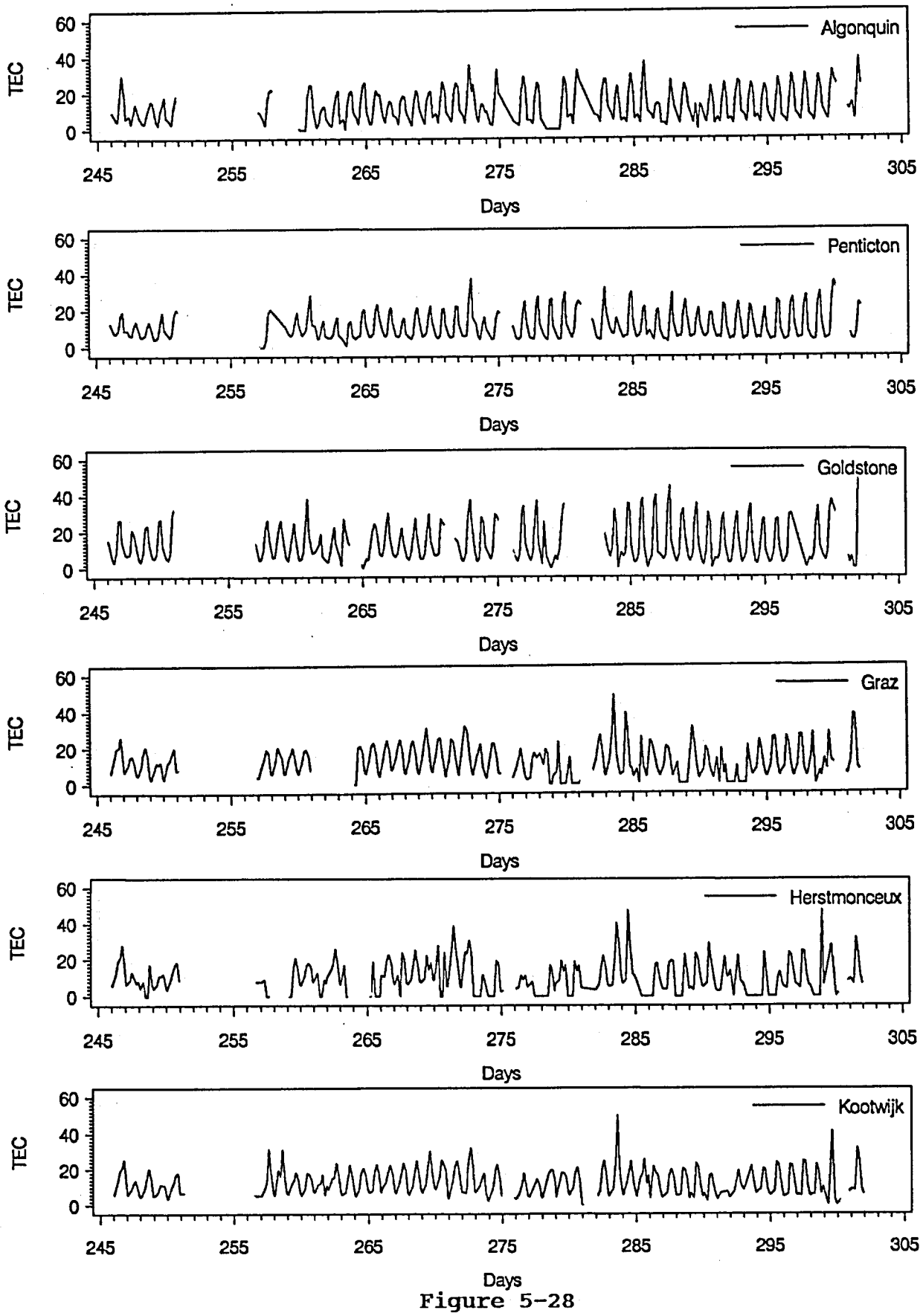

Figure 5-28

Total Electron Content (TEC) for 12 Mid-latitude Stations from 1-Sept-92 to 31-Oct-1992 (in TECU)

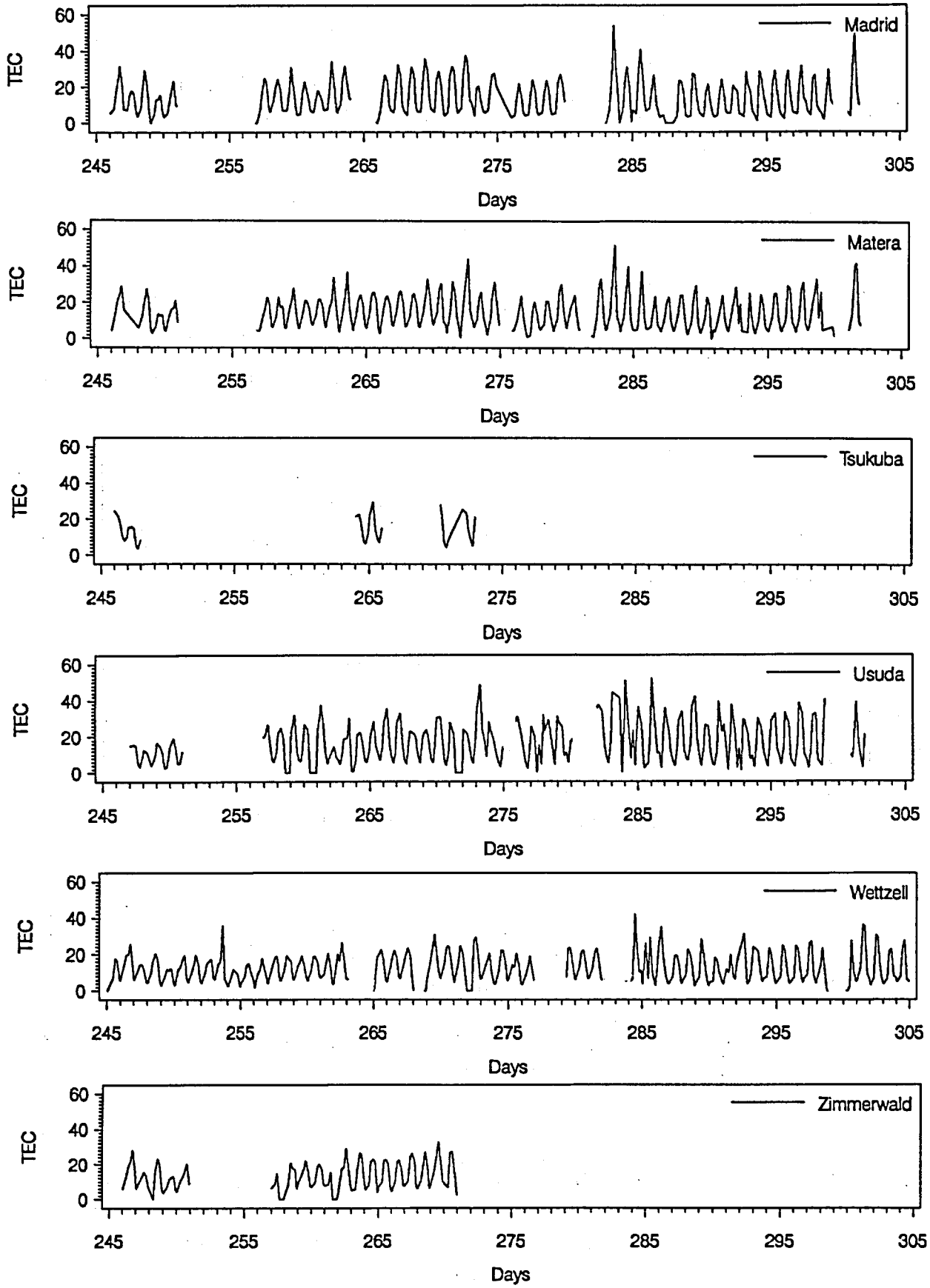

Figure 5-28 (Cont.)

Total Electron Content (TEC) for 12 Mid-latitude Stations from 1-Sept-92 to 31-Oct-1992 (in TECU)

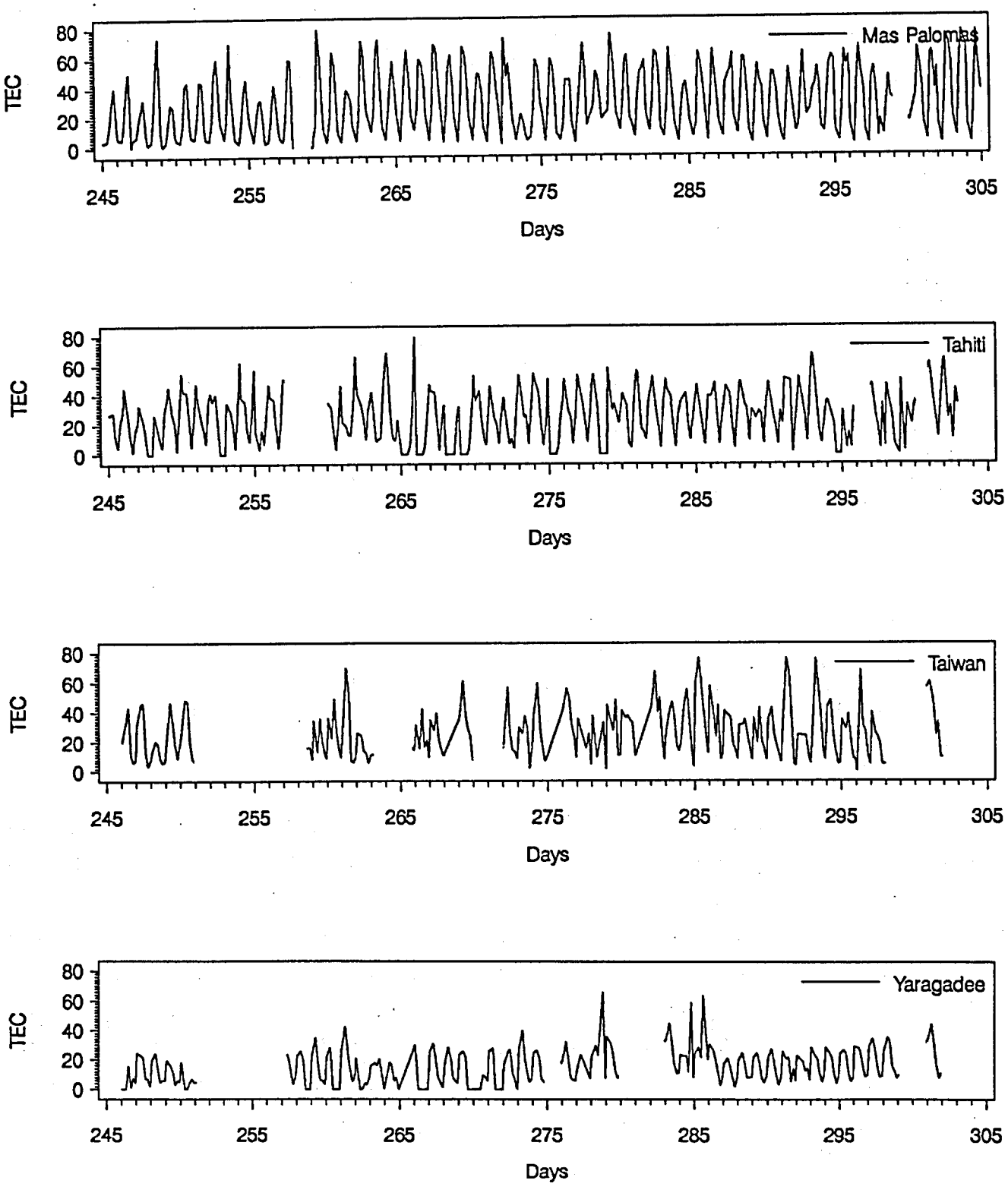

Figure 5-29
Total Electron Content (TEC) for 4 Equatorial Stations
from 1-Sept-92 to 31-Oct-1992 (in TECU)

Station	Type	Geogr. Lat.	Mean TEC	Mean Amplitude
Fairbanks	A	65	10	5
Metsahovi	A	60	11	6
Ny Allesund	A	79	9	5
Onsala	A	57	12	7
Tromso	A	70	11	5
Yellowknife	A	63	10	5
Algonquin	ML	46	13	8
Penticton	ML	49	12	7
Goldstone	ML	35	15	12
Graz	ML	47	14	8
Herstmonceux	ML	51	14	8
Kootwijk	ML	52	13	7
Madrid	ML	40	15	10
Matera	ML	41	16	12
Tsukuba	ML	36	15	8
Usuda	ML	36	17	11
Wettzell	ML	49	13	9
Zimmerwald	ML	47	14	7
Mas Palomas	E	28	32	11
Tahiti	E	-18	29	16
Taiwan	E	25	27	18
Yaragadee	E	-29	18	12

Table 5-25
Mean TEC Values and Mean Daily TEC Amplitudes (in TECU)

In a next step we correlated the daily peak TEC values with the Sunspot Number (SSN) and the Solar Flux (S10.7). For every day we formed mean values of the peak TEC values of all auroral, mid-latitude, and equatorial stations (see Table 5-18). These daily means were then smoothed in a second step by computing running mean values over a time span of 3 days. Figure 5-30 shows the smoothed daily mean peak TEC values for the 3 different latitude regions (auroral, mid-latitude and equatorial). In Figure 5-31 the sunspot number (SSN) and the solar flux at 10.7 cm (S10.7) is shown for the same period.

The mean TEC values of the equatorial stations show the highest correlation with the solar parameters (sunspot number and solar flux). This confirms that the equatorial region of the ionosphere is mainly solar controlled. The mid-latitude and auroral stations show more or less an identical behaviour (apart from a higher elec-

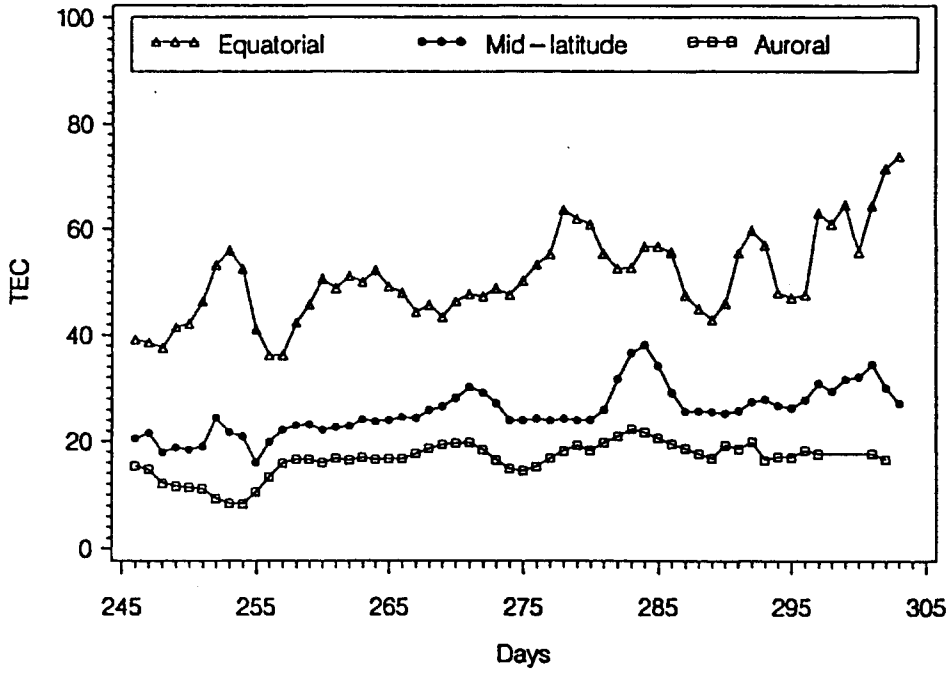

Figure 5-30
Smoothed Daily Mean TEC Peak Values for Different Latitudes (Auroral, Mid-latitude and Equatorial Region)

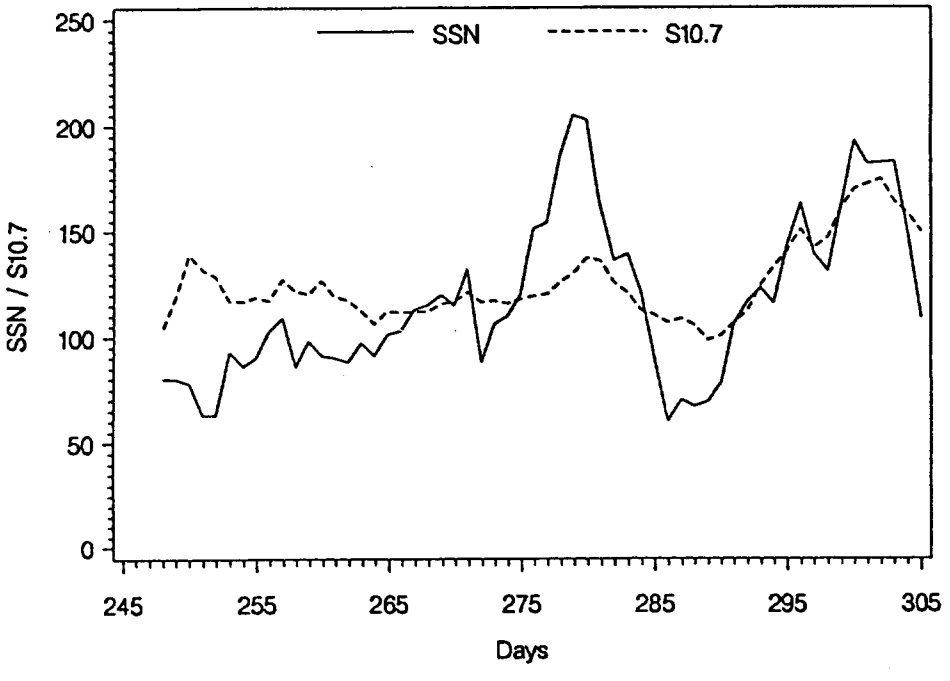

Figure 5-31
Sunspot Numbers (SSN) and Solar Flux (S10.7)

tron content level for the mid-latitude stations). The correlation with the sunspot number and the solar flux is less apparent than for the equatorial stations; there seems to be a delay of approximately two days between the peak of the sunspot numbers at day 279 and the peak of the electron content at day 281.

We will now focus on the irregular part of the ionosphere by first describing known "storm events" in the ionosphere using GPS and then correlating the GPS derived measures with the K_p-index during the considered periods.

The behaviour of the geomagnetic field (which is closely related to the irregular part of the ionosphere, see section 3.1.2) is broadcasted by the Geological Survey of Canada, Ottawa, where the behaviour of different geographic regions (mid-latitude, sub-auroral, auroral etc.) is described and storm events are announced. An example for such a broadcast message is given in Table 5-26.

ENERGY MINES AND RESOURCES CANADA
GEOPHYSICS DIVISION, GEOLOGICAL SURVEY OF CANADA, OTTAWA
GEOMAGNETIC ACTIVITY FORECAST/REVIEW, ISSUED AT 12:05 UT, 17-9-92

		SUB-AURORAL ZONE	AURORAL ZONE	POLAR CAP
PRIOR DAY	15- 9-92	QUIET	UNSETTLED	UNSETTLED
		DRX = 13	DRX = 102	DRX = 41
YESTERDAY	16- 9-92	QUIET	UNSETTLED	UNSETTLED
		DRX = 17	DRX = 86	DRX = 44
TODAY	17- 9-92	MAJOR STORM	MAJOR STORM	ACTIVE
17-9-92	MAJOR MAGNETIC STORM		02.30	UT
17.9.92	Storm conditions may continue for next		24-36	hours.
FORECAST	18- 9-92	MAJOR STORM	MAJOR STORM	ACTIVE
FORECAST	19- 9-92	ACTIVE	ACTIVE	ACTIVE
FORECAST	20- 9-92	UNSETTLED	UNSETTLED	UNSETTLED
17.9.92	STORM ALERT HAS BEEN ISSUED AT		11.45	UT

Table 5-26
Geomagnetic Activity Forecast and Review

In order to visualize the geomagnetic storm on day 261 (17 September 1992) we plotted the L_4 residuals and the differences of the L_4 residuals between subsequent observation epochs (30 second interval) in Figures 5-34 and 5-35. For comparison the residuals and

their changes for a quiet day are shown in the Figures 5-32 and 5-33.

The daily signature of the L_4 residuals is the same for both days (mean value about 20 cm). The short period variations of the L_4 residuals however are different for the two days: whereas on day 260 no variations larger than 25 cm between two subsequent observation epochs (30 second interval) occured, the picture changes for day 261: here changes up to 40 cm may be found. In addition the frequency of the occurrence of enhanced short period variations is much higher than for the preceeding day. This corresponds exactly to the ionospheric conditions described in Table 5-26, where the auroral zone is said to be unsettled for day 260 and a major geomagnetic storm is announced for day 261.

In a next step we analyzed the residuals of all stations and all days using the technique of spectral analysis. With an observation interval of 30 seconds only periods larger than 1 minute may be determined in the spectral analysis. Therefore we proceeded as follows:

- In order to get an impression of the short period variations (periods < 1 minute) we formed the differences of the L_4 residuals between two subsequent observation epochs (see above). The minimum and maximum values as well as the variance of these differences are good measurements for the irregular part of the ionosphere.

- In addition the power spectra of the L_4 residuals were computed using the program SPARES. These power spectra give the frequencies and the corresponding spectral amplitudes detected in the L_4 residuals. These frequencies are a good measure for the irregular behaviour of the ionosphere. The amplitudes of the irregular changes were roughly approximated by the difference of the minimum and maximum L_4 residual.

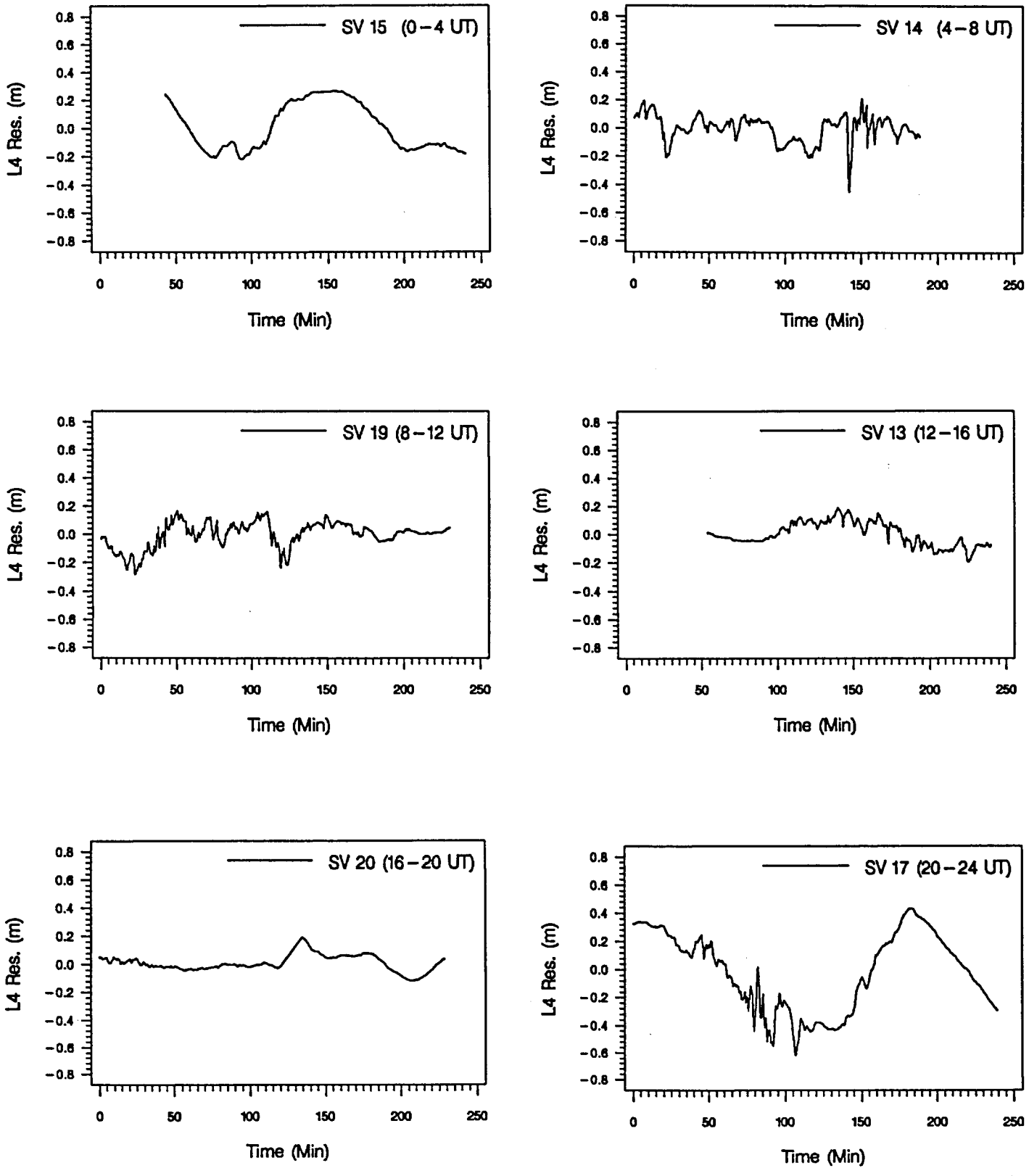

Figure 5-32

L_4 Residuals for Day 260, Station Yellowknife

(PRN 15, PRN 14, PRN 19, PRN 13, PRN 20, PRN 17)

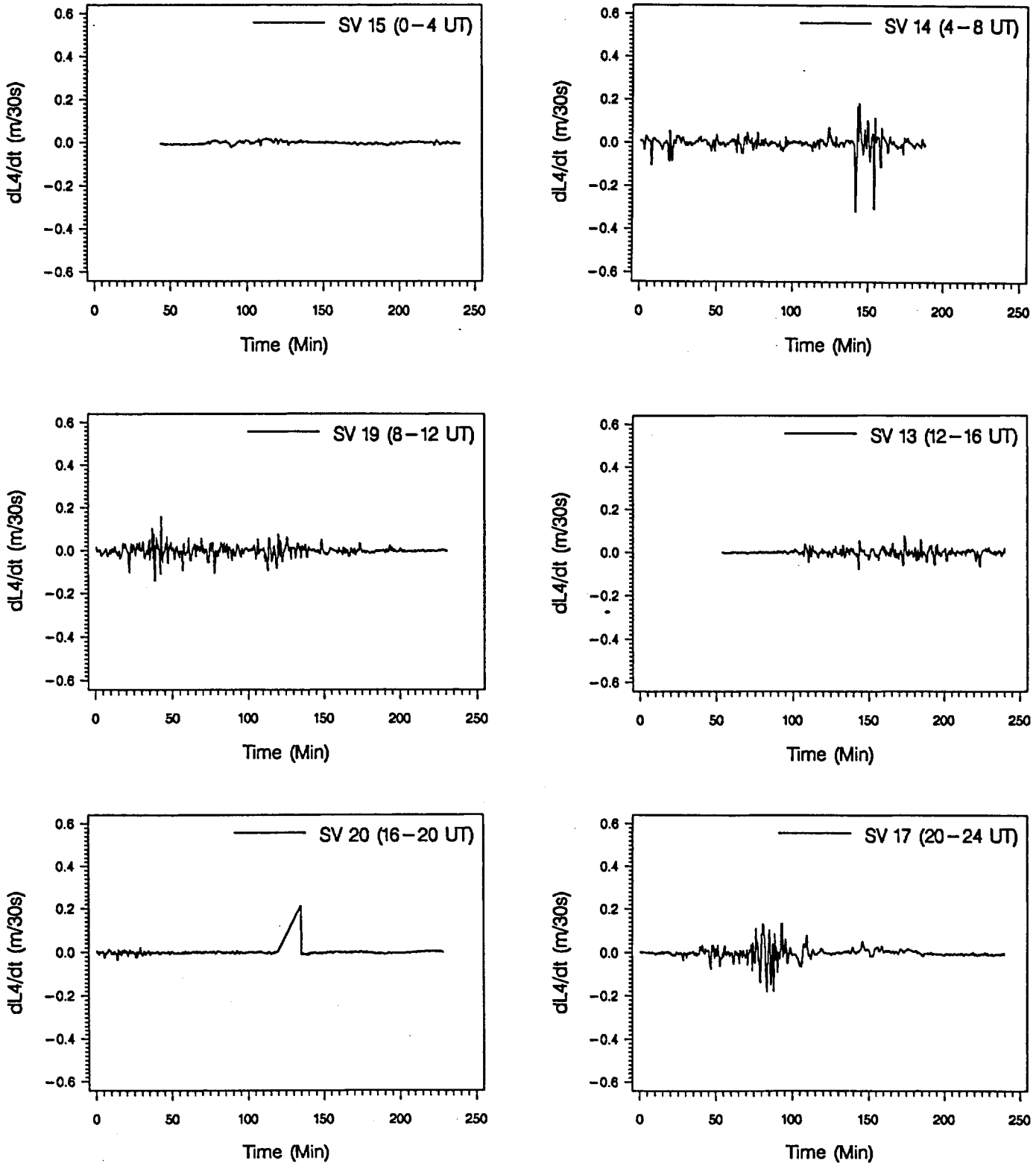

Figure 5-33

Changes in L_4 Residuals per 30 Seconds, Day 260

Station Yellowknife

(PRN 15, PRN 14, PRN 19, PRN 13, PRN 20, PRN 17)

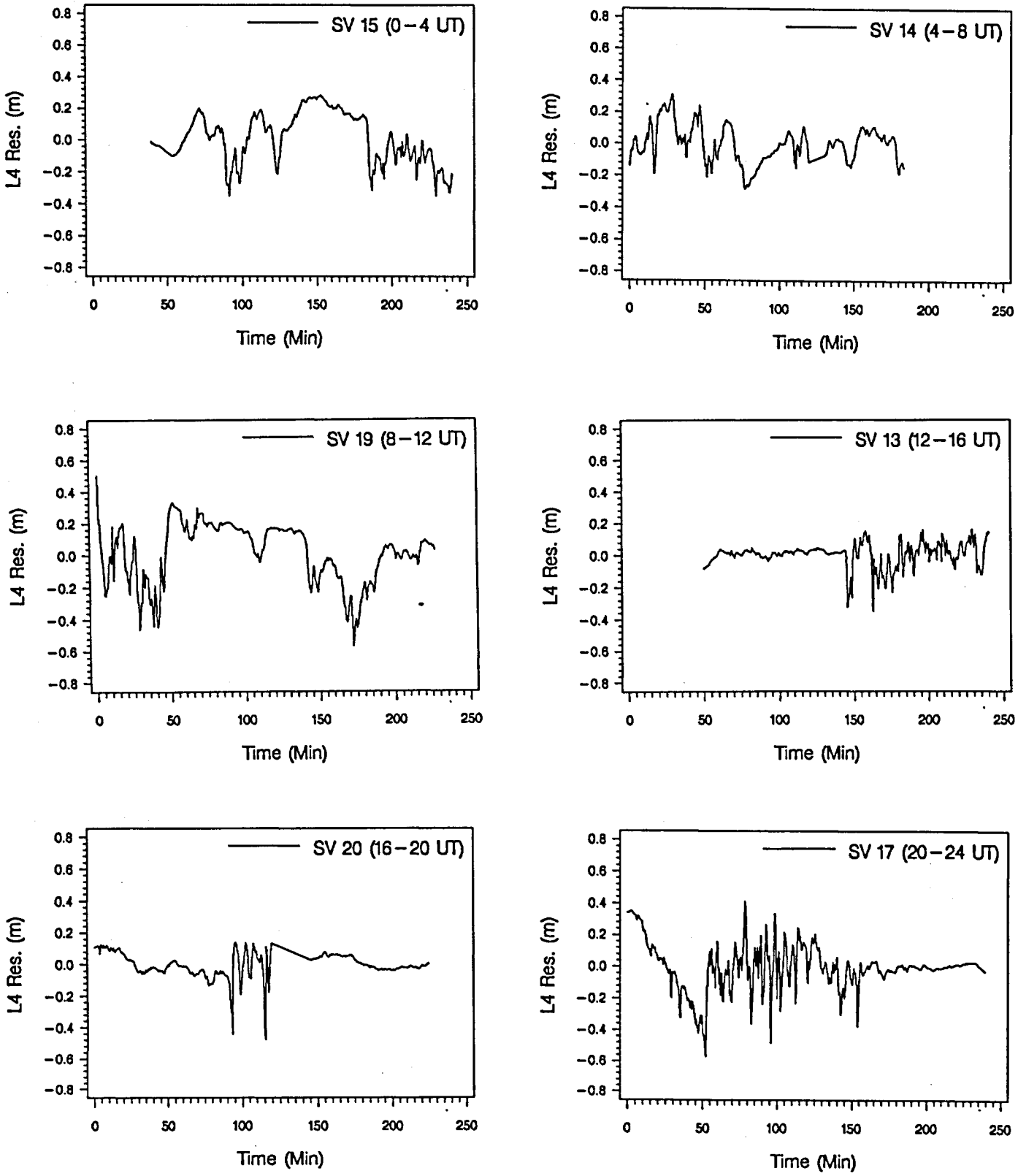

Figure 5-34

L_4 Residuals for Day 261, Station Yellowknife

(PRN 15, PRN 14, PRN 19, PRN 13, PRN 20, PRN 17)

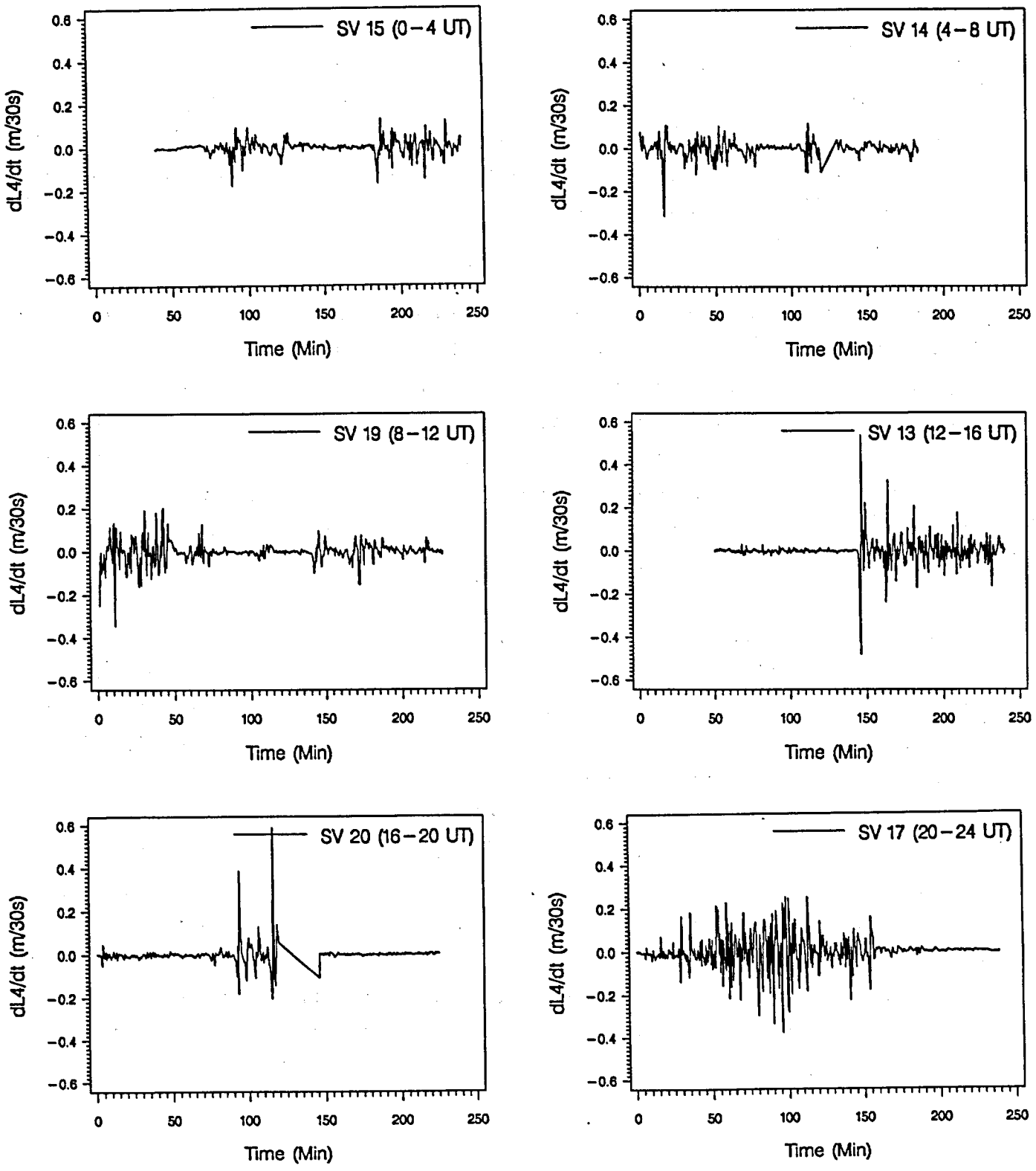

Figure 5-35

Changes in L_4 Residuals per 30 Seconds, Day 261

Station Yellowknife

(PRN 15, PRN 14, PRN 19, PRN 13, PRN 20, PRN 17)

These computations (minimum and maximum values and variance of the changes of the L_4 residuals and the spectral analyses) were performed for all satellites, which had more than 80 % of all possible observations during the 4 hour period of one single-layer model. The computed values were then averaged for each model over the corresponding satellites.

As an example for the output of the program SPARES (see section 4.3.4) we include a part of the result file for day 261 (September 17) of the year 1992 in Table 5-27. The first column denotes the station abbreviation, the second the model number (6 models per day, valid for 4 hours each), and the third the number of satellites which had been used for the computations, because all values in the following columns are mean values including several satellites.

DMIN represents the largest negative value, DMAX the largest positive value of the changes of the L_4 residuals with respect to one model. DVAR denotes the variance of the changes of the L_4 residuals. PMIN and PMAX are results of the spectral analysis: PMIN stands for the minimum detected period (in minutes) in the L_4 residuals, whereas PMAX denotes the period corresponding to the largest spectral amplitude (i.e. the 'main signal') detected in the time series of the L_4 residuals. As described in section 4.3.4 the program SPARES just computes the power spectrum of a given time series of L_4 residuals, i.e. the real amplitudes (in m) of the detected frequencies are not estimated. The program SPARES gives a rough estimate of the amplitudes by indicating the largest negative and the largest positive value of the L_4 residuals (RMIN and RMAX).

IGS: AUTOMATIC IONOSPHERE PROCESSING						DAY 261	1992	
STAT	MOD#	#SV	DMIN (m)	DMAX (m)	DVAR (m)	PMIN (min)	PMAX (min)	RMIN (m)	RMAX (m)
ALGO	1	3	-0.056	0.030	0.005	46.013	146.608	-0.142	0.280
ALGO	2	2	-0.544	0.379	0.038	30.020	113.446	-0.679	0.349
ALGO	3	4	-0.637	0.395	0.041	26.424	125.664	-0.703	0.316
ALGO	4	4	-0.010	0.009	0.002	48.727	208.131	-0.071	0.061
ALGO	5	3	-0.052	0.055	0.004	107.016	244.346	-0.123	0.089
ALGO	6	4	-0.265	0.370	0.025	38.776	103.785	-0.400	0.344
DRAO	1	3	-0.010	0.016	0.003	56.953	157.080	-0.163	0.132
DRAO	2	2	-0.108	0.108	0.020	44.427	107.100	-0.419	0.348
DRAO	3	4	-0.662	0.137	0.028	29.976	97.715	-0.434	0.354
DRAO	4	3	-0.026	0.025	0.004	32.413	158.666	-0.093	0.048
DRAO	5	4	-0.020	0.012	0.002	63.648	141.372	-0.089	0.082
DRAO	6	6	-0.034	0.037	0.003	81.064	172.788	-0.108	0.151
FAIR	1	1	-0.064	0.053	0.013	125.664	209.440	-0.379	0.238
FAIR	2	3	-0.835	0.608	0.094	2.595	16.878	-0.664	0.269
FAIR	3	4	-0.697	0.541	0.063	12.938	53.451	-0.551	0.275
FAIR	4	2	-1.241	0.460	0.057	8.969	117.286	-0.800	0.222
FAIR	5	4	-0.552	1.151	0.058	10.817	76.266	-0.512	0.332
FAIR	6	3	-0.045	0.034	0.007	72.986	157.080	-0.287	0.247

Table 5-27
Result File of the Program SPARES

In order to illustrate the irregular behaviour of the ionosphere during the 60-days test period we plotted for each day the peak value (mean value over 4 stations) of the variance of the changes of the L_4 residuals. In addition we correlated the variance values with the K_p-index, which is a measure for the activity of the geomagnetic field and therefore also for the short period activity of the ionosphere. The figures were generated for all three different latitude regions, where the following stations were taken into account:

- auroral : Tromsoe, Yellowknife, Fairbanks (Figure 5-36)
- mid-latitude : Herstmonceux, Kootwijk, Matera, Wettzell (Figure 5-37)
- equatorial : Tahiti, Mas Palomas, Yaragadee, Taiwan (Figure 5-38)

The inverse values of the minimum periods (PMIN) are given in Figures 5-39 - 5-41.

In Figures 5-36 - 5-38 one can see that for the auroral stations the variance of the changes of the L_4 residuals shows a strong correlation with the K_p-index, whereas this correlation is less obvious for mid-latitude and equatorial stations. Here two different levels for the variances may be observed: for the days with enhanced solar activity (Days 273 - 285, see Figure 5-31) the variance of the changes of the L_4 residuals increases too.

The inverse PMIN values should be correlated to the K_p-index, since a high K_p-index means that short period variations are present in the ionosphere whereas a low K_p-index stands for quiet conditions. The correlation of the inverse PMIN values and the K_p-index is clearly present for the auroral stations whereas it is again less obvious for the mid-latitude and the equatorial stations.

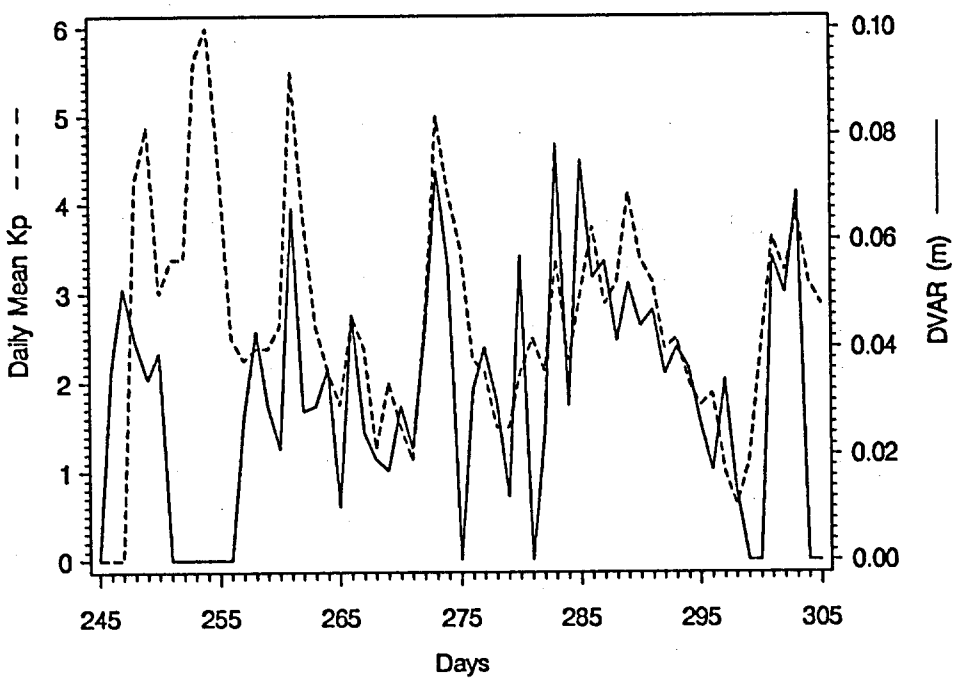

Figure 5-36
Variance of the Changes of L_4 Residuals (per 30 Seconds)
Compared to the (Daily Mean) K_p-Index
Auroral Stations, Days 245 - 305

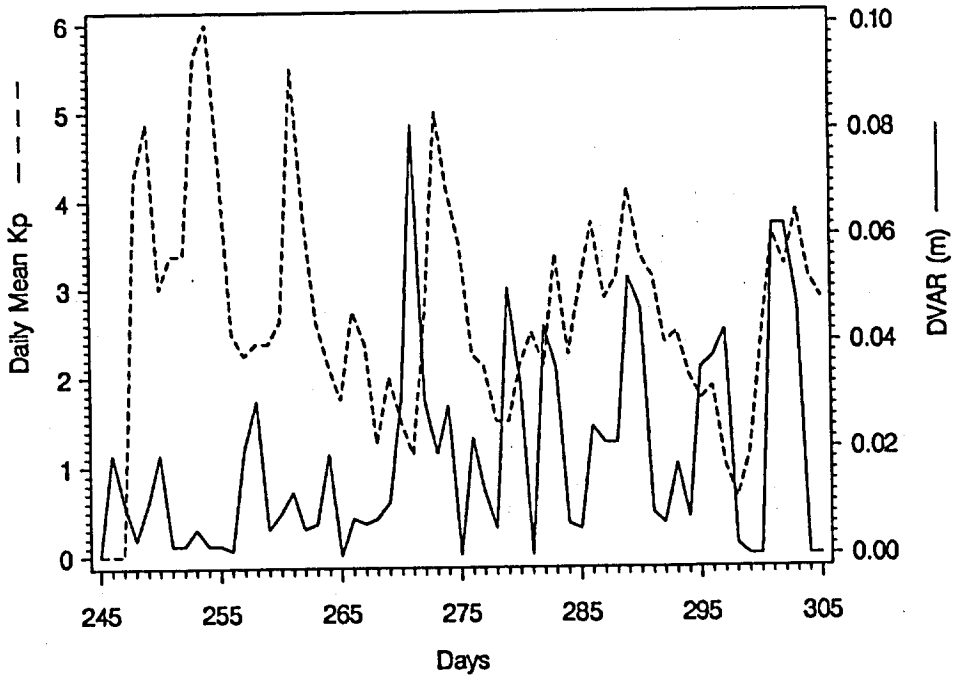

Figure 5-37
Variance of the Changes of L_4 Residuals (per 30 Seconds)
Compared to the (Daily Mean) K_p-Index
Mid-latitude Stations, Days 245 - 305

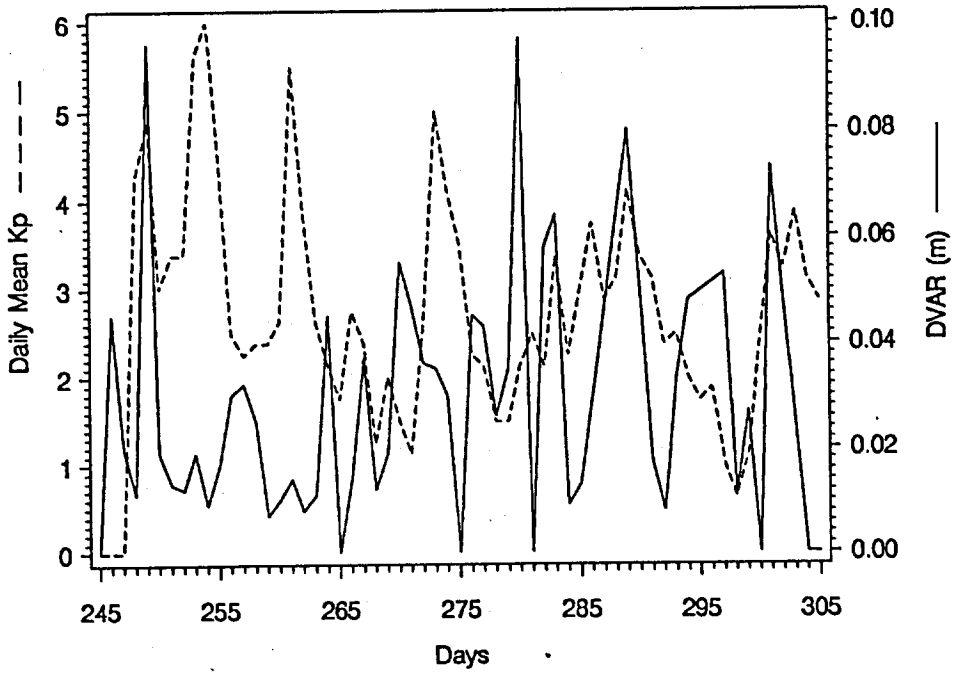

Figure 5-38
Variance of the Changes of L_4 Residuals (per 30 Seconds)
Compared to the (Daily Mean) K_p-Index
Equatorial Stations, Days 245 - 305

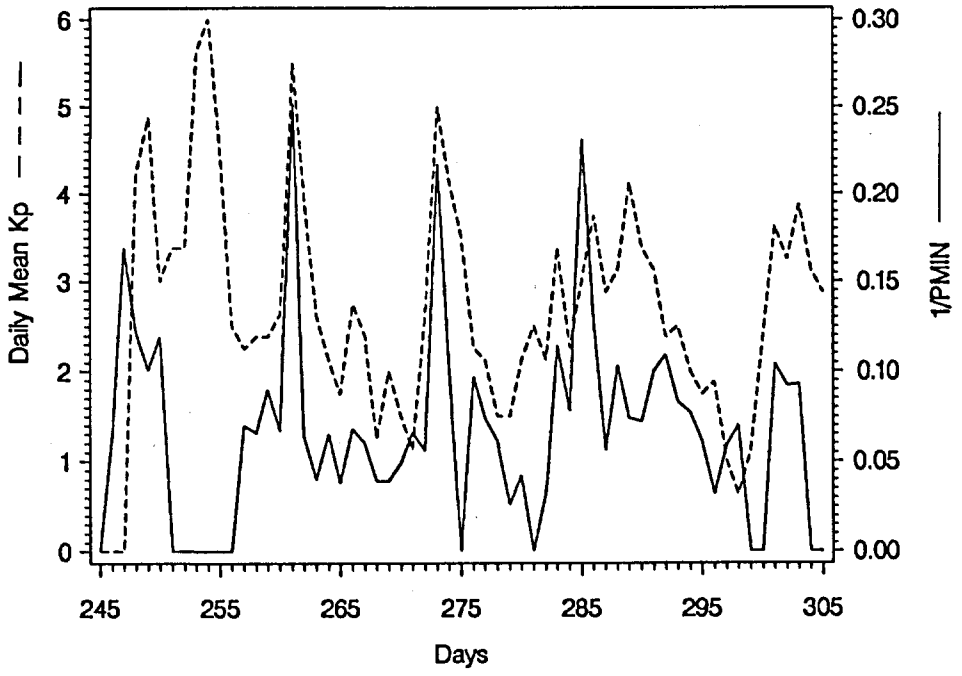

Figure 5-39
Inverse Minimum Periods of the L_4 Residuals (1/Min)
Compared to the (Daily Mean) K_p -Index
Auroral Stations, Days 245 - 305

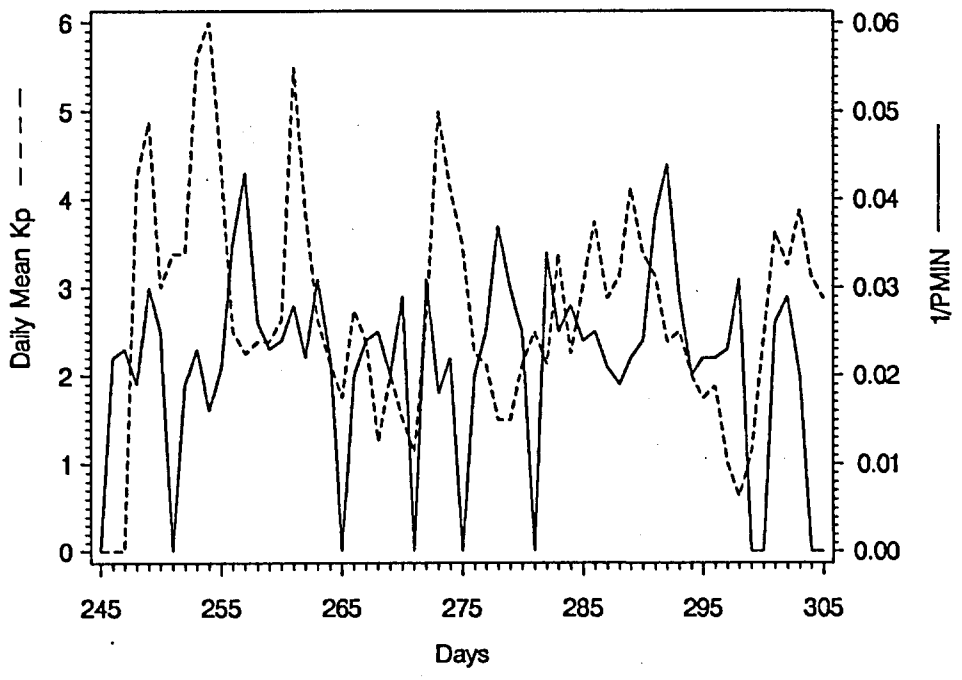

Figure 5-40
Inverse Minimum Periods of the L_4 Residuals (1/Min)
Compared to the (Daily Mean) K_p -Index
Mid-latitude Stations, Days 245 - 305

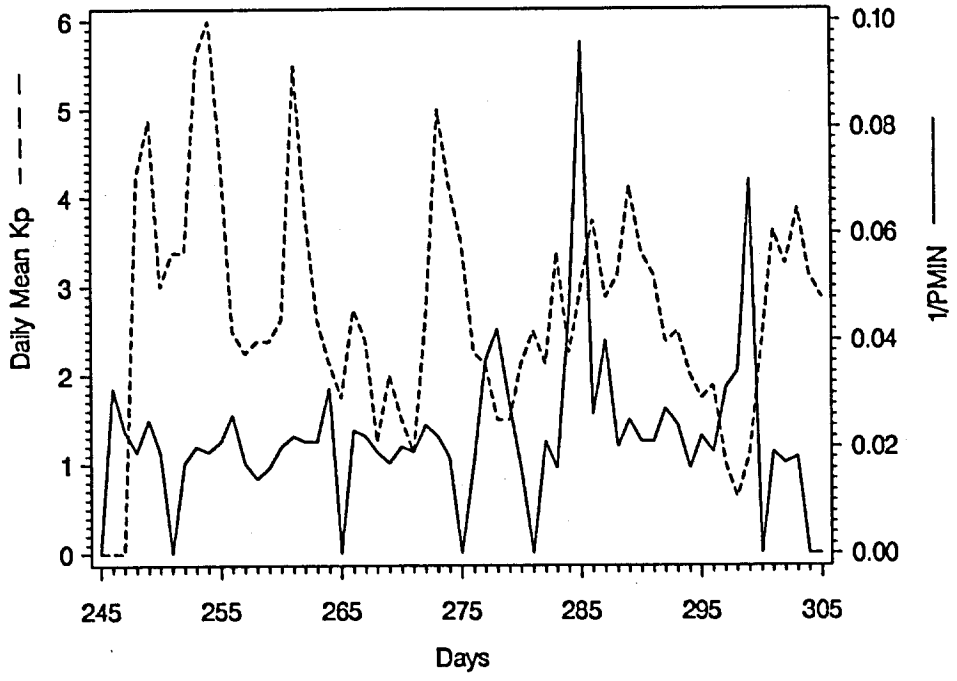

Figure 5-41
Inverse Minimum Periods of the L_4 Residuals (1/Min)
Compared to the (Daily Mean) K_p-Index
Equatorial Stations, Days 245 - 305

The goal of this section was to investigate the capabilities of GPS for ionospheric monitoring. The data of the IGS were used in a automatic way in order to simulate a routine service, as it could be provided in future by some of the analysis centers of the IGS. The main results may be summarized as follows:

- Most of the data from the stations used for the computation arrive in time (assuming a delay of 2 days between observation and data analysis), i.e. a "near real-time" monitoring of the global ionospheric conditions is possible.

- The determination of absolute TEC values is problematic. The main error source seems to be inter-channel calibration problems in the GPS receivers. The accuracy of absolute TEC determination using the programs described in this section is about 3-4 TECU for mid-latitude sites, and may increase to 10-20 TECU for the equatorial and auroral region. Nevertheless the GPS may be used

to determine long period variations (monthly, annual or solar cycle variations) of the TEC.

- Short period disturbances in the ionosphere may very well be detected using GPS. The proposed two measures (variance of the L_4 residuals and the periods determined in the spectral analysis) show a clear correlation with the K_p index for all auroral stations.

- Some of the analysis centers of the IGS should compute (on a routine basis) absolute and relative TEC values for all stations of the IGS and store all the data in a TEC database, which may then be accessed by other interested scientists.

6. CONCLUSIONS

In geodesy the ionosphere is considered as disturbing effect which biases the observations. The goal for the geodesist therefore is to model the ionosphere as accurately as possible in order to eliminate its systematic influence on the observations. In geophysics, however, the influence of the ionosphere on the satellite signals is considered as the 'signal'. In this thesis we tried to cover both aspects by discussing geodetic and geophysical applications of ionosphere modelling and monitoring.

A large number of permanent GPS tracking stations has been built up in the past few years, most of them for the International GPS Service for Geodynamics (IGS). The main task of these stations is the contribution to accurate orbit determination of the GPS satellites and to the computation of earth rotation parameters (ERP). Orbits and earth rotation parameters are the standard products of the IGS, which are routinely produced with a delay of a few days.

Apart from these standard products of the IGS it became obvious that the data of permanent GPS tracking stations would also allow to study the ionosphere. The main goal of the thesis was to demonstrate that the ionosphere may be described by computing single-layer models using data from permanent GPS tracking stations. In these models the total electron content is modelled as a function of geographical latitude and hour angle of the sun. The irregular part of the ionosphere was described by the method of spectral analysis of the residuals of the single-layer models.

In a first geodetic application it was shown that single-layer models generated by one or more dual frequency GPS receivers are very useful for the elimination of systematic ionospheric biases (= scale factors) in geodetic networks. We have tested the proposed single-layer model in a small network with a well known ground truth (the Turtmann Test Network in the Swiss Alps). For different ionospheric conditions the single-layer model was very effective and reduced the scale factors introduced by the ionosphere to the 1 ppm level. In addition it has been shown that the model works also for different geographic latitudes and therefore different iono-

spheric conditions: the model has been used in the equatorial (Hawaii) and in the auroral (Greenland) zones. It became clear that the model is suited for longer observation time spans (1 to 4 hours), where the influence of the short period variations in the ionosphere is averaged out. The influence of short period variations may not be modelled using a single layer model, because the model does not take into account a time-dependency of the ionosphere (apart from the dependency on local time). The model is therefore often also called the model of the 'frozen ionosphere'.

For medium-size (> 10 km) and large networks (up to 2000 km) the influence of the ionosphere is usually eliminated by forming the so-called ionosphere-free linear combination (L_3) of the original carriers L_1 and L_2. The noise of this L_3 linear combination is about 3 times higher than the noise on the carriers L_1 and L_2. For small networks this increased noise degrades the accuracy of the solution. It is therefore preferable (for small networks, such as e.g. dam control networks) to compute an L_1 and L_2 solution and to introduce an ionosphere model.

The single-layer models allow to compute the total electron content not only for the intersection point between the satellite signal path and the ionosphere, but also for an arbitrary point in the ionospheric layer given by its latitude, longitude, and time. This was used to compute the total electron contents for the calibration of the radar altimeter of ERS-1. The computed TEC values showed a good agreement with TEC values obtained from other observation techniques, such as Faraday Rotation and DORIS derived TEC values.

The last geodetic application dealt with the use of ionosphere models for the wide-lane ambiguity resolution in medium-size networks (100 - 300 km). For such baselines the direct ambiguity resolution on the original carriers is not possible because of several increasing systematic effects like orbits, troposphere biases, and last but not least the ionosphere. In these cases the wide-lane ambiguities (= difference between the original ambiguities) may more easily be resolved than the ambiguities in L_1 and L_2, because of the greater wavelength of the wide-lane linear combination. The main problem in this procedure is the fact, that the wide-lane li-

near combination is biased by the ionosphere. Assuming accurate orbits and neglecting clock errors the systematic influence of the ionosphere may directly be seen in the fractional parts of the wide-lane ambiguities before resolution. If ionosphere models are introduced into the ambiguity resolution process the fractional parts of the wide-lane ambiguities are considerably improved. In this study we processed a medium-size network (200 x 300 km) in Switzerland, the EUREF-CH-92 network, which represents the reference frame for the GPS first order survey in Switzerland. The introduction of ionosphere models allowed the resolution of about 85 % of all wide-lane ambiguities.

Monitoring the amount and the changes of the total electron content in the ionosphere is the main geophysical application discussed in this thesis. The increasing number of permanent GPS tracking stations (mainly established for the IGS) represents a potential for ionospheric studies using GPS. At the moment the station distribution of the IGS is not homogeneous at all, since most of the stations are concentrated in the northern hemisphere, whereas the equatorial region and the southern hemisphere show a poor station coverage. This situation may change in future, because for orbit determination a better distribution of the GPS stations is needed and additional GPS tracking stations are planned.

For this study we operated a type of routine ionosphere service, as it could be established in future at some IGS analysis centers. The data of 20 stations of the IGS in different geographical latitudes were processed in a highly automated way over a time span of 60 days (September - October 1992). For all stations we computed six ionosphere models per day (valid for 4 hours each) giving absolute TEC values and the TEC gradients in latitude and local time. In addition the short period variations of the ionosphere were studied by simply computing the variance of the changes of the residuals between two subsequent observation epochs, as well as by applying the technique of spectral analysis.

The major problems for the determination of absolute TEC values using GPS observations are:

- The calibration of the GPS derived absolute TEC values is a serious problem, because other observation techniques, which could be used for the calibration, are biased too by cycle ambiguities (Faraday) or need additional assumptions for the TEC determination.

- The TEC determination using GPS P-code observations suffers from inter-channel calibration problems, which lead to biased TEC values.

- If GPS phase observations are used (as in our case) these calibration problems may be ignored, because uncalibrated channels would lead to a wrong estimate of the additional constant estimated in the program IONEST (see section 4.3). Since this constant is of no interest anyway, we do not have to care about receiver calibrations. However our absolute TEC values are based on all the assumptions made in the single-layer model:
  - all free electrons are concentrated in a spherical shell of infinitesimal thickness in a height of 350 km above the earth's surface,
  - the mapping function for the TEC is 1/cos(z), z = zenith distance, which is only a rough appproximation of the reality, and
  - the single-layer model does not take into account a real time dependency ('frozen ionosphere').

  The absolute TEC values computed using the single-layer model and GPS phase observations have an uncertainity of about 3-4 TECU for mid-latitude ionospheric conditions. For equatorial regions the accuracy may decrease to 10-20 TECU.

Nevertheless, if a 3-day running mean of the daily TEC peak values is compared to the Sunspot Number and the Solar Flux during the test period, there is quite a good correlation (at least for equatorial stations). This indicates that GPS in any case may be used to determine long term variations of the TEC values (monthly, annual or even solar cycle variations).

Short period variations in the ionosphere may very well be detected and monitored by GPS observations. We analyzed the residuals of the single layer models and could clearly defect storm events in the

ionosphere. The variability of the residuals as well as the periods detected in the spectral analysis showed a good correlation with the K_p-index for the auroral stations. The correlation was less apparent for mid-latitude and equatorial stations.

The test demonstrates the capabilities of the GPS for a routine monitoring of the ionosphere. We processed the data with a delay of 2 days between observation and analysis. Most of the data were available at the analysis center within this time span, i.e. it is possible to establish a "near real-time" ionosphere service using the data of the IGS stations. For certain stations the delay between observation and analysis might even be reduced to 1 day. We therefore recommend that some of the analysis centers of the IGS start to compute absolute TEC values using e.g. the models proposed in this study. In addition to the absolute TEC values the variations of the TEC should be analyzed, either by simply differencing the observation of subsequent observation epochs or by applying more sophisticated algorithms like e.g. spectral analysis. We recommend that the results are stored in a ionosphere database, from where the information may be retrieved by interested scientists.

7. REFERENCES

Anodina, T., M. Prilepin (1989). "The GLONASS System." Proceedings of the Fifth International Geodetic Symposium on Satellite Positioning, Las Cruces, New Mexico, March 13-17, Vol. 1, pp. 13-18.

Bent, R.B. and S.K. Llewellyn (1973). "Documentation and Description of the Bent Ionospheric Model." Space & Missiles Organization, Los Angeles, California, AFCRL-TR-73-0657.

Beutler, G., I. Bauersima, S. Botton, W. Gurtner, M. Rothacher, T. Schildknecht (1987a). "Accuracy and Biases in the Geodetic Application of the Global Positioning System." Paper presented at the 19th IUGG, General Assembly, Vancouver 1987.

Beutler, G., I. Bauersima, W. Gurtner, M. Rothacher, T. Schildknecht and A. Geiger (1987b). "Atmospheric Refraction and other Important Biases in GPS Carrier Phase Observations." Paper presented at the 19th IUGG, General Assembly, Vancouver 1987.

Beutler, G., W. Gurtner, U. Hugentobler, M. Rothacher, T. Schildknecht, U. Wild (1988). "Ionosphere and GPS Processing Techniques." Paper presented at the 1988 Chapman Conference on the Use of GPS for Geodynamics, Ft. Lauderdale U.S.A.

Beutler, G., W. Gurtner, M. Rothacher, U. Wild, E. Frei (1989). "Relative Static Positioning with the Global Positioning System: Basic Technical Considerations." Paper presented at the IAG General Meeting, Edinburgh, August 1989.

Beutler, G. (1992a). "The Impact of the International GPS Geodynamics Service (IGS) on the Surveying and Mapping Community." Proceedings, XVII ISPRS Congress, Washington, 1992.

Beutler, G. (1992b). "The 1992 Activities of the International GPS Geodynamics Service (IGS)." 7th International Symposium on "Geodesy and Physics of the Earth", IAG Symposium No. 112, in press.

Bishop, G.J., J.A. Klobuchar, P.H. Doherty (1985). "Multipath Effects on the Determination of Absolute Ionospheric Time Delay from GPS Signals." Radio Science, Vol. 20, pp. 388-396, 1985.

Blewitt, G., W.G. Melbourne, W.I. Bertiger, T.H. Dixon, P.M. Kroger, S.M. Lichten, T.K. Meehan, R.E. Neilan, L.L. Skrumeda, C.L. Thornton, S.C. Wu and L.E. Young (1988). "GPS geodesy with centimeter accuracy." Lecture Notes in Earth Sciences, Vol. 19, Springer Verlag, pp. 30-40.

Blewitt, G. (1990). "Carrier Phase Ambiguity Resolution for the Global Positioning System Applied to Geodetic Baselines up to 2000 km." Journal of Geophysical Research, Vol. 94, No. B8, pp. 10187-10203.

Brockmann, E. (1990). "Untersuchungen zur Korrektion des IAU-Nutationsmodells durch VLBI-Beobachtungen." Diplomarbeit (unpublished).

Brunner, F.K. and M. Gu (1991). "An improved model for the dual frequency ionospheric correction of GPS observations." Manuscripta Geodaetica, Volume 16, pp. 205-214.

Carnebianca, C., G. Mastini, R. Rizzo (1985). "NAVSAT System Configuration Study." ITALSPAZIO, ITS-TR-011/85, ESA Contract No. 5754/84/F/RD(SC).

Davies, K. and G. K. Hartmann (1993). "Total Electron Content (TEC) of the Ionosphere from GPS and GOES Radio Signals." Journal for Satellite-Based Positioning, Navigation and Communication (SPN), No. 1/93, Wichmann, Karlsruhe, 1993.

Francis, C.R., A. Caporali, L. Cavaleri, A. Cenci, P. Ciotti, L. Ciraolo, W. Gurtner, F.H. Massman, D. del Rosso, R. Scharroo, P. Spalla and E. Vermaat (1992). "The Calibration of the ERS-1 Radar Altimeter." ER-RP-ESA-RA-0257, ESA/ESTEC, Noordwijk, The Netherlands.

Frei, E. (1991). "Rapid Differential Positioning With the Global Positioning System (GPS)." PhD Thesis, Geodätisch-geophysikalische Arbeiten in der Schweiz, Vol. 44, 1991.

Georgiadiou, Y. and A. Kleusberg (1988). "On the effect of ionospheric delay on geodetic relative GPS positioning." Manuscripta Geodaetica, Volume 13, pp. 1-8.

Georgiadiou, Y. (1990). "Ionospheric delay modelling for GPS relative positioning." Proceedings of the Second International Symposium on Precise Positioning with the Global Positioning System, Ottawa, Canada, pp. 403-410.

Gorney, D.J. (1990). "Solar cycle effects on the near-earth space environment." Reviews of Geophysics, 28/3 August 1990, pp. 315-336.

Gu, M. and F.K. Brunner (1990). "Theory of the two frequency dispersive range correction." Manuscripta Geodaetica, 1990, Vol. 15, pp. 357-361.

Gurtner, W., G. Beutler, S. Botton, M. Rothacher, A. Geiger, H.-G. Kahle, D. Schneider, A. Wiget (1987). "The Use of the Global Positioning System in Mountainous Aeras." Paper presented at the 19th IUGG, General Assembly, Vancouver 1987.

Gurtner, W., G. Mader, D. MacArthur (1989). " A Common Exchange Format for GPS Data." GPS Bulletin of the CSTG, Vol. 2, No. 3, Rockville, Maryland, USA, 1989.

Gurtner, W. and B. Overgaauw (1991). "Results from the ERS-1 GPS Calibration Campaigns 1990 and 1991." ERS-1 Radar Altimeter Calibration Team Meeting, Berne, December 20, 1991.

Gurtner, W., S. Fankhauser, W. Ehrnsperger, W. Wende, H. Friedhoff, H. Habrich, S. Botton (1992). "EUREF-89 GPS Campaign - Results of the Processing by the "Berne Group" - ." Report on the Symposium of the IAG Subcommission for the European Reference Frame

(EUREF), March 1992, Veröffentlichungen der Bayerischen Kommission für die Internationale Erdmessung, Vol. 52, München.

Hartmann, G.K. and R. Leitinger (1984). "Range errors due to ionospheric and tropospheric effects for signal frequencies above 100 MHz." Bulletin Géodésique No. 58 (1984), pp. 109-136.

Kelley, M.C. (1989). "The Earth's Ionosphere. Plasma Physics and Electrodynamics." International Geophysics Series, Volume 43, Academic Press, New York.

Kertz, W. (1971). "Einführung in die Geophysik. (Vol. II)" BI-Hochschultaschenbücher, No. 535, Mannheim/Vienna/Zürich, 1971.

Klobuchar, J.A. (1986). "Design and characteristics of the GPS ionospheric time delay algorithm for single frequency users." Proceedings of the PLANS-86 conference, Las Vegas, Nevada, pp. 280-286.

Landau, H. (1989). "Zur Nutzung des Global Positioning Systems in Geodäsie und Geodynamik: Modellbildung, Software-Entwicklung und Analyse." Ph.D. Thesis, Studiengang Vermessungswesen, Universität der Bundeswehr München, Neubiberg.

Lanyi, G.E, T. Roth, R.E. Neilan (1987). "A Comparison of Mapped and Measured Total Ionospheric Electron Content Using GPS and Beacon Satellite Observations." The Effect of the Ionosphere on Communication, Navigation and Surveillance Systems, Ionospheric Effects Symposium, 5-7 May 1987, pp. 135-143, Naval Research Laboratory.

Lefevbre, M. (1989). "DORIS." International Coordination of Space Techniques for Geodesy and Geophysics (CSTG), Bulletin No. 11, Munich, pp. 141-151.

Leitinger, R., G.K. Hartmann, F.-J. Lohmar and E. Putz (1984). "Electron content measurements with geodetic Doppler receivers." Radio Science, Vol. 19, No. 3, May-June 1984, pp. 789-797.

McNamara, L.F. and P.J. Wilkinson (1983). "Prediction of the total electron content using the International Reference Ionosphere." Journal of Atmospheric and Terrestrial Physics, Volume 45, Number 2/3, pp. 169 - 174.

Melbourne, W.M. (1985). "The case for ranging in GPS based systems." Proceedings of the First Symposium on Precise Positioning woth the Global Positioning System, Positioning with GPS-1985, Ed. C.C. Goad, Rockville, Maryland, pub. U.S. Department of Commerce, NOAA.

Mervart L., G. Beutler, M. Rothacher and U. Wild (1993). "Ambiguity Resolution Strategies using the Results of the International GPS Geodynamics Service (IGS)." Bulletin Géodésique No. 68 (1994), pp. 29-38.

Mueller, I.I. and G. Beutler (1992). "The International GPS Service for Geodynamics - Development and Current Structure." Proceedings of the Sixth International Geodetic Symposium on Satellite Positioning, Vol. II, pp. 823-835, March 1992, Ohio.

Newby, S.P. (1992). "An Assessment of Empirical Models for the Prediction of the Transionospheric Propagation Delay of Radio Signals". PhD Thesis, Technical Report No. 106, August 1992, Dpt. Surveying Engineering, University of New Brunswick.

Ratcliffe, J.A. (1970). "Sun, Earth and Radio." McGraw-Gill, New York.

Rawer, K., J.V. Lincoln, R.O. Conkright, D. Bilitza, B.S.N. Prasad, S. Mohanty and F. Arnold (1981). "International Reference Ionosphere". World Data Centre A for Solar-Terrestrial Physics, NOAA, Boulder, Colorado, Report UAG-82.

Rishbeth, H., O.K. Garriot (1969). "Introduction to Ionospheric Physics." International Geophysics Series, Vol. 14, Academic Press, New York.

Rothacher, M., G. Beutler, W. Gurtner, T.Schildknecht, U. Wild (1993). "Bernese GPS Software Version 3.4. Documentation, May 1993." Astronomical Institute, University of Berne.

Royden, H.N., R.B. Miller, and L.A. Buenagel (1984). "Comparison of NAVSTAR Satellite L Band Ionospheric Calibrations with Faraday Rotation Measurements." Radio Science, Vol.19, No. 3, May-June 1984.

Royden, H.N., D.W. Green, (1986). "Comparison of two models of total electron content at three midlatitude stations." Proceedings of the International Beacon Satellite Symposium 1986, Ed. a. Tauriainen, University Oulu, Finland, pp. 197-203.

Schneider, D. (1992). "Dreidimensionales Testnetz Turtmann 1985-1990 Teil I." Geodätisch-geophysikalische Arbeiten in der Schweiz, Volume 45, Editor: F. Jeanrichard, 1992.

Schneider, D. (1993). "Neues Konzept der Schweizerischen Landesvermessung: Erste Erfahrungen bei der Realisierung eines GPS-gestützten Landesnetzes." Paper presented at the DVW-Meeting, March 1993, Technical University of Dresden.

Schuh, H. (1978). "Zur Speaktralanalyse von Erdrotationsschwankungen." Arbeiten des Sonderforschungbereichs 78 Satellitengeodäsie der TH München, Veröffentlichungen der Bayerischen Kommission für die internationale Erdmessung, München, 1980.

Seeber, G. (1989). "Satellitengeodäsie." Walter de Gruyter, Berlin, New York, 1989.

Smith, C.A. (1987). "Ionospheric TEC Estimation With a Single-Frequency GPS Receiver." The Effect of the Ionosphere on Communication, Navigation and Surveillance Systems, Ionospheric Effects Symposium, 5-7 May 1987, pp. 145-150, Naval Research Laboratory.

Spilker, J. (1978). "GPS Signal Structure and Performance Characteristics." Navigation: The Journal of the Institute of Navigation, Washington, Vol. 25, No. 2, pp. 121-146.

Wanninger, L. (1992). "Monitoring Total Ionospheric Electron Content And Ionospheric Irregularities Using GPS." Paper presented at the Symposium on Refraction of Transatmospheric Signals in Geodesy, The Hague, The Netherlands, May 19-22, 1992.

Wiget, A., E. Gubler, D. Schneider, G. Beutler, U. Wild (1990). "High-Precision Regional Crustal Motion Network in Switzerland." Proceedings of the Second International Symposium on Precise Positioning with the Global Positioning System, Ottawa, Canada, September 3-7, pp. 835-852.

Wiget, A. and U. Wild (1993). "EUREF-CH-92." Internal Technical Report (in preparation), Swiss Federal Office of Topography.

Wild, U., G. Beutler, W. Gurtner, M. Rothacher (1989). "Estimating the Ionosphere Using One or More Dual Frequency GPS Receivers." Proceedings of the Fifth International Geodetic Symposium on Satellite Positioning, Las Cruces, New Mexico, March 13-17, Vol. 2, pp. 724-736.

Wild, U., G. Beutler, S. Fankhauser, M. Rothacher (1990). "Stochastic Properties of the Ionosphere Estimated from GPS Observations." Proceedings of the Second International Symposium on Precise Positioning with the Global Positioning System, Ottawa, Canada, September 3-7, pp. 411-428.

Wild, U. and G. Beutler (1991). "The Use of Permanent Tracking Station Data for Ionosphere Modelling." Paper presented at the XX General Assembly of the IUGG, Vienna, August 11-24, 1991.

Willis, P., C. Boucher, H. Fagard, M. Gavoret, G. Imbert, M. Kasser, G. Balmino, R. Biancale, A. Cazenave, M. Dorrer, F. Nouel, J.J. Valette (1990). "Positioning With the DORIS System: Present Status and First Results." Proceedings of the Second International Symposium on Precise Positioning with the Global Positioning System, Ottawa, Canada, September 3-7, The Canadian Institute of Surveying and Mapping, pp. 131-144.

Wübbena, G. (1985). "Software developments for geodetic positioning with GPS using TI-4100 code and carrier measurements." Proceedings of the First Symposium on Precise Positioning with the Global Positioning System, Positioning with GPS-1985, Ed. C.C. Goad, Rockville, Maryland, publ. U.S. Department of Commerce, NOAA.

"Geodätisch-geophysikalische Arbeiten in der Schweiz"
(Fortsetzung der Publikationsreihe "Astronomisch-geodätische Arbeiten in der Schweiz")
der Schweizerischen Geodätischen Kommission (ab Bd. 34):

34 1982 Lösung von Parameterbestimmungsproblemen in Himmelsmechanik und Satellitengeodäsie mit modernen Hilfsmitteln. G. Beutler. 257 Seiten.

35 1982 Schwere-Anomalien und isostatische Modelle in der Schweiz:
I. Zum Konzept der isostatischen Modelle in Gebirgen am Beispiel der Schweizer Alpen. E. Klingelé und E. Kissling.
II. Aufbau der Kruste und des oberen Mantels in der Schweiz. E. Kissling.
III. Gravimetrische Untersuchungen in der Kontaktzone Helvetikum/Aar-Massiv.
P.J.Cagienard, H.-G. Kahle, St. Müller und E. Klingelé. 169 Seiten, 1 Karte.

36 1984 Ein gravimetrisches Krusten-Mantel-Modell für ein Profil im nördlichen Alpenvorland bis an die Ligurische Küste. H. Schwendener. 160 Seiten.

37 1986 Les levés aéromagnetiques de la Suisse. E. Klingelé. 69 Seiten.

38 1986 Lokale Schwerefeldbestimmung und gravimetrische Modellrechnungen im Satelliten (GPS)- Testnetz "Turtmann" (Wallis). I. Bernauer, A. Geiger. 106 Seiten.

39 1989 125 Jahre Schweizerische Geodätische Kommission
I. Bedeutung geodätischer Raumverfahren für Landesvermessung und Geodynamik. (R. Sigl)
II. Beitrag der Geodäsie zur Geodynamik. (H.-G. Kahle)
III. L'état actuel de la recherche sur les movements de l'écorce terrestre en Suisse. (F. Jeanrichard)
IV. Die Satellitengeodäsie im Dienste der globalen Geodynamik. (I. Bauersima)
V. Die Veranstaltungen zum 125 Jahr-Jubiläum der Schweizerischen Geodätischen Kommission. (W. Fischer). 62 Seiten.

40 1989 Integrale Schwerefeldbestimmung in der Ivrea- Zone und deren geophysikalische Interpretation. B. Bürki. 186 Seiten.

41 1990 ALGESTAR satellitengestützte Geoidbestimmung in der Schweiz. U. Marti. 61 Seiten plus Punktprotokolle.

42 1990 Höhensysteme, Schwerepotentiale und Niveauflächen: Systematische Untersuchungen zur zukünftigen terrestrischen und GPS-gestützten Höhenbestimmung in der Schweiz. B. Wirth. 204 Seiten.

43 1990 Gravimetrisches Geoid der Schweiz: Potentialtheoretische Untersuchungen zum Schwerefeld im Alpenraum. A. Geiger. 231 Seiten.

44 1991 Rapid Differential Positioning with the Global Positioning System (GPS). E. Frei. 178 Seiten.

45 1992 Dreidimensionales Testnetz Turtmann 1985-1990 Teil I. F. Jeanrichard (Hrsg.)
Autoren: A.Geiger, H.-G. Kahle, R. Köchle, D. Meier, B. Neininger, D. Schneider, B. Wirth. 183 Seiten.

46 1993 Orbits of Satellite Systems in Space Geodesy. M. Rothacher. 243 Seiten.

47 1993 NFP 20. Beitrag der Geodäsie zur geologischen Tiefenstruktur und Alpendynamik. H.-G. Kahle (Hrsg.) Autoren: I. Bauersima, G. Beutler, B. Bürki, M. Cocard, A. Geiger, E. Gubler, W. Gurtner, H.-G. Kahle, U. Marti, B. Mattli, M. Rothacher, Th. Schildknecht, D. Schneider, A. Wiget, B. Wirth. 153 Seiten plus 90 Seiten Anhang.

48 1994 Ionosphere and Geodetic Satellite Systems: Permanent GPS Tracking Data for Modelling and Monitoring: Urs Wild, 155 Seiten.